THE ARC SPECTRUM OF TIN

A Thesis

Submitted to the Faculty

of

Purdue University

by

Wilfred Grenfell Brill

In Partial Fulfillment of the

Requirements for the Degree

of

Doctor of Philosophy

January 1964

ACKNOWLEDGMENTS

It is with great pleasure that the author expresses his deep appreciation to Professor Kenneth L. Andrew whose interest, inspiration, skillful direction, and helpful suggestions throughout the major portion of this investigation were instrumental in bringing it to a satisfactory conclusion.

To the late Professor K. W. Meissner, who suggested the problem and directed the early part of the investigation, the author is grateful.

The author is indebted to Dr. C. J. Humphreys of the Naval Ordnance Laboratory at Corona, California, and to Professor A. G. Shenstone of Princeton University, who made available the results of their measurements of the arc spectrum of tin in the far infrared and vacuum ultraviolet regions, respectively.

The author is grateful to his wife, Joan, who assisted in checking the thousands of numbers involved in the various phases of the reduction of the data.

Financial support received from the Purdue Research Foundation, the National Science Foundation, and the National Aeronautics and Space Administration is gratefully acknowledged.

TABLE OF CONTENTS

LIST OF TABLES

LIST OF ILLUSTRATIONS

ABSTRACT

Brill, Wilfred Grenfell. Ph. D., Purdue University, January 1964. The Arc Spectrum of Tin. Major Professor: Kenneth L. Andrew.

The arc spectrum of tin has been investigated photographically from 2064 A to 13608 A using plane- and concave-grating spectrographs and Fabry-Perot interferometers crossed with a plane grating spectrograph and with a quartz prism spectrograph. The light sources employed were electrodeless discharge tubes containing tin halides. In the wavelength region investigated, 376 lines have been measured; of these, 141 are new and 314 were measured interferometrically. The wavelength measurements in the far infrared and vacuum ultraviolet regions of the spectrum supplied by other laboratories are included and bring the line list to a total of 591.

An analysis of the arc spectrum of tin has been carried out with the result that 529 of the lines are now classified and 38 new energy levels have been found, bringing the total number of even levels to 62 and the number of odd levels to 138. Two lines were found to be due to forbidden transitions between levels of the same parity.

In addition, 42 lines belonging to the first spark spectrum of tin were measured and one new even energy level for this spectrum was found.

author

INTRODUCTION

The present state of knowledge of the arc spectrum of tin as given in the third volume of Atomic Energy Levels[1] (AEL) rests primarily upon the measurements of Meggers[2], the infrared measurements of Randall and Wright[3], and the unpublished vacuum ultraviolet measurements of Shenstone and of Barrow and Rowlinson. A study of the 38 energy levels of even parity and 125 levels of odd parity listed in AEL shows that many of the levels predicted by theory have not yet been observed. This is particularly true for the levels of the $5s^2 5pnf$ configurations and the higher $5s^2 5pnp$ configurations, all of which should combine with the $5s^2 5p5d$ levels to produce lines in the longer wavelength region of the spectrum.

The problem, therefore, was to make a new investigation of the arc spectrum of tin, obtaining as many lines as possible in the region from 2000 A to 13000 A with particular emphasis on the longer wavelengths. In order to find new levels, to determine the level values more accurately, and to classify the lines with greater certainty, measurements of these lines were to be made as accurately as possible.

One additional result of the investigation would be the determination of the suitability of lines of the tin spectrum for use as calculated Ritz standards in the vacuum ultraviolet as has been done with the spectra of copper, germanium, and other elements[4].

HISTORICAL BACKGROUND

Nearly 200 publications related to the atomic spectra of tin have appeared up to the present time, of which 96 published prior to 1912 have been summarized by Kayser[5]. Only the more important papers will be mentioned here, but those of significance that have appeared since 1912 are included in the general references.

The first observation of the tin spectrum was reported by Wheatstone[6,7] at a meeting of the British Association for the Advancement of Science held at Dublin on August 12, 1835. By means of a prism, he investigated the spectra of the spark taken from pools of mercury and molten zinc, cadmium, bismuth, tin, and lead. He found that "none of these metals gave an uninterrupted spectrum, but each presented a few (tin gave seven) bright, definite lines, widely separated from each other; the number, position, and colour of these lines differ in each of the metals employed. These differences are so obvious that any one metal may instantly be distinguished by the appearance of its spark." He also examined the spectra produced by various amalgams and alloys and "found that when the metals differed much in volatility the lines appertaining to the most volatile metal only were observed; in other cases lines belonging to both were seen."

The first accurate investigation was made in 1859 by Plücker[8] who observed the spectrum produced by a Geissler tube containing stannous chloride. In addition to chlorine lines, he found six lines which he attributed to the compound and, using a prism spectrometer, he determined

the wavelengths of these lines with respect to the Fraunhofer absorption lines of the solar spectrum. A later comparison showed that five of the lines he measured belong to the spark spectrum of tin and the sixth to the arc spectrum.

The first extensive measurements in the arc spectrum of tin were reported in 1883 by Liveing and Dewar[9]. Using a spectrograph with quartz lenses and a speculum grating, they investigated the ultraviolet arc spectra of several elements and, for tin, gave the wavelengths of 45 lines between 2194 A and 3326 A.

The most important contribution to the arc spectrum of tin prior to 1912 came in 1893 when Kayser and Runge[10] published the results of their investigation of the arc spectra of tin, lead, arsenic, antimony, and bismuth. They used a spectrograph with a Rowland concave grating of 6.5 meter radius and the wavelengths they gave are in the Rowland system in which the wavelengths of the sodium D-lines are 5896.16 A and 5890.19 A. For the tin spectrum, they measured 73 lines between 2053 A and 5632 A. In addition, they discovered the first significant regularities in the arc spectrum of tin when they found thirteen pairs of lines having a wave number difference in air of 5187 cm^{-1} and eight pairs with a difference of 1736 cm^{-1}. Much later these were recognized as the separations of the $5s^2 5p^2\ ^1D_2$ and $5s^2 5p^2\ ^3P_2$ levels and the $5s^2 5p^2\ ^3P_2$ and $5s^2 5p^2\ ^3P_1$ levels, respectively, of the neutral tin atom.

The first description of the Zeeman effect for tin was given in 1897 by Zeeman[11] who investigated one line of the arc spectrum and three lines of the spark spectrum. He observed no effect of the magnetic field on the arc line, but one of the spark lines was split into three components while the other two appeared to undergo a change. He used a spectrograph

with a grating of six-foot radius which gave a reciprocal dispersion of 4.46 A/mm in second order. The magnetic field strength was 32,000 gauss and the light source was a condensed spark between pure tin electrodes.

The results of the first important investigation of the infrared arc spectrum of tin were published by Randall[12] in 1911. He used a plane grating monochromator with a thermopile detector mounted at the exit slit to determine the wavelengths in the Rowland system of 22 tin lines between 8554 A and 13022 A.

Arnolds[13] made an important contribution in 1914 when he published the first measurements of the arc and spark spectra of tin in the International system in which the wavelength of the red line of the cadmium spectrum is 6438.4696 A. His paper gives 68 lines between 2194 A and 7800 A which appeared in the arc spectrum. He used a spectrograph with a Rowland concave grating of 6.34 m radius and the standards were interferometrically measured lines of the iron spectrum.

Saunders[14] made measurements in the far ultraviolet region of the tin arc spectrum using a vacuum spectrograph with a one-meter concave grating and gave the wavelengths of 15 lines between 1811 A and 2355 A. He also found three lines having the constant wave number differences found by Kayser and Runge[10] and he discovered four lines belonging to a fourth group.

In 1916, Zumstein[15] sought regularities in the arc spectra of lead and tin and, for the former, found five groups of three lines which had constant frequency differences. Since tin belongs to the same group in the periodic table, similar groups were sought and found for tin. Three of the five groups he found were contained in the regularities found by Kayser and Runge, having separations of 5186 cm^{-1} and 1736 cm^{-1}, while

the additional constant differences given by Zunstein were 1692 cm^{-1} and 288 cm^{-1}. The former is now known to be the separation of the $5s^2 5p^2\ ^3P_1$ and $5s^2 5p^2\ ^3P_0$ levels, but the latter is not real.

In 1921, Walters[16] filled the gap between the measurements in the visible region and the infrared measurements of Randall[12] when he published the wavelengths of 49 lines between 5631 A and 9146 A which he obtained with a tin arc light source. He used a grating spectrograph with a reciprocal dispersion of about 10 A/mm in first order and lines of the iron spectrum in first, second, and third orders were used as standards.

In 1924, McLennan, Young, and McLay[17] published the results of their investigation of the tin spectrum. With the aid of a small Hilger quartz prism spectrograph, they measured 50 lines produced by a tin arc between 1855 A and 2251 A; and they made absorption experiments using tin vapor heated to about 1200 °C and measured 17 absorption lines between 2171 A and 3175 A. In addition, using a vacuum spectrograph with fluorite optics, they investigated the reversal spectrum of tin in a carbon arc in hydrogen and measured 40 such reversals between 1756 A and 1911 A. They were able to arrange most of the lines of the tin arc spectrum into an array as combinations between six levels of low energy and 44 levels of higher energy. The separations of the six low levels were 1692, 1735, 288, 4897, and 8549 cm^{-1}. One of their low levels and the five lowest of the higher levels are not real. Using the series they had established, they found the absolute term value of the lowest level to be 59158 cm^{-1}.

In a publication the following year, Sponer[18] criticized the work of McLennan, Young, and McLay because of intensity fluctuations in their series lines, because of large variations in the constant differences of

the terms, and because many lines appeared at two different places in their table. Sponer removed their non-existent low energy level and replaced the constant differences of 288 cm^{-1} and 4897 cm^{-1} with their sum, giving for the first time the correct five low levels with differences of 1692, 1735, 5185, and 8549 cm^{-1}. In addition, she was the first to give the correct inner quantum numbers (0, 1, 2, 2, and 0, respectively) to these levels. Sponer also rejected the previously mentioned five higher levels, giving an array of combinations between five low levels and 42 higher levels.

Zumstein[19] published a second paper concerning the arc spectrum of tin in 1926. Using a 25-ampere arc, he made new measurements in the region between 1950 A and 2170 A and found 12 new lines. Also, using tin heated to about 1600 °C in a small carbon tube, he measured 53 absorption lines (38 of which were new) between 2000 A and 6000 A. He combined his results with those of other investigators and listed 162 lines between 1756 A and 5632 A. Most of these he was able to classify as combinations between five low energy levels and 49 higher levels.

The following year, Sur[20] attempted to explain the results of Zumstein on the basis of Hund's[21] theory, and correctly identified the five lowest energy levels as $^3P_0$, $^3P_1$, $^3P_2$, $^1D_2$, and $^1S_0$, respectively, and the four next higher levels as $^3P_0$, $^3P_1$, $^3P_2$, and $^1P_1$, respectively.

Back[22] and Green and Loring[23] independently made new Zeeman effect investigations of the tin arc spectrum, the former having studied 33 lines between 2269 A and 5632 A and the latter 26 lines between 2334 A and 5632 A. Their results are in good agreement and definitely established the quantum numbers of the $5s^25p^2$ levels, the $5s^25p6s$ levels, and a few other levels. Also, Green and Loring discovered one $5s^25p6p$ level

with J = 1, the first 6p level to be found. They gave 59690 cm^{-1} as the absolute value of the $5s^2 5p^2\ ^3P_0$ term which corresponds to an ionization potential of 7.37 volts. In addition, from their investigation of the first spark spectrum of tin, they found the separation of the $5s^2 5p\ ^2P^\circ_{\frac{3}{2}}$ and $5s^2 5p\ ^2P^\circ_{\frac{1}{2}}$ levels of Sn II (the limits of all $5s^2 5pnx$ series of Sn I) to be 4252 cm^{-1}.

An important contribution to the arc spectrum of tin was made in 1931 by Randall and Wright[3] who, using an arc of 80 amperes between a carbon rod and a pool of tin, and a grating spectrometer with a thermopile detector, determined the wavelengths of 62 lines (46 of which were new) between 9852 A and 24740 A with an estimated accuracy of ± 2 A. The principal purpose of their investigation was to find the nine undiscovered levels of the $5s^2 5p6p$ configuration; they succeeded in doing this, but two of the levels were later shown to be ficticious. They also found one level of the $5s^2 5p7p$ configuration, four levels of the $5s^2 5p4f$ configuration, and one level of the $5s^2 5p5f$ configuration.

The most extensive investigation of the tin arc spectrum up to the present time was made by Meggers[2] in 1940. His line list includes 377 lines attributed to the tin arc spectrum between 1697 A and 24738 A. Thirty-seven of these are from the infrared measurements of Randall and Wright (with all wavelength values reduced by 1.8 A), while the remaining lines were obtained photographically. In the wavelength region between 2000 A and 12536 A, the light source was an arc in air of six to twelve amperes between a copper rod as upper electrode and a pool of molten tin in a cupped lower copper electrode. The spectrograms were obtained using various stigmatic spectrographs at the National Bureau of Standards. The spark spectrum also was photographed down to 2000 A to

aid in the detection of spark lines which appeared in the arc spectrum. Lines of the iron arc spectrum were used as standards. An arc of one to four amperes between water-cooled electrodes of pure tin, or tin versus copper, in an atmosphere of pure nitrogen, and a normal-incidence vacuum spectrograph of 4.2 A/mm reciprocal dispersion were used by Professor A. G. Shenstone who photographed the region between 1400 A and 2200 A at Princeton University. Of the 377 lines, Meggers was able to classify 294 as combinations between 37 energy levels of even parity and 56 levels of odd parity. His list of levels includes all of those due to the $5s^2 5p^2$, $5s^2 5p6p$, $5s^2 5p7p$, $5s^2 5p6s$, $5s^2 5p7s$, and $5s^2 5p8s$ configurations and all but the $^3F^\circ_4$ levels of the $5s^2 5p5d$ and $5s^2 5p6d$ configurations, in addition to levels of the $5s^2 5p4f$ and $5s^2 5p5f$ configurations and a few from higher $5s^2 5pns$ and $5s^2 5pnd$ configurations. Of special interest are two levels which Meggers believed might belong to the $5s5p^3$ configuration, for this is the first that levels of this configuration had been observed.

Continuing his investigations of absorption spectra in the Schumann region, Garton[24,25] found 45 lines (most of which were new) in the absorption spectrum of tin vapor between 1600 A and 1800 A, in addition to a strong triplet in the 1300-1400 A region which exhibited the ground state splitting. He did not give the wavelengths of the lines he found, but did list three new levels with J = 1 at 75952 (±10), 61766 (±5), and 60401 (±5) cm^{-1}. In his experiments, Garton used metallic tin vaporized in a King furnace at temperatures of 1400-1800 °C and observed the absorption on a hydrogen continuous background with a Hilger medium quartz spectrograph.

In 1958, the third volume of Atomic Energy Levels[1] which contains the levels of Sn I through Sn VI, was published. The level values for

Sn I are based primarily upon the measurements of Meggers[2], the infrared measurements of Randall and Wright[3], and the unpublished vacuum ultraviolet measurements of Shenstone and of Barrow and Rowlinson. The level designations are those given by Meggers and Shenstone, and the absolute value of the $5s^2 5p^2\ ^3P_0$ term, 59231.8 cm^{-1}, and the ionization potential, 7.342 volts, are based chiefly on the series of Barrow and Rowlinson. The tables include 38 energy levels of even parity and 125 levels of odd parity.

EXPERIMENTAL PROCEDURES

Light Sources

For an investigation of the type proposed, the employment of a suitable light source is of great importance. In order to investigate the atomic spectrum of an element, one would like to have a light source that emits a spectrum which contains a maximum number of lines of the element and no lines or bands due to impurities, a spectrum whose lines are sharp and of high intensity. In addition, the light source should be reliable, convenient to operate, and should require little or no attention during long exposures.

The first light source investigated was a conventional arc in air from a copper upper electrode to a pool of molten tin in a lower copper electrode. With the exception of the long wavelength region where longer exposure times were needed, nearly all of the lines reported by Meggers[2] were found to be emitted by the air arc. In addition, some new lines believed to belong to the tin spectrum were found in the region above 5000 A. Before work with the air arc was begun, it was realized that, while this source emitted lines of high intensity, it would not be suitable for extensive investigation due to the breadth of the spectral lines and to the presence of strong bands. One feature not expected was the lack of stability of the arc. Although on two or three occasions the arc did burn steadily for as long as 45 minutes, the usual length of operation was less than five minutes before the arc either ceased or jumped to the copper lower electrode containing the tin. Increasing the

diameter of the lower electrode had little effect on the stability of the arc, but the use of graphite in place of the copper electrodes did noticeably improve the stability as did using higher currents. Both of these changes produce a higher temperature at the electrodes and indicate that the lack of stability is at least partly due to the low vapor pressure of tin; although tin melts at about 232 °C, a temperature of almost 1500 °C must be attained before its vapor pressure reaches one mm Hg.

The second light source to be investigated was the arc in vacuum. Such a source should be more suitable for this investigation because the lines it emits are much sharper than those of the air arc and because the lines and bands due to the presence of air should be absent. However, the source proved to be far from ideal; even though the lines emitted were quite sharp compared to those of the air arc, they were considerably less intense, and the vacuum arc suffered from the same stability problem as did the air arc. In addition, although the pressure in the arc chamber could be maintained sufficiently low to cause the extinction of the discharge in a Geissler tube connected to the chamber, band spectra were still prevalent; in particular, the nitrogen bands appeared stronger at these very low pressures than at higher pressures. An arc in helium was also tried. At low pressures the helium was strongly excited while the tin lines were weak but sharp, while at higher pressures the tin lines became broader and more intense as in the air arc. The arc in helium seemed somewhat more stable than that in vacuum.

While the work with the air arc was being carried on, another member of the spectroscopy group, Mr. Herbert Kleiman, was making a study of the characteristics of electrodeless discharge tubes of the type described by Corliss, Bozman, and Westfall[26]. In the course of his investigation, he

made two tubes containing stannous chloride with neon carrier gases and several tubes containing stannic chloride with helium, neon, argon, and krypton carrier gases. The tubes were excited by the 2450 Mc/sec output of a Raytheon Microtherm microwave generator. Since stannic chloride is a liquid with a rather high vapor pressure at room temperature, the tubes containing this compound had to be cooled considerably in order to obtain a sufficiently low vapor pressure during opeartion. This cooling was provided by immersing the lower end of the tube in liquid nitrogen. The parabolic antenna of the Microtherm was mounted above the tube. The tubes containing stannous chloride, on the other hand, operated very well without heating or cooling when mounted vertically above the Microtherm antenna. Spectrograms taken with these tubes showed that the tin spectrum was strongly excited, being stronger than the air arc in the long wavelength region but somewhat less intense in the ultraviolet. Also, the lines were much sharper than those of the air arc and the source was convenient to use. The principal shortcomings of these tubes were the presence of lines of the chlorine and carrier gas spectra and bands in the 3000 A to 5000 A region. Nevertheless, the electrodeless discharge tubes appeared considerably more promising than did the arc sources and it was decided to make further investigations of this type of source.

The first electrodeless discharge tubes made for this investigation contained only metallic tin and neon in order to eliminate the lines due to chlorine and the bands due to the compound. To make such a tube, a small piece of tin was introduced into a quartz tube blank before the blank was sealed onto a vacuum system. After the tube was evacuated it was heated strongly with an oxygen-gas flame in order to drive off the more volatile impurities and to outgas the quartz blank. The carrier

gas was then admitted to give a reading of a few mm Hg on a McLeod gauge and the tube was sealed off. The tubes containing only metallic tin and a carrier gas never operated satisfactorily. Mercury was present in the earliest tubes and its spectrum was dominant. The addition of a cold trap in the line between the tube and the vacuum system eliminated the mercury, but indium and zinc lines were then found. The indium proved to be an impurity in the tin and, although it was present only in a very small amount, its vapor pressure was sufficiently high compared to that of tin to cause its spectrum to be excited much more readily than that of tin. The zinc was found to be present in the quartz and the high temperatures at which these tubes were operated drove zinc from the quartz in sufficient amounts to produce a relative strong spectrum. Tubes were made containing various carrier gases at various pressures and they were operated at temperatures up to about 1000 °C in a furnace and at higher temperatures when heated with the oxygen-gas flame, but the tin spectrum was never strongly excited because of the low vapor pressure of tin.

In order to obtain a material with a higher vapor pressure, a few tin compounds other than the halides were tried, the only satisfactory one of which was stannous sulfide. Two tubes containing this compound with helium and neon carrier gases operated reasonably well in a furnace at 700-800 °C. The tin spectrum was excited, but the lines were weaker than those emitted by the tin chloride tubes. Lines of the zinc spectrum were present as were lines of the sulfur spectrum, but they were relatively weak. That only the very strongest zinc lines appeared is no doubt due to the lower temperature at which these tubes operated.

A survey of other tin compounds showed that only the halides had the

correct properties for an electrodeless discharge tube that would operate with little or no heating or cooling. For this reason, a return to stannous chloride was made. Tubes containing this compound without a carrier gas had lifetimes of only a few hours, as the compound dissociated with the tin plating on the walls of the tubes and the chlorine gas raising the pressure inside the tubes to the point where they would no longer operate. The presence of a carrier gas retarded this effect so that a few hundred hours of operation could be obtained from each tube. Tubes containing stannous iodide and stannous bromide without carrier gas were also made. Since neither of these compounds was readily available, they had to be produced in the laboratory. This was accomplished, in the case of the iodide, by reacting the tin with iodine under vacuum and then driving the compound into the tube blank. This method proved unsatisfactory because the impurities which were present in the tin were also present in the compound. The stannous chloride, however, was quite pure and it was found that it could be used to produce the iodide and bromide according to the reactions

$$SnCl_2 + 2\ HI \longrightarrow SnI_2 + 2\ HCl$$

and

$$SnCl_2 + 2\ HBr \longrightarrow SnBr_2 + 2\ HCl$$

The hydrogen chloride was driven off by heating, leaving the red-orange crystals of stannous iodide or the pale yellow-green crystals of stannous bromide.

The final arrangement used to make the tin halide electrodeless discharge tubes is shown in Figure 1. Each of the tin halides was contained in a glass tube which could easily be sealed to the tube-making apparatus. After the system was evacuated, the quartz tube blank was surrounded by a furnace at about 1000 °C for an hour. During this time,

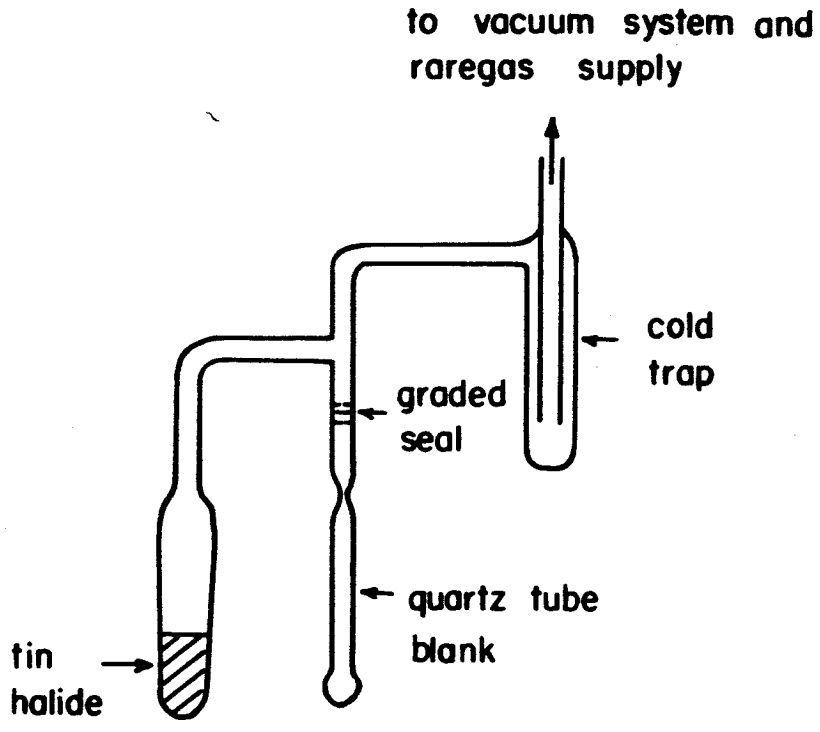

FIGURE 1 ARRANGEMENT USED TO MAKE ELECTRODELESS DISCHARGE TUBES

the tin halide in the side tube was occasionally heated to the boiling point with the hand torch and some of the compound was driven over into the trap. At the end of the outgassing, the trap was cooled with liquid nitrogen and the furnace was removed from the tube blank. When the blank had cooled, the tin halide was heated again and a small amount was driven into the blank. The carrier gas was then added if the tube contained stannous chloride. Next, the tube was sealed off and removed from the system. The tubes made in this way proved to be quite free of impurities.

In order to determine the effect of the diameter of the tubes, tubes with inside diameters of from four to ten millimeters were studied. The tubes with the smallest diameter proved to be the most satisfactory as they were more stable in operation and the spectral lines were more intense since the discharge was confined to a smaller region so that more of the light entered the spectrograph. The tube with the ten millimeter inside diameter radiated heat so rapidly that it would not operate without external heating and then the tin spectrum was weak and the discharge was not stable.

Tubes containing these tin halides were used throughout the rest of the investigation and they proved to be very satisfactory. The iodide tubes operate best when the upper half of the tube is surrounded by a small resistance furnace. Too low a temperature results in the tin spectrum being weak compared to that of the iodine, while a temperature that is too high causes an increase in the intensity of the bands and a decrease in the intensity of the tin spectrum. The stannous bromide and stannous chloride tubes operate satisfactorily without heating or cooling. However, the bromide tends to dissociate, but much more slowly than the

chloride without carrier gas, so that the tin deposit on the inside of the tube soon greatly reduces the light output. It was found that a very gentle draft of air on the back side of the tube causes the tin to condense there, leaving the front of the tube clear. An additional benefit is an increase in the light output due to the reflection from the coating on the back side of the tube. The lines of the tin arc spectrum are of comparable intensity in all three tin halide tubes, but the spark spectrum is the strongest in the chloride tube and weakest in the iodide tube. This greatly simplified the identification of the spark lines.

One type of light source which was not investigated is the hollow cathode. However, others in this laboratory have worked with hollow cathode sources with germanium, silicon, and lead and have found that, although the lines are quite sharp, the intensity is low compared to that of the electrodeless discharge tubes so that long exposure times are necessary to obtain even the strongest lines in the long wavelength region.

Spectrographic and Interferometric Equipment

The Purdue 30-foot concave grating spectrograph[27] was used for much of the work during the early part of this investigation. The grating has a ruled area 5-3/8 inches wide and two inches high with 15,000 rulings per inch and it is in a Paschen-Runge mounting. The reciprocal dispersion of this instrument is about 1.7 A/mm in first order and it has a theoretical resolving power of about 80,000 in this order. The one great advantage of this instrument is its ability to photograph all regions of the spectrum with one exposure, but the astigmatism of the instrument is a serious disadvantage since it permits making only one exposure on a plate and prohibits using a Fabry-Perot interferometer.

The concave grating spectrograph was not available during most of this investigation as it was undergoing extensive modification, including the installation of a new grating.

The exposure times required for the concave grating spectrograph ranged from a few seconds for the strong lines in the lower wavelength region of the tin spectrum to several hours for the lines in the long wavelength region. Exposure times of three to twelve hours were sufficient to obtain all but the weakest lines in the 6000 Å to 12000 Å region.

The optical arrangement used with the concave grating spectrograph is shown in Figure 2. The tin source was focused on the slit by means of a concave mirror. The standard source was either an electrodeless discharge tube containing ferric iodide and krypton or an iron-neon hollow cathode and it was mounted behind a horizontal slit which was positioned so as to produce a virtual image near the position of Sirk's focus[28]. Because of this, the lines of the standard were much shorter than those of the tin source and this permitted easy identification of the respective lines. In order to ascertain whether the different conditions of illumination of the grating produced shifts between the lines of the standard and the tin spectra, an experiment was carried out in which four strong tin lines were measured in different orders, first with the standard imaged on the slit and next with it at Sirk's focus. There was no detectable shift in the wavelengths of the tin lines for the two conditions.

During the early part of this investigation, an electrically operated shutter was designed and installed on the grating side of the slit of the concave grating spectrograph to enable one to focus a light source on the slit when the photographic plates are in position. At the same

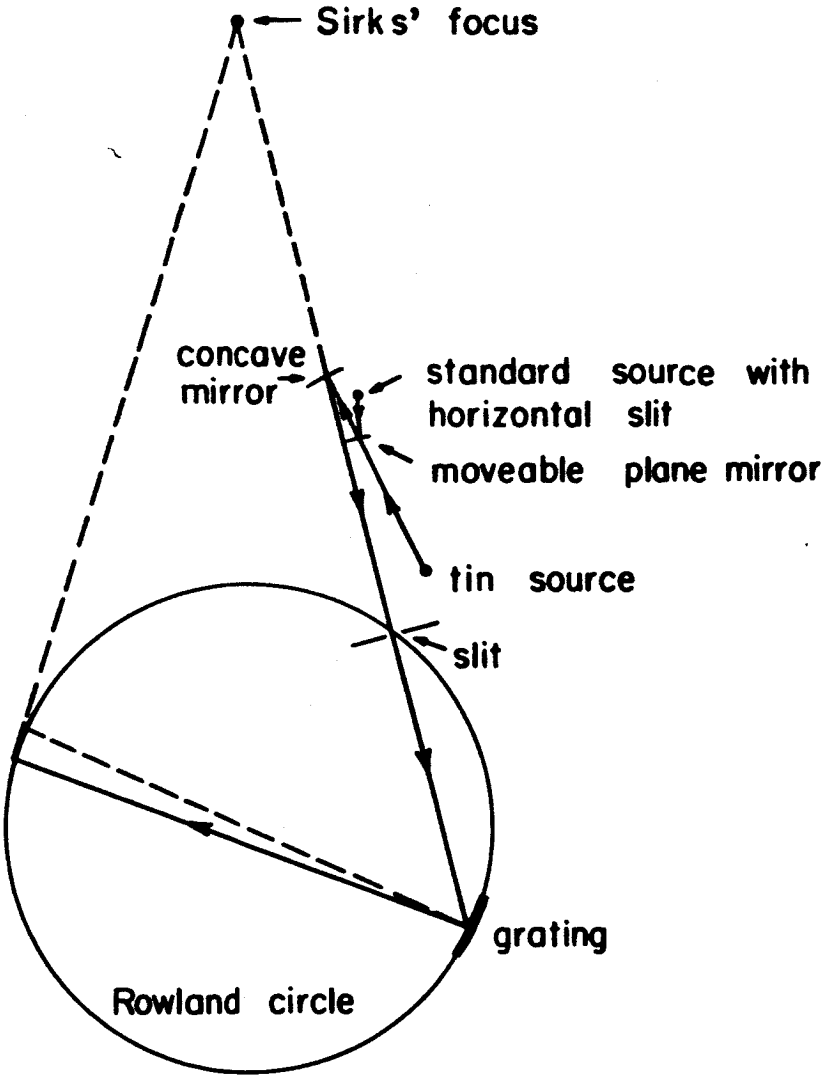

FIGURE 2 OPTICAL ARRANGEMENT FOR THE CONCAVE GRATING SPECTROGRAPH

from 12009 A to 13608 A, even though the stronger lines in this region were obtained when the longer focal length slower lens was used. The shorter focal length lens made it possible to obtain interference patterns for five lines between 12313 A and 12981 A. The instrument is very fast with this lens, but the reciprocal dispersion is about 88 A/mm so that the lines are quite close together.

An exposure time of less than one second with the Steinheil spectrograph was sufficient to cause the strongest lines in the visible region to be overexposed, but exposure times ranging up to 60 hours were used to obtain the weakest lines in the infrared. For the interference patterns, the exposure times varied from less than one second to 60 hours.

A Hilger E-1 quartz prism spectrograph was used to obtain interferograms in the ultraviolet region of the spectrum down to 2064 A. It has a reciprocal dispersion of about 1.5 A/mm at 2100 A and about 10.4 A/mm at 3800 A. Since the interference fringes were in good focus over only one-half of the photographic plate, five plates were necessary to cover the region from 2064 A to 3801 A. The exposure times ranged from one second or less for the strong lines in the region above 2400 A to 20 hours for the weak lines in the lowest wavelength region.

The optical arrangement used with the Steinheil and Hilger spectrographs is shown in Figure 3. Lines of the argon spectrum emitted by an electrodeless discharge tube were used as standards for the grating measurements above 11300 A and lines of the iodine spectrum emitted by the stannous iodide tube were used below this wavelength down to 3575 A. The argon source replaced the tin source when the standard exposure was made and the decker on the slit was positioned so that the argon lines were shorter than the tin lines in order to permit easy identification of the

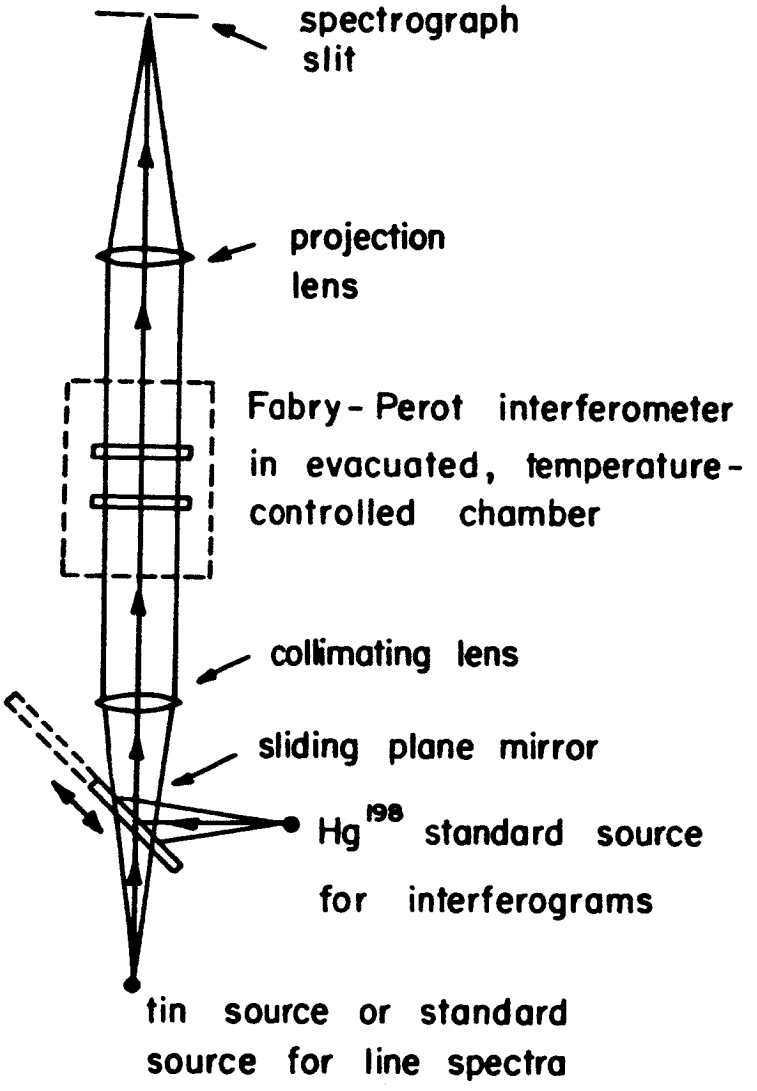

FIGURE 3 OPTICAL ARRANGEMENT USED WITH THE STEINHEIL AND HILGER SPECTROGRAPHS

two spectra. The standard line for all interferometric measurements was the green line emitted by a water-cooled electrodeless discharge tube containing Hg^{198} and argon at a pressure of 3 mm Hg. It was excited by the output of a 250 Mc/sec oscillator. The vacuum wavelength of the green line emitted by this tube, measured with respect to the krypton International standard line by Dr. Victor Kaufman, is 5462.27085 A with an uncertainty believed to be less than $\pm$0.00010 A. Exposures with the mercury source were made immediately before and after each exposure with the tin source in order to detect changes in the temperature or pressure which may have occurred during the tin exposure.

The plates of the Fabry-Perot interferometer used with the Steinheil and Hilger spectrographs were of crystalline quartz of 65 mm diameter cut perpendicular to the optic axis and were aluminized by evaporation in a high vacuum. The spacers which separated the interferometer plates were made of Invar. Spacers of 5- and 18-mm length were used with the Steinheil spectrograph in the 3575 A to 12009 A region and 18- and 30-mm length in the 12009 A to 12981 A region. Spacers of 2-, 5-, and 12-mm length were used in the ultraviolet with the Hilger spectrograph. The interferometer was mounted in an evacuable, double-walled cylindrical chamber which was provided with two plane end windows of crystalline quartz also cut perpendicular to the optic axis. Water at a constant thermostatically controlled temperature of about 23 °C was circulated between the walls of the housing, thus eliminating variations in the interferometer length due to temperature changes. The interferometer chamber was evacuated by means of a Welch diffusion- and fore-pump combination to a pressure of less than 10 μ Hg as indicated by the absence of a discharge in a Geissler tube connected to the chamber. This

arrangement permits the direct determination of vacuum wavelengths.

The interferometer was illuminated by light made parallel by a collimating lens and the interference fringes were focused on the spectrograph slit by a 125 mm focal length glass achromat in the case of the five millimeter spacer with the Steinheil spectrograph and by quartz-fluorite achromats of 350- or 500-mm focal length for the other exposures.

Photographic Details

Eastman Kodak Spectroscopic Plates were used throughout this investigation. The types of plates used in the various wavelength regions are as follows:

Plate Type	Concave Grating	Steinheil	Hilger E-1
103a-O-UV	1942 A to 2450 A		2064 A to 2400 A
103a-O	2450 A to 4800 A	3575 A to 4800 A	
103a-F	4800 A to 7000 A	4800 A to 6900 A	2400 A to 3801 A
I-N	6000 A to 9000 A	6800 A to 9000 A	
I-M	9000 A to 9850 A		
I-[illegible]	9850 A to 10200 A	9000 A to 10200 A	
I-Z	9850 A to 12009 A	10000 A to 13608 A	

The I-N, I-M, I-[illegible], and I-Z plates were hypersensitized prior to use in order to obtain the maximum sensitivity. The hypersensitization of the I-M, I-[illegible], and I-Z plates was produced by bathing the plates for three minutes in a solution of one part 28 per cent ammonia in 20 parts distilled water after which the plates were rinsed in water, bathed for three minutes in ethyl alcohol, and then dried in a stream of warm air produced by a blower and heating coil in an enclosure. The hypersensitization of the I-N plates consisted of pre-fogging by a one-minute exposure to the light of a type NE-51 neon lamp mounted in a Dialco type 952208-931 pilot light assembly located six feet from the plate.

Prior to developing, the 103a-O-UV plates were washed for one minute in ethylene dichloride and allowed to dry. This was necessary in order to remove the ultraviolet sensitizer which otherwise would interfere with the developing of the plate.

All of the plates were developed for five minutes in Kodak D-19 developer, rinsed in water for about 30 seconds, fixed in Kodak Acid Fixer for approximately twice the time required for the plates to clear, and finally rinsed for at least 30 minutes in running water. Following this, the plates were placed in a nearly vertical position and allowed to dry without external heating in order to minimize distortions in the emulsion.

Comparators

The photographic plates were measured with one of two Zeiss-Abbe comparators, one having a travel of 100 mm and the other 200 mm. Settings on sharp lines can be made to an accuracy of about $\pm$0.001 mm with these comparators. The 2-1/2 inch by 18 inch plates taken on the concave grating spectrograph had to be cut into three pieces so that they could be measured with the 200 mm comparator. The 65 mm by 180 mm Steinheil grating spectrograms also were measured with the larger comparator. All plates were measured three times in order to obtain more accurate results.

The interferograms obtained with the Steinheil spectrograph were measured with the smaller comparator. In general, each fringe pattern was measured only once and four or six fringe diameters were measured.

Before the interferograms obtained with the Hilger spectrograph were measured, the larger comparator was modified in order to make possible photoelectric setting[29] on the fringes. The optical arrangement used is shown in Figure 4. The light from a straight-filament lamp mounted

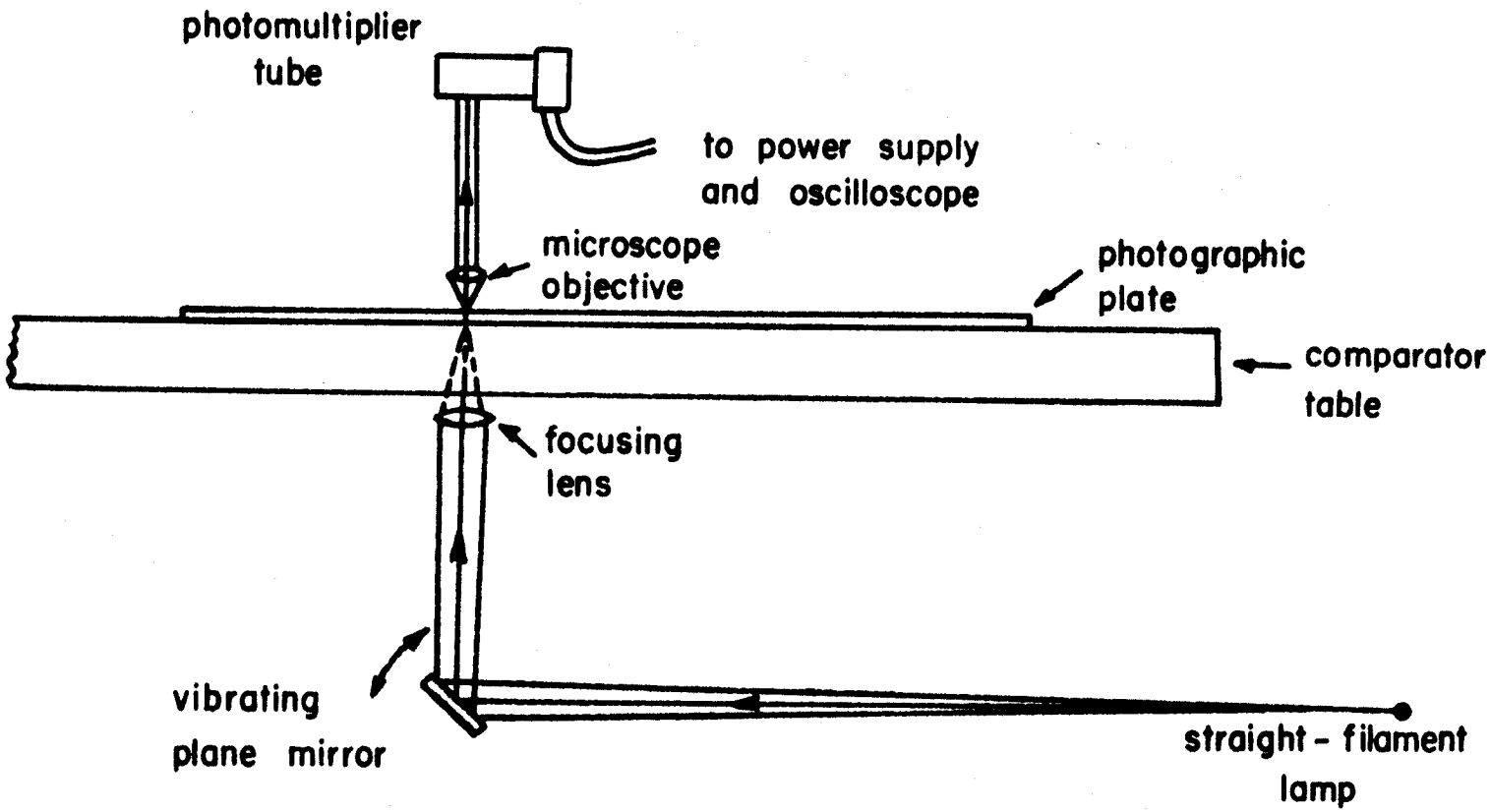

FIGURE 4 OPTICAL ARRANGEMENT OF THE PHOTOELECTRIC COMPARATOR

parallel to the lines on the photographic plate is reflected from a vibrating plane mirror and focused on the plate. The light passing through the plate is picked up by a photomultiplier tube located in place of the eyepiece of the microscope and the electrical output of this tube is connected to the vertical amplifier of a Hewlett-Packard Model 130B oscilloscope. The plane mirror is mounted at a 45 degree angle on a flat spring, one end of which is held rigid while the other end is connected to the driver mechanism of an eight-inch loudspeaker. This loudspeaker is driven by a 60 c/sec voltage so that the image of the straight filament sweeps the plate in each direction 60 times per second. The amplitude of this sweep is determined by the amplitude of the 60 c/sec signal fed to the loudspeaker. With the sweep circuit of the oscilloscope set to operate at 120 c/sec, the pattern displayed by the scope in one period is essentially a plot of the plate darkening versus position along the sweep of the light beam, and the pattern displayed in the next period is the mirror image of the first due to the fact that the light sweep is in the opposite direction while the oscilloscope sweep is in the same direction as in the first period. Thus, if a spectral line or fringe is present in the region swept by the light beam, its profile appears at two positions on the oscilloscope screen and moving the comparator table so as to bring the line to the center of the sweep causes the line profiles on the screen to approach one another. By taking all readings at the positions where the line profiles coincide, very accurate measurements can be made.

The circuit shown in Figure 5, designed by K. L. Andrew, was used to obtain the voltage which drives the mirror and to supply the 120 c/sec synchronizing voltage for the oscilloscope. The resistance-capacitance

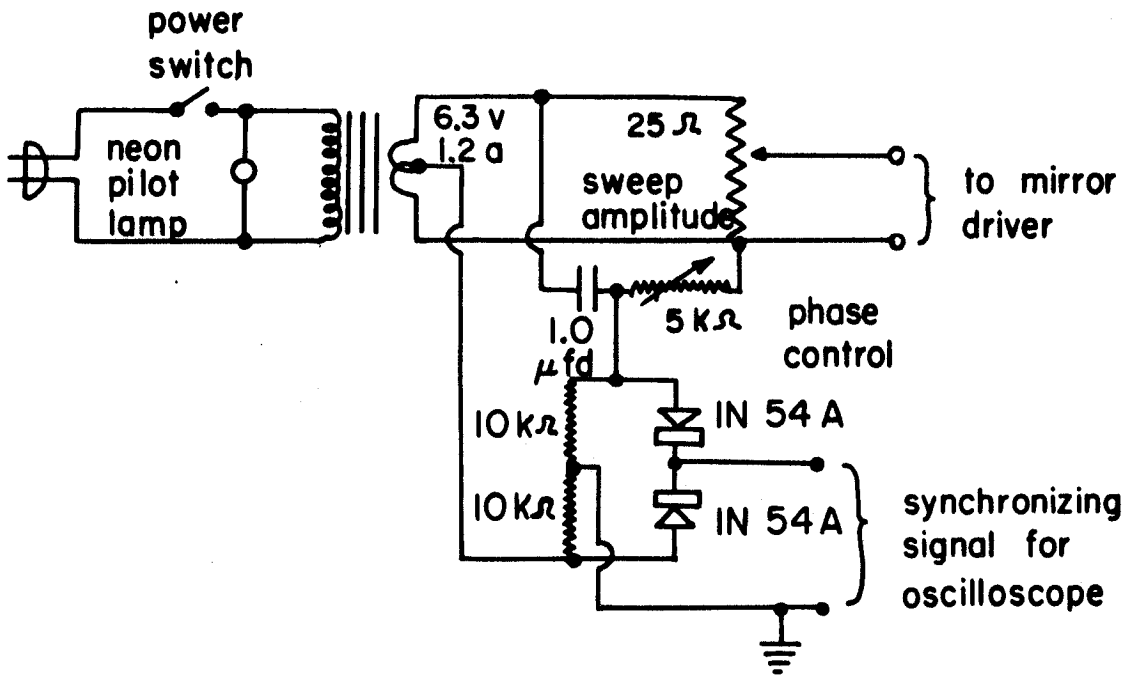

FIGURE 5 CIRCUIT USED WITH THE PHOTOELECTRIC COMPARATOR

network shifts the phase of this latter voltage by approximately 90 degrees in order to make the oscilloscope sweep coincide with that of the light beam. The direct current for the straight-filament lamp was supplied by a transformer-operated full-wave bridge rectifier circuit with more than adequate filtering.

While the photoelectric setting device enables one to make very accurate settings on the lines or fringes, the particular arrangement used here does have some disadvantages. As originally set up, it was very difficult to tell which line was being scanned since the line could be seen readily only be removing the photomultiplier tube from the microscope. A more serious disadvantage was that the intensity of the straight-filament lamp was not sufficient to permit measuring plates having a high background as the output of the photomultiplier was then low compared to the noise level. However, within these limitations, the photoelectric setting arrangement worked very well and it was possible to make settings on sharp fringes consistently to within ± 0.001 mm. This arrangement of the comparator was used to measure all of the Hg^{198} standard plates and all of the ultraviolet plates except for those of the lowest wavelength region which have a high background. It was not used to measure any line spectra, and the tin interferograms taken on the Steinheil spectrograph either had lines too closely spaced or had high backgrounds and could not be measured photoelectrically.

One device not usually considered suitable for wavelength measurements is the Bausch and Lomb eyepiece which consists of a 20-mm scale combined with a lens which gives a magnification of seven. The smallest division of the scale is 0.1 mm, and readings on sharp fringes can be made to ± 0.05 mm or better. This eyepiece was used to measure the

diameters of weak fringe patterns which could not easily be seen through the comparator microscope. Surprisingly enough, in these cases the uncertainties in the resulting wavelengths usually were smaller than when the same fringe patterns were measured with the comparator.

Far Infrared and Vacuum Ultraviolet Regions

Measurements in the far infrared and the vacuum ultraviolet regions of the spectrum are not possible with the equipment presently available in the spectroscopy section of the Physics Department of Purdue University. However, to aid in this work, measurements of the far infrared region of the arc spectrum of tin were very kindly carried out and made available by Dr. C. J. Humphreys of the Naval Ordnance Laboratory at Corona, California. Measurements of the vacuum ultraviolet tin arc spectrum which have been performed by Professor A. G. Shenstone of Princeton University were very graciously made available for this investigation, although they have not yet been published*.

The light sources used by Dr. Humphreys were electrodeless discharge tubes containing a rare gas and stannous chloride, made by the author, or stannous iodide, fabricated at Corona. The spectrometer[31] used to record the spectrum has a 15,000 ruling per inch grating and a lead sulfide detector. The wavelengths of 110 lines between 10946 A and 24712 A were obtained with this equipment.

The light source used by Professor Shenstone was an arc of two to four amperes in an enclosed chamber containing nitrogen at atmospheric pressure. A normal-incidence vacuum spectrograph having a two-meter

---

* Most of the vacuum ultraviolet wavelengths obtained by Professor Shenstone have been given by Kelly in Vacuum Ultraviolet Emission Lines[30].

glass grating with 30,000 rulings per inch and a reciprocal dispersion of about 4.2 A/mm was used to obtain 126 lines between 1600 A and 2000 A.

Reduction of Data

The reduction of the grating measurements was carried out in the conventional manner. The three comparator readings for each line were first averaged. Then two lines of the standard spectrum at or near the ends of the region were used to determine the scale factor

$$\sigma = \frac{\lambda_1 - \lambda_2}{s_1 - s_2} \qquad (1)$$

where s_1 and s_2 are the average comparator readings of the two standard lines and λ_1 and λ_2 are their respective wavelengths. The wavelengths of the other lines on the plate were then calculated from the relation

$$\lambda = \lambda_1 + \sigma(s - s_1) = \lambda_2 - \sigma(s_2 - s) \qquad (2)$$

where s is the average comparator reading of the line in question. In general, the dispersion is not linear, so a correction curve must be drawn. This curve is obtained by plotting the differences between the actual and calculated wavelengths of the standard lines on the plate as a function of the wavelength. It usually has a shape resembling that of a parabola. The corrections for the other lines are taken from the graph and are added to the calculated wavelengths to obtain the correct wavelengths.

In the case of the concave grating measurements, lines of the iron spectrum as emitted by an electrodeless discharge tube or a hollow cathode served as standards. The wavelengths of these iron lines[32,33] are known to better than $\pm$0.001 A, so very smooth correction curves were obtained. However, since the standard lines were in second and third

orders and the tin lines were in first order, an additional small correction to the tin wavelengths was necessary because of the dispersion of air.

A similar procedure was used for the reduction of the Steinheil grating plates above 11300 A where lines of the argon spectrum[34] were used as standards. However, in the region below 11300 A, the lines of the iodine spectrum[35] which were used as standards appeared on only the stannous iodide plates, but since the same camera settings were used for all three tin halide sources, it was possible to adjust the comparator readings for the bromide and chloride plates to those of the iodide plates. Then the comparator readings of all three sources were averaged so that only one wavelength for each line was calculated.

An estimation of the possible error in each wavelength value was made. This estimate was based upon the deviation of the comparator settings on the line, the magnitude of the scatter of the standard lines about the correction curve, and the estimated accuracy of the standard lines.

The least-squares method described by Meissner[36] was used to reduce the interference pattern measurements. Most of the actual calculations were performed by a digital computer, the Univac Solid-State 80 (USS 80). The program for this computer was conceived by Professor K. L. Andrew and is essentially an elaborate and more flexible version of the program he had written for the Burroughs 205 (Datatron) digital computer[37]. The method of reduction is based upon the fundamental relation of Fabry-Perot interferometry

$$\lambda_x(p_x + \epsilon_x) = 2t = \lambda_s(p_s + \epsilon_s) \qquad (3)$$

where λ_x and λ_s are the vacuum wavelengths of the unknown and standard

lines, respectively, $p_x + \epsilon_x$ and $p_s + \epsilon_s$ are their corresponding central order numbers, and t is the spacer length. The program first calculates the diameter and its square for each interference ring, and uses the latter values to compute ΔD^2, the difference of the squares of successive ring diameters. It next calculates D_o^2, the square of the diameter of the innermost fringe, and ϵ for each ring. The final value of ϵ for a given pattern is the average of the values obtained from each ring and the uncertainty, $\Delta\epsilon$, is taken to be 2.5 times the root-mean-square deviation of the individual values of ϵ from the average. The computer uses Edlén's formula[38] to convert the approximate air wavelengths of the tin lines into vacuum wavelengths which are necessary because the interferometer chamber was evacuated. The integral part of the order number is then determined from the value of 2t and this approximate vacuum wavelength. This integral part is combined with the fractional part, ϵ, to compute the final wavelength. The uncertainty, $\Delta\lambda$, is computed from $\Delta\epsilon$. The vacuum wavelength is converted to an air wavelength and the latter, along with its uncertainty, is punched on an IBM card in addition to being printed.

Since the optics used to obtain the interferograms are less than perfect, the quantity $\Delta D^2/\lambda$ is not quite constant. In order to obtain better values of ΔD^2, the values of $\Delta D^2/\lambda$ for all the patterns on the plate are fitted by a weighted least-squares method to the curve

$$\frac{\Delta D^2}{\lambda} = A + B\lambda + C\lambda^2 \qquad (4)$$

where A, B, and C are constants determined by the computer. This relation is then used to compute an adjusted value of ΔD^2 for each fringe pattern with the result that adjusted values of λ and $\Delta\lambda$ are obtained.

In the case of the standard lines, the same procedure is used to determine ϵ and $\Delta\epsilon$. The integral order number is determined from the vacuum wavelength and the approximate value of 2t. Then the "exact" 2t and its uncertainty are calculated. The value of 2t which was used to determine the tin wavelengths is the average of the values obtained with the standard exposures taken before and after the tin exposure.

In order to make the greatest possible use of the computing facilities, additional programs for the USS 80 were written by the author. The first of these was an average program. Its primary purpose is to average wavelengths or wave numbers according to the relation

$$\bar{x} = \frac{\sum_{i=1}^{n} w_i x_i}{\sum_{i=1}^{n} w_i} \tag{5}$$

where n is the number of values averaged and w_i is the weight assigned to the value x_i and is equal to $(\Delta x_i)^{-p}$, where Δx_i is the extimated uncertainty associated with the value x_i and p has a value of zero or two depending on whether a linear or a weighted average is desired. The uncertainty in the average value is determined from the equation

$$\Delta\bar{x} = \sqrt{n^q \sum_{i=1}^{n} \left(\frac{w_i \Delta' x_i}{\sum_{i=1}^{n} w_i} \right)^2 + \left(\bar{x} \cdot \frac{\Delta 2t}{2t} \right)^2} \tag{6}$$

where q is an integer equal to zero or one, and

$$\Delta' x_i = \sqrt{(\Delta x_i)^2 + (x_i - \bar{x})^2} \tag{7}$$

The second term under the radical in the expression for $\Delta\bar{x}$ takes into account the uncertainty of 2t and is included only in the final average for a given interferometrically measured line on a given plate. The factor n^q is included to avoid obtaining uncertainties that are too small

if non-independent values are averaged as, for example, in the average of the adjusted and unadjusted wavelengths determined from a single set of measurements.

The average program was used to calculate the weighted average of the wavelengths obtained with different sources with the concave grating spectrograph. These average values, in turn, were averaged with the Steinheil grating wavelengths to yield the final grating wavelengths for the lines. These are the values which appear in the table in the next chapter. The average program also was used to average the adjusted and unadjusted wavelength values determined by the Fabry-Perot program. The adjusted values were given twice the weight of the unadjusted values.

Another program was written to calculate the correction due to phase-change effects. This correction is necessary since the change of phase of the light waves upon reflection at the surfaces of the interferometer plates usually is not such that equation (3) is valid. In general,

$$\lambda_s(p_s + \epsilon_s) = 2t_o - 2\frac{\beta_s\lambda_s}{2\pi}$$

$$= 2t_o - 2\frac{(\delta_s + n_s\pi)\lambda_s}{2\pi} \qquad (8)$$

where t_o is the physical separation of the reflecting surfaces of the interferometer plates, β_s is the change of phase of the light of wavelength λ_s upon reflection, and $\delta_s = \beta_s - n_s\pi$, where n_s is an integer. Equation (8) can be written

$$\lambda_s(p_s + n_s + \epsilon_s) = 2t_o - \frac{\delta_s\lambda_s}{\pi} = 2t \qquad (9)$$

where 2t is the value normally calculated from equation (3). This is

because the integer $p_s + n_s$ is really the value calculated from the standard wavelength and the approximate value of 2t; the actual values of p_s and n_s cannot be determined.

Proceeding in a similar manner, for the unknown wavelength we have

$$\lambda_x(p_x + n_x + \epsilon_x) = 2t_o - \frac{\delta_x\lambda_x}{\pi}$$

$$= 2t - \frac{\delta_x\lambda_x}{\pi} + \frac{\delta_s\lambda_s}{\pi}$$

$$= 2t - 2\delta t \qquad (10)$$

In order that there be no correction, we must have $\delta t = 0$ which means that

$$\delta_x\lambda_x = \delta_s\lambda_x \qquad (11)$$

so that either $\lambda_x = \lambda_s$ or $\delta = \alpha\lambda^{-1}$, where α is a constant.

Therefore, in general the effective value of 2t for $\lambda_x \neq \lambda_s$ will differ from the calculated value by an amount $2\delta t$ which, as will be shown, can be calculated if two or more different spacers are used. (Since the phase change is a strong function of the properties of the reflecting film, the same pair of interferometer plates must be used with all spacers.)

The actual calculations for the phase-change corrections were carried out in terms of wave numbers rather than wavelengths because the corrections are then much more nearly constant. The conversion from air wavelength to vacuum wave number was performed by a separate program which used Edlén's formula[38]. (This program will be referred to as the $\lambda\lambda\nu$ program since it is capable of converting an air wavelength, a vacuum wavelength, or a vacuum wave number into the corresponding air wavelength, vacuum wavelength, and vacuum wave number.)

Because of the phase-change effects, if we use two different spacers we will obtain two slightly different wave numbers for the same line,

$$\nu_1 = \frac{P_1}{2t_1} \quad \text{and} \quad \nu_2 = \frac{P_2}{2t_2} \tag{12}$$

where $P_1 = p_1 + n_1 + \epsilon_1$, $P_2 = p_2 + n_2 + \epsilon_2$, and $2t_1$ and $2t_2$ are the values determined from the standard wavelength. The subscripts refer to the different spacers. The true wave number of the line is

$$\nu = \frac{P_1}{2t_1 - 2\delta t} = \frac{P_2}{2t_2 - 2\delta t} \tag{13}$$

from which

$$2\delta t = \frac{P_1 \cdot 2t_2 - P_2 \cdot 2t_1}{P_1 - P_2} \tag{14}$$

If we write

$$\nu = \nu_1 + \delta\nu_1 = \nu_2 + \delta\nu_2 \tag{15}$$

then

$$\delta\nu_1 = \nu - \nu_1 = \frac{P_1}{2t_1 - 2\delta t} - \frac{P_1}{2t_1} \tag{16}$$

so that

$$\delta\nu_1 = \frac{P_1 \cdot 2\delta t}{2t_1(2t_1 - 2\delta t)} \tag{17}$$

Substituting in from the expression for $2\delta t$, we obtain

$$\delta\nu_1 = \frac{(\nu_2 - \nu_1)2t_2}{2t_2 - 2t_1} \tag{18}$$

And, in a similar manner,

$$\delta\nu_2 = \frac{(\nu_2 - \nu_1)2t_1}{2t_2 - 2t_1} \tag{19}$$

Then we can write

$$\delta\nu_1 \cdot 2t_1 = \delta\nu_2 \cdot 2t_2 = \frac{(\nu_2 - \nu_1)2t_1 \cdot 2t_2}{2t_2 - 2t_1} = K \qquad (20)$$

where K is a function of the wave number only. Thus, once the value of K is known, the corrections to the wave numbers are easily calculated from

$$\delta\nu_i = \frac{K}{2t_i} \qquad (21)$$

From this equation it can easily be seen that K is equivalent to the change in the order number required to produce $\delta\nu$. The computer made use of equation (20) in order to compute a value of K for each pair of spacers; thus, if a given line was measured with one spacer, no value of K could be calculated, one value was calculated for two spacers, three values for three spacers, and so forth. The program also computed the uncertainty for each value of K from the relation

$$\Delta K = \frac{2t_1 \cdot 2t_2}{2t_2 - 2t_1} \sqrt{(\Delta\nu_1)^2 + (\Delta\nu_2)^2} \qquad (22)$$

where $\Delta\nu_1$ and $\Delta\nu_2$ are the uncertainties in the values of ν_1 and ν_2, respectively. A modification of the average program was included in the phase-change program and was used to average the different values of K for each wave number. The lines of each light source were dealt with separately in order to avoid the effects due to any wave number shifts between sources. Therefore, a total of 808 values for K were obtained in the wave number region from 7701 cm^{-1} to 48327 cm^{-1}. The uncertainties were rather large, usually larger than the value of K. In order to draw a graph of K versus ν, the values of K were averaged over regions of 500 cm^{-1} so that the number of points was reduced by a factor of ten and the scatter of the points was considerably reduced. The resulting

plot is shown in Figure 6. In most of the region above 14000 cm^{-1}, the uncertainties are greater than K so that the exact shape of the curve is in doubt. In particular, the peak in the curve at 27000 cm^{-1} may not be real since there are few lines in this region of the spectrum with the result that the uncertainties are particularly large.

The values of K for each observed wave number were read from the curve. A final version of the average program used these values together with the uncorrected wave numbers to compute the final corrected wave number with uncertainty for each line of each light source.

The average grating wavelengths were converted into wave numbers by means of the λλν program and then were averaged with the interferometric values obtained for the stannous bromide source to yield the final wave number values for the lines measured by the author. The bromide source was used in this case because its lines were sharper than those of either the iodide or chloride sources. The final line list was completed when the lines measured by Humphreys, Meggers, and Shenstone were included. Again the λλν program was used to calculate the vacuum wave numbers.

The final program written for the USS 80 was to calculate improved values of the energy levels. However, this computer was replaced by an IBM 7090 digital computer before the level list was completed so that the results obtained were incomplete. Mr. Leon Radziemski wrote a similar but more sophisticated and more versatile version of the level calculation program for the 7090 based upon the author's iterative method of computation used in the USS 80 program. Approximate values of the even and odd energy levels and the observed wave numbers comprise the input data. Since each line represents the difference between one even and one odd level, it is obvious that the value of one level can be

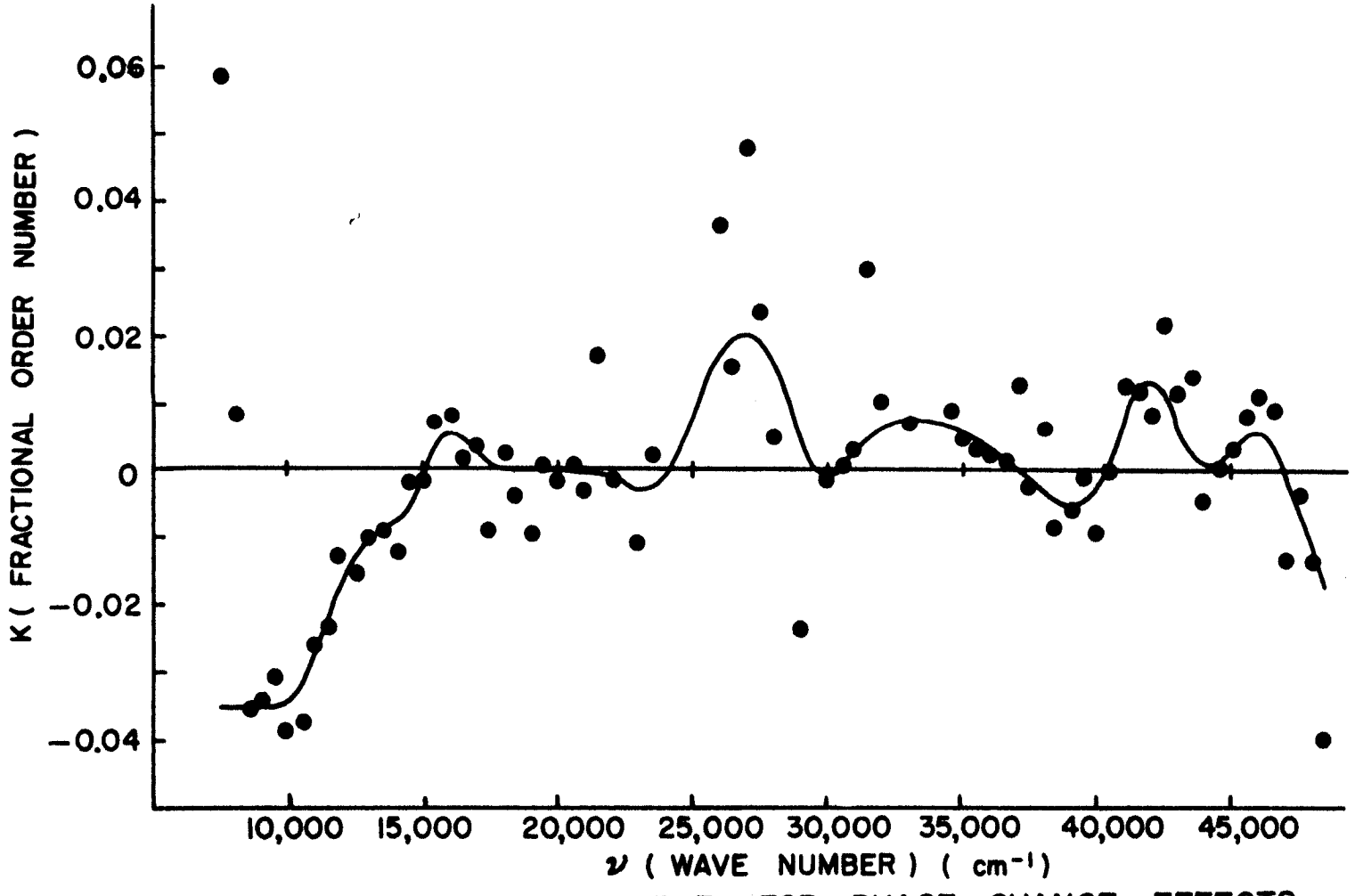

FIGURE 6 CORRECTION CURVE FOR PHASE-CHANGE EFFECTS

computed from the observed wave number and the other level. Thus, since there are eleven observed combinations between the first odd level and the even levels in the case of the arc spectrum of tin, eleven values can be computed for the first odd level. These are averaged to yield a new value for this level, and the uncertainty also is computed. The value of the second odd level is computed in the same way and the process is repeated until the values of all the odd levels have been determined with respect to the input values of the even levels. The same procedure is next used to calculate the even level values with respect to the improved set of odd level values just obtained. This iterative process is repeated until the difference between two successive sets of values for the levels is much less than the corresponding set of uncertainties. This condition is normally achieved in a few iterations depending on the accuracy of the input level values. The level values appearing in the next chapter were computed by the 7090 in the manner just described.

EXPERIMENTAL RESULTS

Observed Lines

The tin lines observed in this investigation are listed in Tables 1 and 2. The first table includes 591 lines which could be identified with no other element nor with the spark spectrum of tin. Lines which were obtained with only one light source are not included in the table. Of the lines listed in Table 1, 110 in the infrared were measured by Dr. C. J. Humphreys of the Naval Ordnance Laboratory at Corona, California, 126 in the vacuum ultraviolet were measured by Professor A. G. Shenstone of Princeton University, and 18 are lines measured by Meggers[2]. These lines are designated by the letters H, S, and M, respectively, in the uncertainty columns of the table. The line at 8007 A is the only line observed by Meggers but not found in this investigation which could be classified and it was included in the line list for this reason. The other lines of Meggers which appear in the table fill the gap between the region investigated by the author and the vacuum ultraviolet. Of the 376 lines measured by the author, 141 are new, 146 are newly classified, five have been re-classified, and only 30 are unclassified.

The first column of Table 1 gives the intensities of the lines. The values listed for the lines of Humphreys and Shenstone are the values assigned by them. For the lines above 3000 A measured by the author, the intensity figures are visual estimates of the darkening of the photographic plates. Due to the different sensitivities of the plates and the different exposure times, these numbers cannot be directly related to the

absolute intensities of the lines. The intensities of the lines between 2000 A and 3000 A were determined from microphotometer tracings of the photographic plates and the figures thus obtained were adjusted to give values which correspond to those determined visually.

The second and third columns of the table contain the wavelengths and their estimated uncertainties determined from the grating measurements. For the lines measured by the author, the wavelength values are the weighted averages of the results obtained with the concave grating spectrograph and the Steinheil spectrograph. Only the values obtained with the electrodeless discharge tubes are included in order to avoid shifts due to different types of excitation.

The fourth and fifth columns of the table give the wavelengths and their estimated uncertainties as determined from the interferometric measurements. Although interferometric measurements over the entire wavelength region were made for all three tin halide sources, the values given in the table are those obtained from the bromide tube, with the exception of a few lines which were not measureable with this source in which case, as indicated in the table, the value obtained with the iodide tube appears. The lines emitted by the bromide tube are the sharpest and are believed to be the least perturbed because the tube operates at a lower temperature than the iodide tube and the pressure in the tube is much lower than that in the chloride tube. The agreement between the wavelengths determined with the iodide and bromide tubes is excellent in most cases, but some wavelengths from the chloride tube show deviations larger than expected. Further investigation is needed in order to determine whether these shifts are real or whether they are due to measuring errors caused by the poor fringes of this source.

The sixth and seventh columns of the table give the wave numbers and their estimated uncertainties. In the case of the author's measurements, the wave numbers were computed as previously described and are the weighted averages of the grating and interferometric values.

The eighth column gives the level combinations of the lines which are classified. The levels are identified by numbers and are listed in Tables 3 and 4. The superscript ° identifies a level of odd parity.

The final column of Table 1 gives the differences between the observed and the calculated wave numbers. In general, the magnitude of the differences gives an indication of the accuracy of the measurements. However, in the case of the measurements of Shenstone and Meggers, large differences frequently indicate a shift in the value of the odd levels due to the use of different types of light sources; they used arcs at atmospheric pressure while electrodeless discharge tubes operating at comparatively low pressures were used by Humphreys and the author. The largest shift found is 2.6 cm^{-1} which occurred in the case of level 43°. In general, where a shift is observed, the value of the level determined from the arc measurements is the lower.

Lines of the spark spectrum of tin also were present on the plates which were measured. The lines which can be classified as belonging to the first spark spectrum appear in Table 2. In this case, the interferometric values are from the stannous chloride source since, as was previously noted, the spark lines were strongest in this source and not all of the lines appeared with the other sources. The levels referred to in the eighth column of the table are listed in Tables 5 and 6.

Table 1. Observed Lines of Sn I

Intensity	Air Wavelength (A) and Uncertainty Grating λ	Δλ	Interferometer λ	Δλ	Vacuum Wave Number (cm^{-1}) and Uncertainty ν	Δν	Combination	$\nu_o - \nu_c$ (cm^{-1})
5[a]	24712.70	H			4045.40	H	14 - 7°	-0.02
40	24638.08	H			4057.65	H	11°- 8	+0.09
50	24314.54	H			4111.64	H	7 - 4°	+0.06
20	23656.0	H			4226.10	H	24°-14	+0.02
10	22683.54	H			4407.28	H	20°-10	-0.14
200	22500.69	H			4443.10	H	14°- 9	+0.02
30	22181.20	H			4507.09	H	14 - 6°	+0.04
80	22131.65	H			4517.18	H	25°-14	+0.14
50	22107.51	H			4522.12	H	9 - 4°	+0.08
5[a]	22077.74	H			4528.21	H		
100	21685.93	H			4610.03	H	24°-13	-0.01
10[a]	21518.06	H			4645.99	H	47 -23°	+0.13
25	21091.99	H			4739.84	H	7 - 3°	+0.08
500	20862.18	H			4792.05	H	14°- 8	+0.03
25	20848.89	H			4795.11	H	51 -23°	+0.13
10	20821.97	H			4801.31	H	8 - 3°	+0.05
40	20812.50	H			4803.49	H	10°- 6	+0.03
200	20622.72	H			4847.70	H	13°- 7	-0.02
150	20597.99	H			4853.52	H	14°- 7	-0.01
15	19590.47	H			5103.13	H	20 -10°	-0.01
10	19382.38	H			5157.92	H	53 -22°	-0.16
100	19298.72	H			5180.28	H	24°-12	-0.38
150	19215.10	H			5202.82	H	16°- 9	-0.03
100	19082.58	H			5238.95	H	15°- 8	-0.32
150	18860.77	H			5300.56	H	15°- 7	-0.21
200	18482.28	H			5409.13	H	24°-11	+0.08
10	18271.57	H			5471.49	H	25°-12	-0.12

Table 1. Observed Lines of Sn I (Continued)

Intensity	Air Wavelength (A) and Uncertainty Grating λ	Δλ	Interferometer λ	Δλ	Vacuum wave Number (cm^{-1}) and Uncertainty ν	Δν	Combination	$\nu_o - \nu_c$ (cm^{-1})
100	17809.81	H			5613.35	H	16°- 7	+0.05
100	17735.73	H			5636.80	H	30°-14	-0.02
20	17200.34	H			5812.25	H	24°-10	-0.11
10	17160.20	H			5825.85	H	29°-13	-0.12
300	17019.18	H			5874.12	H	13°- 6	-0.02
400	17002.43	H			5879.91	H	14°- 6	-0.04
300	16380.00	H			6103.34	H	25°-10	+0.02
30	15971.95	H			6259.27	H		
20	15800.69	H			6327.11	H	15°- 6	-0.08
200	15752.76	H			6346.36	H	19°- 9	-0.53
75	15630.51	H			6396.00	H	29°-12	-0.59
80	15579.90	H			6416.77	H	27°-10	-0.66
1000	15466.80	H			6463.70	H	18°- 8 32°-14	+0.01 -0.34
5	15375.36	H			6502.14	H	46 -18°	+0.07
40	15364.02	H			6506.94	H	47 -18° 53 -19°	+0.23 +0.11
100	15167.13	H			6591.40	H	30°-12	+0.02
100	15159.04	H			6594.92	H	18 - 9° 49 -18°	-0.06 +0.42
300	15056.65	H			6639.77	H	16°- 6	+0.05
150	15020.18	H			6655.89	H	28 -12° 51 -18°	+0.29 +0.07
200	14794.80	H			6757.28	H	19°- 7	-0.05
100	14659.34	H			6819.73	H	30°-11	-0.05
10	14559.97	H			6866.27	H	19 - 8°	-0.39
5	14473.46	H			6907.31	H	33°-13	-0.16
10	14379.59	H			6952.40	H		
30	14345.95	H			6968.70	H	17 - 7°	+0.01
20	14303.61	H			6989.33	H	28°-10	+0.07
15	14224.34	H			7028.28	H	29°-10	-0.01
15	14214.22	H			7033.29	H	33 -12°	+0.08

Table 1. Observed Lines of Sn I (Continued)

Intensity	Air Wavelength (Å) and Uncertainty Grating λ	Δλ	Interferometer λ	Δλ	Vacuum Wave Number (cm^{-1}) and Uncertainty ν	Δν	Combination	$\nu_o - \nu_c$ (cm^{-1})
70	14133.52	H			7073.44	H	16 - 6°	-0.03
40	14067.82	H			7106.48	H	38°-14	+0.02
20	13994.74	H			7143.59	H	52 -17°	-0.03
10[a]	13756.52	H			7267.29	H	35°-13	-0.06
0	13608.3	.7			7346.5	.4	10 - 4°	0.0
3000	13607.95	H			7346.64	H		+0.17
100[a]	13475.87	H			7418.64	H	32°-12	+0.03
2	13459.23	.13			7427.81	.07	6 - 2°	-0.12
6000	13458.47	H			7428.23	H		+0.30
45	13346.91	H			7490.32	H	38°-13	-0.09
50	13318.31	H			7506.41	H	49 -16°	+0.01
50	13187.26	H			7581.00	H	20°- 8	+0.20
1	13081.48	.24			7642.30	.14	20°- 7	0.00
1500	13080.53	H			7642.86	H		+0.56
50	13072.22	H			7647.72	H		
80	13029.27	H			7672.93	H	20 - 9°	+0.11
3	13020.21	.22			7678.27	.13	21 - 9°	0.00[b]
2000	13019.62	H			7678.62	H		+0.35
100	13004.08	H			7687.79	H	22 - 9°	+0.21
300	12990.26	H			7695.97	H	22°- 9	+0.34
5	12981.00	.07	12981.009	.009	7701.455	.006	6 - 1°	-0.003
2500	12980.58	H			7701.71	H		+0.25
00	12934.1	.6			7729.4	.3	21°- 8	-1.0
200	12932.56	H			7730.31	H		-0.08
2	12888.67	.12			7756.63	.07	23 - 8°	-0.06
1000	12888.57	H			7756.69	H		0.00
0	12845.1	.8			7782.9	.5	19°- 6	-0.8
200	12843.74	H			7783.77	H		+0.01
20	12830.23	H			7791.96	H	21°- 7	+0.08
000	12811.0	1.5			7803.7	.9		
80	12789.22	H			7816.95	H	48 -15°	-0.01
000	12788.3	.9			7817.5	.5		+0.6
20	12682.89	H			7882.48	H	41°-13	-0.05
							41 -14°	+0.23

Table 1. Observed Lines of Sn I (Continued)

Intensity	Air Wavelength (Å) and Uncertainty Grating λ	Δλ	Interferometer λ	Δλ	Vacuum wave Number (cm^{-1}) and Uncertainty ν	Δν	Combination	$\nu_o - \nu_c$ (cm^{-1})
30	12553.86	H			7963.50	H	53 -15°	+0.11
4	12536.39	.07	12536.310	.013	7974.646	.009	10 - 3°	(+0.004
1000	12535.99	H			7974.85	H		+0.21
5	12530.79	.05	12530.778	.005	7978.168	.003	12 - 4°	(0.000
1000	12530.55	H			7978.31	H		+0.14
40	12427.25	H			8044.63	H	22°- 8	(+0.05
00	12425.7	1.0			8045.6	.6		+1.0
500	12335.68	H			8104.35	H	20 - 7°	(-0.11
4	12335.56	.05	12335.524	.007	8104.450	.005		-0.003
50	12327.83	H			8109.51	H	33°-10	(-0.28
3	12327.62	.18			8109.65	.12		-0.15
1500	12313.15	H			8119.18	H	22 - 7°	(-0.04
6	12313.11	.05	12313.084	.006	8119.221	.004		0.000
3	12054.68	.15			8293.26	.11	47 -12°	(0.00
25	12054.66	H			8293.28	H		+0.01
1500	12009.52	H			8324.45	H	23°- 8	(-0.09
8	12009.381	.024	12009.397	.007	8324.535	.004		-0.001
16	11932.816	.017	11932.821	.012	8377.956	.007	11 - 3°	(+0.002
4000	11932.80	H			8377.97	H		+0.02
200	11854.12	H			8433.58	H	50 -12°	(-0.21
8	11853.814	.022	11853.839	.014	8433.782	.010		0.000[b]
300	11848.26	H			8437.75	H	39°-11	(-0.03
8	11848.182	.023	11848.219	.009	8437.781	.007		0.000[b]
2500	11825.22	H			8454.19	H	7 - 2°	(-0.16
14	11824.986	.016	11824.994	.008	8454.351	.005		-0.001
3	11753.41	.10			8505.84	.07	42°-12	-0.10
12000	11740.11	H			8515.48	H	8 - 2°	(-0.38
22	11739.600	.015	11739.591	.007	8515.852	.005		-0.001
500	11694.43	H			8548.74	H	13 - 4°	(-0.05
9	11694.346	.020	11694.360	.007	8548.791	.006		+0.004
12	11670.739	.017	11670.746	.005	8566.088	.004	20 - 6°	(+0.003
1000	11670.74	H			8566.09	H		+0.01
3	11665.17	.13			8570.18	.10	43°-12	+0.04
200	11651.92	H			8579.93	H	22 - 6°	(-0.92
9	11650.641	.021	11650.669	.011	8580.854	.009		+0.001

Table 1. Observed Lines of Sn I (Continued)

Intensity	Air Wavelength (A) and Uncertainty Grating λ	Δλ	Interferometer λ	Δλ	Vacuum Wave Number (cm^{-1}) and Uncertainty ν	Δν	Conbination	$\nu_o - \nu_c$ (cm^{-1})
100	11648.29	H			8582.60	H		
8	11648.209	.025	11648.239	.014	8582.644	.011	23 - 6°	(−0.03 +0.008
20	11616.148	.015	11616.152	.005	8606.347	.004		
4000	11615.91	H			8606.53	H	12 - 3°	(+0.001 +0.18
80	11532.88	H			8668.49	H		
8	11532.576	.019	11532.580	.012	8668.714	.007	20° - 6	(−0.23 −0.007
50	11500.78	H			8692.68	H		
7	11500.737	.023	11500.701	.013	8692.736	.011	38° -10	(−0.05 +0.001
8000	11454.50	H			8727.80	H		
24	11454.409	.015	11454.407	.005	8727.875	.003	7 - 1°	(−0.07 −0.001
4	11445.93	.09			8734.34	.07	42° -11	0.00
-[c]	11439.22	H			8739.46	H		
20	11336.944	.016	11336.945	.004	8818.304	.003		
1500	11336.76	H			8818.45	H	21° - 6	(+0.001 +0.14
3	11323.22	.08			8829.00	.06		
6000	11277.65	H			8864.67	H		
24	11277.468	.015	11277.483	.005	8864.801	.004	9 - 2°	(−0.13 −0.002
6	11222.548	.021	11222.552	.005	8908.190	.004		
20	11222.28	H			8908.41	H	46 -11°	(0.000 +0.22
150	11216.72	H			8912.82	H		
10	11216.698	.016	11216.703	.008	8912.836	.006	47 -11°	(−0.01 +0.002
5000	11191.81	H			8932.66	H		
26	11191.695	.025	11191.710	.005	8932.739	.004	14 - 4°	(−0.08 +0.001
2	11151.15	.13			8965.23	.10	63 -19°	0.00[b]
4	11125.85	H			8985.62	H		
6	11125.67	.06	11125.700	.018	8985.739	.014	24° - 8	(−0.13 −0.003
3	11120.68	.10			8989.79	.08	44 -10°	−0.11
8	11109.73	.06	11109.711	.008	8998.669	.006		
27	11109.65	H			8998.72	H	48 -11°	(0.000 +0.05
4	11107.29	.07			9000.63	.06	49 -11°	0.00
4	11085.43	.08			9018.38	.07	40° -10	0.00[b]
3	11050.10	.07			9047.21	.06	24° - 7	−0.03
20	11032.44	H			9061.70	H		
8	11032.14	.06	11032.129	.004	9061.951	.003	51 -11°	(−0.25 +0.001
5	11031.06	.06			9062.83	.05	46° -12	+0.05

Table 1. Observed Lines of Sn I (Continued)

Intensity	Air Wavelength (A) and Uncertainty Grating λ	Δλ	Interferometer λ	Δλ	Vacuum Wave Number (cm^{-1}) and Uncertainty ν	Δν	Combination	$\nu_o-\nu_c$ (cm^{-1})
4	10993.48	.10			9093.81	.08	58°-14	-0.05
60	10946.93	H			9132.48	H		
12	10946.893	.022	10946.912	.006	9132.496	.004	22°- 6	(-0.02 -0.006
5	10931.75	.07			9145.16	.06	53 -11°	+0.06
38	10893.861	.016	10893.868	.005	9176.963	.004	13 - 3°	-0.002
10	10817.34	.04	10817.366	.003	9241.863	.002	27°- 9	-0.004
20	10807.609	.016	10807.612	.005	9250.204	.004	46 -10°	+0.001
13	10776.76	.03	10776.756	.006	9276.689	.005	25°- 8	-0.008
2	10760.02	.19			9291.12	.17	46°-11	-0.06
3	10737.18	.08			9310.88	.07	49°-12	-0.03
3	10734.07	.14			9313.58	.12		
6	10705.73	.06	10705.778	.007	9338.193	.006	25°- 7	-0.005
6	10702.91	.06	10702.922	.005	9340.684	.004	48 -10°	+0.002
9	10700.669	.018	10700.679	.007	9342.643	.006	49 -10°	0.000
6	10698.78	.06	10698.743	.005	9344.332	.005	56°-13	-0.004
3	10597.44	.09			9433.66	.08		
4	10539.94	.11			9485.12	.10	52 -10°	+0.06
4	10537.82	.07			9487.03	.06	53 -10°	-0.08
11	10467.077	.015	10467.100	.007	9551.132	.008	26°- 7	-0.002
36	10456.377	.014	10456.386	.006	9560.915	.005	14 - 3°	0.000
12	10423.776	.014	10423.787	.004	9590.815	.004	27°- 8	-0.001
3	10404.97	.07			9608.16	.07		
3	10382.43	.10			9629.02	.09		
4	10371.73	.08			9638.95	.08	45°-10	+0.09
10	10357.371	.019	10357.366	.009	9652.318	.008	27°- 7	0.000
7	10350.96	.06	10350.944	.013	9658.307	.012	26 - 9°	-0.005
4	10222.73	.06			9779.44	.05	27 - 8°	-0.04
2	10200.01	.11			9801.23	.11		
10	10187.03	.05	10187.056	.005	9813.689	.005	28°- 9	0.000
6	10083.08	.04	10083.005	.007	9914.959	.007	56°-12	+0.003
3	10071.45	.08			9926.34	.08	24 - 7°	-0.11

Table 1. Observed Lines of Sn I (Continued)

Intensity	Air Wavelength (A) and Uncertainty Grating λ	Δλ	Interferometer λ	Δλ	Vacuum Wave Number (cm^{-1}) and Uncertainty ν	Δν	Combination	$\nu_o - \nu_c$ (cm^{-1})
2	10054.86	.15			9942.71	.15	49°-10	+0.09
3	10039.45	.07	10039.441	.008	9957.984	.008		
3	9949.18	.08			10048.32	.09	58°-12	-0.11
4	9941.91	.07	9941.926[d]	.010	10055.656	.010	51°-10	-0.007
6	9916.66	.06	9916.680	.008	10081.256	.008	25 - 7°	-0.004
8	9855.97	.06	9855.976	.004	10143.347	.004	56°-11	0.000
22	9850.372	.020	9850.381	.003	10149.109	.003	15 - 4°	0.000
6	9837.30	.06	9837.269	.008	10162.635	.009	28°- 8	-0.003
10	9813.89	.06	9813.879	.004	10186.858	.004	28 - 9°	+0.002
7	9809.19	.06	9809.191	.007	10191.726	.008	29 - 9°	+0.002
20	9805.17	.04	9805.184	.005	10195.892	.005	31 - 9°	0.000[b]
9	9799.64	.06	9799.631	.005	10201.668	.005	29°- 8	-0.002
5	9778.07	.08	9778.085	.007	10224.148	.008	28°- 7	+0.007
16	9742.480	.024	9742.486	.008	10261.507	.008	30 - 8°	-0.004
12	9740.913	.022	9740.903	.005	10263.174	.005	29°- 7	+0.002
6	9645.48	.09	9645.565	.005	10364.617	.006	25°- 6	+0.001
8	9623.76	.04	9623.776	.006	10388.083	.006	24 - 6°	+0.005
12	9616.010	.017	9616.014	.004	10396.468	.004	30°- 8	-0.001
2	9537.82	.06			10481.70	.07	32 - 8°	-0.05
4	9478.98	.09	9479.075	.004	10546.660	.005	56°-10	0.000
4	9474.55	.09	9474.633	.008	10551.605	.009	26 - 6°	+0.023
8	9451.39	.03	9451.391	.004	10577.552	.004	26°- 6	+0.001
14	9414.936	.019	9414.949	.006	10618.494	.006	28 - 7°	0.000
14	9410.620	.019	9410.630	.006	10623.368	.007	29 - 7°	+0.005
6	9408.39	.05	9408.452	.005	10625.826	.005	30 - 7°	+0.007
10	9361.819	.016	9361.838	.003	10678.734	.004	27°- 6	-0.001
5	9360.619	.021	9360.608	.003	10680.136	.003	58°-10	0.000
10	9272.494	.022	9272.511	.005	10781.607	.006	31°- 8	-0.001
6	9219.81	.04	9219.913	.006	10843.118	.009	31°- 7	+0.008
5h	9144.50	.07			10932.53	.09	62 -12°	0.00[b]

Table 1. Observed Lines of Sn I (Continued)

Intensity	Air Wavelength (Å) and Uncertainty				Vacuum Wave Number (cm^{-1}) and Uncertainty		Combination	$\nu_o - \nu_c$ (cm^{-1})
	Grating		Interferometer					
	λ	Δλ	λ	Δλ	ν	Δν		
5	9091.62	.03	9091.634	.003	10996.105	.004	33 - 7°	+0.001
12	9022.699	.019	9022.6913	.0018	11080.126	.002	28 - 6°	0.000
16	9018.75	.03	9018.7288	.0022	11084.994	.003	29 - 6°	0.000
9	9016.72	.03	9016.733	.003	11087.449	.004	30 - 6°	-0.002
9	8907.277	.013	8907.279	.003	11223.692	.003	32° - 8	-0.003
7	8885.996	.020	8886.012	.003	11250.554	.005	28° - 6	-0.004
1	8860.37	.10	8860.320	.014	11283.175	.017	33° - 8	+0.001
4	8855.289	.014	8855.287	.003	11289.589	.003	29° - 6	0.000
2	8837.43	.06	8837.477	.013	11312.342	.016	39 - 9°	+0.001
10	8812.284	.013	8812.2882	.0022	11344.675	.003	33° - 7	0.000
0	8802.98	.08	8803.05[d]	.03	11356.58	.04	36 - 7°	-0.02
5	8786.742	.018	8786.752	.005	11377.646	.006	37° - 9	-0.002
2	8769.38	.06	8769.477	.012	11400.062	.016	34° - 8	+0.001
4	8725.352	.019	8725.332[d]	.003	11457.734	.005	33 - 6°	-0.001
2	8702.65	.06	8702.692	.012	11487.544	.015	17 - 5°	-0.009
10	8693.909	.012	8693.896	.004	11499.162	.006	16 - 4°	+0.003
5	8681.891	.012	8681.8820	.0025	11515.077	.004	70°-11	0.000[b]
5	8650.523	.015	8650.504	.006	11556.842	.008	42 - 9°	+0.001
15	8648.05	.03	8648.029	.005	11560.152	.007	45 - 9°	0.000[b]
11	8598.36	.03	8598.367	.004	11626.922	.006	44 - 8°	+0.010
5	8586.471	.015	8586.447	.004	11643.060	.006	35° - 8	+0.001
3	8563.978	.021			11673.61	.03		
3	8561.426	.018			11677.090	.024		
28	8552.538	.013	8552.531	.003	11689.233	.004	10 - 2°	-0.002
5	8541.352	.019	8541.332	.005	11704.558	.007	35° - 7	-0.002
4	8541.089	.018			11704.893	.025		
2	8535.628	.017	8535.640	.006	11712.367	.008	38 - 7°	-0.002
1	8528.15	.08			11722.65	.11		
8	8525.277	.015	8525.283	.003	11726.595	.004	37° - 8	-0.001
7	8498.945	.015	8498.972	.006	11762.902	.009	36° - 7	+0.006

Table 1. Observed Lines of Sn I (Continued)

Intensity	Air wavelength (Å) and Uncertainty Grating λ	Δλ	Interferometer λ	Δλ	Vacuum Wave Number (cm^{-1}) and Uncertainty ν	Δν	Combination	$\nu_o - \nu_c$ (cm^{-1})
5	8480.799	.018	8480.802	.007	11788.100	.009	37°- 7	+0.002
3	8459.162	.016	8459.179	.006	11818.234	.009	36 - 6°	-0.002
5	8457.991	.014	8457.994	.005	11819.888	.006	46 - 9°	+0.008
6	8454.669	.015	8454.678	.004	11824.523	.006	47 - 9°	0.000
11	8432.236	.015	8432.2262	.0025	11856.006	.004	17 - 4°	+0.001
20	8422.619	.014	8422.624	.005	11869.524	.006	31°- 6	-0.004
5	8394.500	.014	8394.498	.004	11909.291	.005	41°- 9	-0.001
5	8393.730	.020	8393.7466	.0025	11910.358	.004	48 - 9°	0.000
14	8391.215	.013	8391.225	.003	11913.938	.004	18 - 4°	-0.001
6	8381.597	.016	8381.600	.003	11927.619	.004	38°- 7	+0.001
16	8356.973	.016	8356.9779	.0020	11962.761	.003	10 - 1°	+0.002
10	8349.374	.019	8349.3839	.0021	11973.641	.003	51 - 9°	0.000
7	8345.193	.018	8345.1974	.0024	11979.648	.004	49 - 8°	-0.002
13	8337.658	.024	8337.656	.005	11990.483	.006	43 - 7°	0.000[b]
4	8275.227	.020	8275.236[d]	.011	12080.929	.014		
12	8249.730	.014	8249.728	.004	12118.280	.006	19 - 4°	+0.002
5	8247.152	.023	8247.151[d]	.003	12122.067	.005	52 - 8°	0.000
5	8245.752	.014	8245.746	.007	12124.131	.009	53 - 8°	+0.010
6	8243.572	.013	8243.566	.003	12127.339	.005	16 - 3°	+0.002
5	8160.024	.020	8160.013	.003	12251.514	.004	46 - 7°	-0.004
3h	8132.70	.09			12292.66	.14	64 -12°	0.00[b]
11	8120.580	.014	8120.564	.003	12311.030	.005	42°- 8	0.000
20	8114.044	.015	8114.030	.004	12320.942	.006	12 - 2°	+0.003
6	8100.187	.016	8100.1897	.0021	12341.996	.003	48 - 7°	-0.001
3	8098.910	.018	8098.900	.003	12343.962	.005	49 - 7°	+0.003
4	8081.149	.015	8081.140	.005	12371.089	.007	33°- 6	-0.004
4	8078.437	.022	8078.434	.005	12375.234	.007	43°- 8	+0.007
2h	8075.873	.019			12379.16	.03		
2	8070.31	.03			12387.69	.05	54 - 9°	+0.03
8h	8068.869	.021	8068.869	.004	12389.904	.005	55 - 9°	0.000[b]

Table 1. Observed Lines of Sn I (Continued)

Intensity	Air wavelength (Å) and Uncertainty Grating λ	Δλ	Interferometer λ	Δλ	Vacuum wave Number (cm^{-1}) and Uncertainty ν	Δν	Combination	$\nu_o - \nu_c$ (cm^{-1})
6	8046.401	.018	8046.410	.003	12424.486	.005	44°- 8	-0.001
9	8038.488	.016	8038.4910	.0025	12436.726	.004	43°- 7	-0.002
14	8029.848	.015	8029.849	.007	12450.111	.010	42 - 6°	0.000
6	8028.077	.014	8028.081	.006	12452.854	.009	44 - 6°	+0.002
5	8022.295	.014			12461.833	.022	57 - 8°	-0.002
4	8021.348	.018	8021.365[d]	.008	12463.283	.013	45°- 9	-0.010
	8007.7	M			12484.5	M	17 - 3°	+0.4
1	8006.50	.09			12486.42	.14	52 - 7°	+0.04
5	8005.231	.014	8005.2112	.0024	12488.427	.004	53 - 7°	-0.002
9	7970.954	.012	7970.9418	.0020	12542.119	.003	18 - 3°	+0.001
3	7927.26	.03	7927.386	.005	12611.033	.009	48°- 9	+0.004
9	7910.426	.014	7910.414	.003	12638.086	.004	22 - 5°	+0.003
4			7909.289	.008	12639.884	.012	23 - 5°	+0.016
5	7863.693	.013	7863.709	.004	12713.150	.006	46 - 6°	+0.001
5	7852.691	.014	7852.695	.005	12730.980	.008	35°- 6	+0.003
6	7816.881	.019	7816.878	.003	12789.312	.005	36°- 6	-0.001
7	7808.126	.016	7808.1364	.0025	12803.631	.004	48 - 6°	+0.002
4	7806.94	.03	7806.941[d]	.022	12805.59	.03	49 - 6°	0.00
8	7801.502	.014	7801.510	.006	12814.507	.009	37°- 6	-0.008
3HH	7798.583	.020	7798.594	.009	12819.300	.014	54 - 7°	+0.001
5HS	7794.91	.03	7794.908	.005	12825.359	.009	56 - 7°	+0.002
6h	7769.12	.03	7769.157	.004	12867.869	.006	46°- 8	-0.001
4H	7765.60	.03	7765.614	.003	12873.740	.004	45°- 7	-0.004
4h	7761.767	.017	7761.782	.003	12880.095	.005	51°- 9	0.000
18	7754.883	.015	7754.881	.004	12891.556	.006	13 - 2°	-0.002
3H	7736.155	.018			12922.76	.03	59 - 9°	0.00[b]
5	7719.816	.025	7719.849	.003	12950.058	.005	53 - 6°	-0.003
6	7717.478	.019	7717.478	.003	12954.036	.005	38°- 6	0.000
5	7713.90	.04	7713.938	.003	12959.982	.006	48°- 8	+0.004
4	7695.96	.03	7695.954	.005	12990.266	.008	47°- 7	-0.002

Table 1. Observed Lines of Sn I (Continued)

Intensity	Air Wavelength (A) and Uncertainty Grating λ	Δλ	Interferometer λ	Δλ	Vacuum Wave Number (cm^{-1}) and Uncertainty ν	Δν	Combination	$\nu_o - \nu_c$ (cm^{-1})
3	7695.12	.03			12991.68	.05	61 - 8°	0.00[b]
12	7685.288	.015	7685.2703	.0024	13008.323	.004	23 - 4°	+0.003
3	7677.52	.06	7677.523	.004	13021.451	.007	48° - 7	-0.028
7	7593.777	.015	7593.758	.004	13165.083	.007	13 - 1°	+0.001
5	7586.608	.023	7586.602	.004	13177.503	.006	49° - 7	0.000
4h	7557.10	.04	7557.047	.007	13229.037	.011	51° - 8	-0.008
5	7530.627	.023	7530.593	.003	13275.510	.006	14 - 2°	+0.001
7HHS	7527.529	.019	7527.518	.009	13280.930	.015	54 - 6°	-0.001
3HH	7524.13	.04			13286.91	.07	56 - 6°	-0.08
3HH	7523.636	.024			13287.79	.05	57 - 6°	+0.01
6h	7490.784	.021	7490.727	.004	13346.159	.009	41° - 6	-0.001
4h	7488.677	.020	7488.649	.009	13349.858	.018	52° - 8	-0.010
4h	7485.658	.024			13355.20	.04	60 - 7°	0.00[b]
7h	7455.886	.015	7455.867	.005	13408.561	.009		
5h	7425.639	.017	7425.645[d]	.009	13463.137	.014	43° - 6	-0.009
14h	7398.554	.013	7398.570	.004	13512.406	.008	44° - 6	0.000
4	7332.18	.05	7332.203	.007	13634.711	.012	22 - 3°	-0.003
4h	7309.63	.05	7309.626	.005	13676.822	.009		
4H	7286.884	.023			13719.51	.05		
4h	7278.76	.04			13734.81	.07	5 - 3[e]	-0.01
6	7192.15	.03	7192.173	.004	13900.173	.008	45° - 6	+0.011
4	7184.58	.04			13914.87	.07	58° - 7	-0.15
6	7132.386	.015	7132.382	.012	14016.695	.018	47° - 6	+0.010
8	7116.542	.013	7116.539	.003	14047.902	.006	48° - 6	+0.005
5h	7096.480	.025	7096.428[d]	.014	14087.69	.04	60° - 8	0.00[b]
4	7094.45	.07			14091.64	.14		
4	7050.08	.13			14180.3	.3		
4	7025.01	.12			14230.93	.24		
6	6982.82	.12	6982.788	.006	14316.980	.012	51° - 6	+0.016
13h	6924.363	.014	6924.356	.006	14437.791	.012	52° - 6	+0.004

Table 1. Observed Lines of Sn I (Continued)

Intensity	Air Wavelength (Å) and Uncertainty Grating λ	Δλ	Interferometer λ	Δλ	Vacuum Wave Number (cm^{-1}) and Uncertainty ν	Δν	Combination	$\nu_o - \nu_c$ (cm^{-1})
10	6898.525	.016	6898.510	.004	14491.884	.008	15 - 2°	+0.004
7	6748.632	.021	6748.618	.003	14813.758	.007	24 - 4°	-0.003
5	6691.00	.04	6690.972	.016	14941.38	.04	58° - 6	-0.06
10	6679.75	.04	6679.716	.005	14966.563	.011		
6	6678.82	.04	6678.815	.004	14968.584	.008	25 - 4°	+0.009
5	6675.00	.06	6674.939	.004	14977.274	.009	26 - 4°	+0.010
8H	6650.483	.018	6650.491	.010	15032.337	.020	59° - 6	0.000[b]
9	6629.02	.05	6628.996	.006	15081.075	.014		
5h	6604.31	.06	6604.347	.003	15137.361	.007	28 - 5°	+0.004
7	6462.050	.017	6462.0506	.0017	15470.689	.004	5 - 2[e]	-0.004
10	6444.363	.019	6444.3690	.0023	15513.136	.006	30 - 4°	+0.001
5	6406.19	.05	6406.251	.004	15605.440	.009	26 - 3°	-0.002
9	6354.145	.018	6354.1577	.0016	15733.378	.004	32 - 4°	0.000
16	6310.613	.015	6310.6169	.0018	15841.931	.005	16 - 2°	0.000
8	6275.683	.015	6275.6907	.0018	15930.095	.005	34 - 4°	-0.002
12	6203.509	.019	6203.509	.003	16115.449	.009	16 - 1°	-0.005
5	6202.983	.020	6202.996	.003	16116.783	.008	35 - 4°	+0.001
7	6196.399	.017	6196.3811	.0021	16133.987	.006	28 - 3°	0.000
18	6171.585	.014	6171.5980	.0019	16198.777	.005	17 - 2°	0.000
13	6154.451	.015	6154.4455	.0015	16243.922	.004	36 - 4°	+0.002
4	6153.60	.04	6153.566[d]	.003	16246.242	.007		
24	6149.619	.015	6149.6035	.0023	16256.711	.006	18 - 2°	0.000
7	6110.20	.04	6110.1966	.0018	16361.556	.005	32 - 3°	+0.001
18	6073.265	.018	6073.266	.004	16461.048	.010	19 - 2°	-0.002
20	6069.117	.014	6069.117	.003	16472.302	.007	17 - 1°	+0.001
8	6060.79	.04	6060.8043	.0022	16494.893	.006	37 - 4°	-0.001
16	6054.686	.020	6054.6738	.0021	16511.594	.006	33 - 3°	-0.002
15	6037.58	.03	6037.6043	.0018	16558.276	.005	34 - 3°	0.000
5	6022.49	.04	6022.544	.003	16599.683	.010	38 - 4°	-0.002
9	6011.11	.04	6011.0965	.0021	16631.294	.006	39 - 4°	0.000

Table 1. Observed Lines of Sn I (Continued)

Intensity	Air Wavelength (A) and Uncertainty Grating λ	Δλ	Interferometer λ	Δλ	Vacuum Wave Number (cm^{-1}) and Uncertainty ν	Δν	Combination	$\nu_o - \nu_c$ (cm^{-1})
16	5970.34	.04	5970.2915	.0012	16744.962	.003	35 - 3°	+0.002
8	5934.08	.06	5934.0058	.0018	16847.354	.006	41 - 4°	+0.001
12	5925.33	.04	5925.3039	.0019	16872.096	.006	36 - 3°	-0.001
4	5922.99	.05	5923.037	.003	16878.554	.008	44 - 4°	+0.018
6	5801.78	.04	5801.7935	.0014	17231.272	.004	49 - 4°	-0.002
10	5761.75	.04	5761.7295	.0015	17351.087	.005	23 - 2°	-0.004
7	5753.58	.04	5753.5531	.0013	17375.745	.004	53 - 4°	+0.001
45	5631.676[d]	.004	5631.6758	.0010	17751.777	.003	2° - 5	-0.008
4	5387.81	.11			18555.3	.4		
5	5218.70	.05	5218.700	.005	19156.525	.016	24 - 2°	-0.006
12	5176.87	.04	5176.8607	.0013	19311.348	.005	25 - 2°	+0.001
20	5174.55	.04	5174.5348	.0013	19320.028	.005	26 - 2°	-0.008
4h	5164.64	.06	5164.6435[d]	.0021	19357.029	.008		
11	5160.17	.04	5160.1536	.0021	19373.871	.008	27 - 2°	+0.001
5h	5145.25	.07	5145.235	.006	19430.043	.022	24 - 1°	-0.013
16	5104.58	.04	5104.5593	.0019	19584.871	.007	25 - 1°	+0.001
9h	5034.89	.05	5034.8802	.0019	19855.908	.008	30 - 2°	+0.003
13	4979.66	.04	4979.646	.006	20076.146	.023	32 - 2°	-0.003
11	4931.34	.04	4931.3234	.0016	20272.873	.006	34 - 2°	+0.004
8	4912.73	.04	4912.7119	.0016	20349.674	.007	32 - 1°	+0.002
3	4888.27	.07	4888.310	.008	20451.26	.03		
7	4886.33	.04	4886.3281	.0018	20459.551	.008	35 - 2°	-0.002
3h	4878.33	.05	4878.329[d]	.003	20493.098	.013		
6h	4797.65	.03	4797.6600	.0024	20837.670	.010	37 - 2°	+0.005
6	4773.60	.04	4773.657	.003	20942.446	.012	38 - 2°	-0.010
10	4766.44	.04	4766.4595	.0017	20974.068	.008	39 - 2°	+0.003
4	4717.87	.05	4717.859	.003	21190.125	.012	41 - 2°	+0.001
7	4712.07	.04	4712.1069	.0020	21215.994	.009	38 - 1°	+0.014
3	4711.10	.20	4710.9327	.0016	21221.281	.007	44 - 2°	-0.025
5	4633.89	.04	4633.8980	.0024	21574.062	.011	49 - 2°	+0.018

Table 1. Observed Lines of Sn I (Continued)

Intensity	Air wavelength (Å) and Uncertainty Grating λ	Δλ	Interferometer λ	Δλ	Vacuum wave Number (cm^{-1}) and Uncertainty ν	Δν	Combination	$\nu_o - \nu_c$ (cm^{-1})
6	4603.10	.05	4603.0745	.0024	21718.525	.011	53 - 2°	+0.010
55	4524.734[d]	.004	4524.7344	.0008	22094.549	.004	4° - 5	-0.006
3h	4396.19	.06	4396.133	.003	22740.874	.015		
3h	4230.67	.08			23630.3	.5		
60	3801.013[d]	.002	3801.0108	.0007	26301.324	.005	2° - 4	-0.004
1	3745.61	.04			26690.3	.3		
35	3655.778[d]	.003	3655.7764	.0011	27346.180	.008	8° - 5	+0.001
55			3330.6072	.0007	30015.921	.006	3° - 4	0.000
65			3262.3310	.0006	30644.093	.006	4° - 4	-0.006
30			3223.5697	.0005	31012.555	.005	5° - 4	+0.003
25			3218.6805	.0007	31059.662	.006	14° - 5	+0.001
65			3175.0354	.0010	31486.603	.009	2° - 3	-0.007
50			3141.8232	.0006	31819.435	.006	16° - 5	-0.001
60			3034.1150	.0011	32948.950	.012	1° - 2	-0.003
50			3032.7778	.0009	32963.476	.010	19° - 5	+0.003
65			3009.1333	.0009	33222.479	.010	2° - 2	+0.001
41			2913.5593	.0007	34312.233	.008	22° - 5	+0.014
60			2863.3147	.0012	34914.305	.014	2° - 1	+0.023
61			2850.6195	.0005	35069.789	.006	6° - 4	+0.006
64			2839.9765	.0008	35201.209	.009	3° - 3	+0.006
51			2813.5822	.0005	35531.416	.006	7° - 4	+0.001
22			2812.5575	.0006	35544.360	.008	25° - 5	+0.027
9			2790.1822	.0008	35829.387	.010	4° - 3	+0.006
26			2787.9197	.0006	35858.463	.008	27° - 5	+0.009
43			2785.0257	.0004	35895.722	.005	8° - 4	-0.001
52			2779.8113	.0004	35963.052	.005	9° - 4	0.000
41			2761.7803	.0006	36197.834	.007	5° - 3	0.000
2			2744.1573	.0007	36430.284	.010	28° - 5	+0.009
52			2706.5049	.0009	36937.068	.013	3° - 2	-0.001
40			2661.2436	.0004	37565.242	.006	4° - 2	-0.006

Table 1. Observed Lines of Sn I (Continued)

Intensity	Air Wavelength (A) and Uncertainty				Vacuum Wave Number (cm^{-1}) and Uncertainty		Combination	$\nu_o - \nu_c$ (cm^{-1})
	Grating		Interferometer					
	λ	$\Delta\lambda$	λ	$\Delta\lambda$	ν	$\Delta\nu$		
12			2636.9923	.0004	37910.694	.006	35°- 5	-0.002
9			2635.3926	.0007	37933.705	.009	5°- 2	+0.004
10			2631.1935	.0006	37994.239	.008	37°- 5	+0.006
42			2594.4209	.0006	38532.726	.008	10°- 4	-0.004
50			2571.5940	.0005	38874.742	.007	11°- 4	-0.001
15			2558.0944	.0007	39079.880	.010	45°- 5	0.000
7			2548.4572	.0009	39277.653	.015	48°- 5	+0.038
35			2546.5487	.0006	39257.050	.009	4°- 1	-0.004
15			2531.0975	.0005	39496.680	.009	51°- 5	-0.001
26			2523.9069	.0005	39609.200	.007	14°- 4	-0.005
40			2495.7241	.0004	40056.453	.007	15°- 4	-0.002
13			2491.6993	.0009	40121.151	.014	58°- 5	-0.004
43			2483.4096	.0005	40255.067	.007	6°- 3	+0.002
14			2476.4013	.0004	40368.983	.007	16°- 4	+0.002
32			2455.2516	.0004	40716.699	.007	7°- 3	+0.002
24			2433.4769	.0008	41081.003	.012	8°- 3	-0.002
53			2429.4952	.0007	41148.327	.010	9°- 3	-0.007
50			2421.6943	.0005	41280.865	.008	18°- 4	-0.004
37			2408.1505	.0004	41513.017	.005	19°- 4	0.000
38			2380.7400	.0004	41990.938	.007	6°- 2	+0.006
20			2357.8813	.0004	42397.990	.007	20°- 4	+0.006
49			2354.8499	.0012	42452.564	.022	7°- 2	+0.001
39			2334.8124	.0006	42816.864	.011	8°- 2	-0.008
12			2332.3659	.0005	42861.772	.010	22°- 4	+0.007
35			2317.2301	.0009	43141.715	.016	23°- 4	-0.002
34			2286.6812	.0004	43718.015	.009	10°- 3	+0.003
16			2282.2480	.0007	43802.927	.014	24°- 4	+0.004
36			2268.9296	.0010	44060.024	.019	11°- 3	0.000
20			2267.1874	.0005	44093.877	.010	25°- 4	-0.001
18			2251.1486	.0004	44408.004	.008	27°- 4	+0.007

Table 1. Observed Lines of Sn I (Continued)

Intensity	Air Wavelength (A) and Uncertainty Grating λ	Δλ	Interferometer λ	Δλ	Vacuum Wave Number (cm^{-1}) and Uncertainty ν	Δν	Combination	$\nu_o-\nu_c$ (cm^{-1})
27			2246.0573	.0012	44508.657	.022	8°- 1	-0.021
24			2231.7243	.0005	44794.482	.010	14°- 3	-0.004
6			2222.5276	.0008	44979.820	.016	28°- 4	0.000
7			2220.6002	.0009	45018.859	.018	29°- 4	+0.007
14			2211.0333	.0010	45213.629	.020	30°- 4	-0.021
26			2209.6597	.0008	45241.734	.016	15°- 3	-0.003
25			2199.3455	.0010	45453.881	.021	10°- 2	+0.002
24			2194.4991	.0005	45554.252	.010	16°- 3	-0.010
13			2171.3015	.0008	46040.889	.016	32°- 4	+0.013
6			2168.4986	.0010	46100.393	.022	33°- 4	+0.037
5			2163.0156	.0007	46217.240	.015	34°- 4	-0.002
21			2151.4268	.0008	46466.164	.017	18°- 3	+0.013
20			2148.7266	.0007	46524.550	.014	13°- 2	0.000[b]
16			2148.4581	.0005	46530.362	.011	14°- 2	+0.009
6			2147.8377	.0010	46543.801	.020	37°- 4	+0.023
12			2141.4194	.0008	46683.288	.018	38°- 4	-0.010
16			2140.7311	.0007	46698.296	.015	19°- 3	-0.002
10			2128.0013	.0007	46977.616	.015	15°- 2	+0.012
6	2123.62	M			47074.5	M	41°- 4	-0.9
12			2121.2008	.0012	47128.21	.03	42°- 4	0.00
7	2118.38	M			47191.0	M	43°- 4	-1.4
19			2113.9370	.0017	47290.13	.04	16°- 2	0.00
19			2100.9122	.0009	47583.270	.020	20°- 3	+0.005
6	2098.82	M			47630.7	M	45°- 4	+1.3
16			2096.4284	.0018	47685.03	.04	46°- 4	-0.02
17			2094.3276	.0010	47732.856	.022	21°- 3	+0.009
5	2092.422	M			47776.3	M	48°- 4	-0.8
20			2091.5900	.0009	47795.322	.021	17°- 2	0.000[b]
4	2085.62	M			47932.1	M	49°- 4	-1.1
14			2080.6306	.0013	48047.05	.03	22°- 3	0.00

Table 1. Observed Lines of Sn I (Continued)

Intensity	Air Wavelength (Å) and Uncertainty Grating λ	Δλ	Interferometer λ	Δλ	Vacuum Wave Number (cm^{-1}) and Uncertainty ν	Δν	Combination	$\nu_o-\nu_c$ (cm^{-1})
18			2073.0746	.0015	48222.15	.04	14°- 1	-0.01
14	2072.89	M			48226.4	M	53°- 4	+0.1
18			2068.5755	.0018	48327.02	.04	23°- 3	+0.02
16			2064.002	.003	48434.09	.07	19°- 2	-0.08
2	2061.57	M			48491.2	M	55°- 4	-1.1
4	2059.612	M			48537.3	M	56°- 4	+0.1
9	2058.31	M			48568.0	M	57°- 4	-0.5
10	2054.03	M			48669.2	M	58°- 4	-1.5
18	2040.905	M			48982.1	M	16°- 1	+0.2
20	2040.660	M			48988.0	M	24°- 3	-0.2
7	2028.597	M			49279.3	M	25°- 3	+0.1
14	2026.975	M			49318.7	M	20°- 2	-0.4
12	2020.833	M			49468.6	M	21°- 2	-0.1
14	2015.764	M			49593.0	M	27°- 3	-0.3
13	2008.048	M			49783.5	M	22°- 2	+0.6

Intensity	Vacuum Wavelength (Å) and Uncertainty Grating λ	Δλ	Interferometer λ	Δλ	Vacuum Wave Number (cm^{-1}) and Uncertainty ν	Δν	Combination	$\nu_o-\nu_c$ (cm^{-1})
30h	1994.982	S			50125.8	S	19°- 1	-0.2
5	1993.439	S			50164.6	S	28°- 3	-0.5
30h	1991.890	S			50203.6	S	29°- 3	-0.6
100r?v	1984.182	S			50398.6	S	30°- 3	-0.3
HHH	1977.82	S			50560.7	S		
100rv	1971.452	S			50724.0	S	24°- 2	0.0
1h	1969.986	S			50761.8	S	80°- 4	+0.5
10h	1969.137	S			50783.7	S	31°- 3	-0.4
5HH	1967.495	S			50826.1	S		
100	1960.215	S			51014.8	S	25°- 2	-0.2
500rv	1952.141	S			51225.8	S	32°- 3	-0.3
5h?	1949.885	S			51285.1	S	33°- 3	-0.6

Table 1. Observed Lines of Sn I (Continued)

Intensity	Vacuum Wavelength (A) and Uncertainty Grating λ	Δλ	Interferometer λ	Δλ	Vacuum Wave Number (cm^{-1}) and Uncertainty ν	Δν	Combination	$\nu_o - \nu_c$ (cm^{-1})
30h	1948.229	S			51328.7	S	27°- 2	-0.5
10h?	1945.415	S			51402.9	S	34°- 3	+0.4
50h	1942.690	S			51475.0	S	22°- 1	+0.3
1	1936.261	S			51645.9	S	35°- 3	+0.4
50h	1933.178	S			51728.3	S	37°- 3	-0.8
50HH	1928.976	S			51841.0	S	84°- 4	+1.8
30h	1927.966	S			51868.1	S	38°- 3	-0.4
100h	1926.764	S			51900.5	S	28°- 2	-0.5
500rv	1925.305	S			51939.8	S	29°- 2	-0.2
3H	1922.157	S			52024.9	S		
100h	1913.528	S			52259.5	S	41°- 3	-1.2
200h	1911.613	S			52311.8	S	42°- 3	-1.6
300H	1909.305	S			52375.1	S	43°- 3	-2.6
3h	1907.425	S			52426.7	S	44°- 3	-0.2
2	1904.049	S			52519.7	S	31°- 2	-0.3
1	1901.346	S			52594.3	S		
50h	1897.299	S			52706.5	S	25°- 1	-0.3
200rHr	1891.415	S			52870.5	S	46°- 3	+0.1
5h	1888.165	S			52961.5	S	48°- 3	-1.0
200rHv	1886.042	S			53021.1	S	(27°- 1 33°- 2	+0.1 -0.4
3h	1884.256	S			53071.3	S		
100H	1882.647	S			53116.7	S	49°- 3	-1.8
5HH	1881.191	S			53157.8	S	94°- 4	+1.3
20h	1878.643	S			53229.9	S	51°- 3	-1.6
50h	1873.302	S			53381.7	S	35°- 2	+0.3
30H	1872.254	S			53411.6	S	53°- 3	-0.1
30h	1871.297	S			53438.9	S	36°- 2	-0.9
2h	1870.411	S			53464.2	S	37°- 2	-0.7
100rv	1865.933	S			53592.5	S	28°- 1	-0.3
100r	1865.523	S			53604.3	S	38°- 2	-0.2

Table 1. Observed Lines of Sn I (Continued)

Intensity	Vacuum Wavelength (Å) and Uncertainty Grating λ	Δλ	Interferometer λ	Δλ	Vacuum Wave Number (cm^{-1}) and Uncertainty ν	Δν	Combination	$\nu_o-\nu_c$ (cm^{-1})
10H	1862.951	S			53678.3	S	55°- 3	+0.6
30h	1861.432	S			53722.1	S	56°- 3	-0.4
200R+H	1860.330	S			53753.9	S	57°- 3	+0.1
2H	1856.849	S			53854.7	S	58°- 3	-1.3
30	1854.253	S			53930.1	S	40°- 2	0.0
50rhv	1852.003	S			53995.6	S	41°- 2	-1.0
100RH	1848.768	S			54090.1	S	60°- 3	-0.1
15h	1848.054	S			54111.0	S	43°- 2	-2.6
r	1837.583	S			54419.3	S	63°- 3	0.0[b]
10HHH	1837.45	S			54423.2	S		
10h	1833.094	S			54552.6	S	45°- 2	+2.0
5h	1829.298	S			54665.8	S	47°- 2	-1.3
5	1828.183	S			54699.1	S	48°- 2	+0.8
200R	1823.021	S			54854.0	S	49°- 2	-0.3
2	1820.186	S			54939.4	S	50°- 2	+0.1
100rv	1819.273	S			54967.0	S	51°- 2	-0.4
100R	1815.771	S			55073.0	S	35°- 1	-0.2
50rv	1813.020	S			55156.6	S	37°- 1	-0.1
E+r	1804.971	S			55402.6	S	54°- 2	0.0
E+R	1804.628	S			55413.1	S	55°- 2	-0.4
10h	1803.187	S			55457.4	S	56°- 2	-1.0
1h	1796.514	S			55663.4	S		
5H	1795.743	S			55687.3	S	41°- 1	-1.1
HHH	1793.32	S			55762.5	S	79°- 3	0.0[b]
E+R	1790.776	S			55841.7	S	61°- 2	0.0[b]
E+r	1789.836	S			55871.0	S	62°- 2	-0.2
10h	1787.407	S			55947.0	S	80°- 3	+0.4
E+R	1780.491	S			56164.3	S	64°- 2	0.0[b]
r	1779.128	S			56207.3	S	65°- 2	+0.1
5rr	1778.009	S			56242.7	S	(45°- 1 66°- 2	+0.3 -0.2

Table 1. Observed Lines of Sn I (Continued)

Intensity	Vacuum Wavelength (A) and Uncertainty Grating λ	Δλ	Interferometer λ	Δλ	Vacuum Wave Number (cm^{-1}) and Uncertainty ν	Δν	Combination	$\nu_o-\nu_c$ (cm^{-1})
20R$\underline{v}$	1773.364	S			56390.0	S	48°- 1	-0.1
r	1772.769	S			56408.9	S	67°- 2	0.0[b]
1h	1765.817	S			56631.0	S	50°- 1	-0.1
50R$\underline{v}$	1764.943	S			56659.1	S	51°- 1	-0.1
	1753.69	S			57022.6	S	84°- 3	-1.8
10H	1753.412	S			57031.7	S		
r?	1751.996	S			57077.8	S		
E+20R	1751.485	S			57094.4	S	54°- 1	0.0
r	1750.352	S			57131.4	S		
E+r$\underline{v}$	1745.718	S			57283.0	S	58°- 1	-0.6
R	1737.22	S			57563.2	S	62°- 1	+0.2
r$\underline{v}$	1736.01	S			57603.4	S		
10h	1733.66	S			57681.4	S	80°- 2	-1.0
r	1729.51	S			57819.8	S	89°- 3	0.0[b]
H	1729.22	S			57829.5	S		
R	1727.15	S			57898.9	S	65°- 1	-0.1
r	1726.08	S			57934.7	S	66°- 1	0.0[b]
R	1719.88	S			58143.6	S	68°- 1	0.0[b]
r	1714.54	S			58324.7	S	69°- 1	0.0[b]
r	1714.08	S			58340.3	S	94°- 3	-1.3
H	1713.63	S			58355.7	S		
r	1708.72	S			58523.3	S	71°- 1	0.0[b]
r	1706.63	S			58595.0	S	72°- 1	0.0[b]
r	1706.26	S			58607.7	S	73°- 1	0.0[b]
r	1704.17	S			58679.6	S	74°- 1	0.0[b]
r	1703.86	S			58690.3	S	75°- 1	0.0[b]
r	1703.60	S			58699.2	S	100°- 3	0.0[b]
r	1702.19	S			58747.8	S	76°- 1	0.0[b]
r	1701.87	S			58758.9	S	77°- 1	0.0[b]
5	1697.59	S			58907.0	S	85°- 2	0.0[b]

Table 1. Observed Lines of Sn I (Continued)

Intensity	Vacuum Wavelength (A) and Uncertainty Grating λ	Δλ	Interferometer λ	Δλ	Vacuum Wave Number (cm^{-1}) and Uncertainty ν	Δν	Combination	$\nu_o-\nu_c$ (cm^{-1})
r	1696.15	S			58957.0	S	105°- 3	0.0[b]
h	1695.77	S			58970.3	S	78°- 1	0.0[b]
H	1693.48	S			59050.0	S		
H	1687.80	S			59248.7	S		
h	1682.67	S			59429.4	S		
r?	1682.00	S			59453.0	S	81°- 1	0.0[b]
H	1680.45	S			59507.9	S		
H	1679.71	S			59534.1	S		
H	1676.32	S			59654.5	S	90°- 2	0.0[b]
H	1670.89	S			59848.3	S		
r?	1670.59	S			59859.1	S		
H	1667.43	S			59972.5	S		
H	1665.52	S			60041.3	S		
H	1662.92	S			60135.2	S		
2	1657.00	S			60350.0	S		
r on H	1655.71	S			60397.1	S	83°- 1	0.0[b]
r	1648.91	S			60646.1	S	86°- 1	0.0[b]
h	1640.33	S			60963.3	S		
r	1633.58	S			61215.2	S	88°- 1	0.0[b]
r	1619.52	S			61746.7	S	93°- 1	0.0[b]
r	1614.82	S			61926.4	S		
r	1610.02	S			62111.0	S	99°- 1	0.0[b]
rh	1605.65	S			62280.1	S		
rh	1603.19	S			62375.6	S	104°- 1	0.0[b]

[a] Intensity uncertain

[b] This line alone determines the value of one of the levels involved.

[c] Confused, no intensity estimate

[d] This value was obtained with the SnI_2 electrodeless discharge light source.

[e] This is a forbidden transition.

Table 1. Observed Lines of Sn I (Continued)

The letter H, M, or S in the uncertainty columns of the table indicates that the lines were measured by Humphreys, Meggers, or Shenstone, respectively.

The symbols which describe the character of the lines are defined as follows:

h, H, HH, HHH - increasing degrees of haziness

S - asymmetric

E - emission line

r - fine and weak reversal

R - strong reversal

r - reversal on the red side of an emission line

v - reversal on the violet side of an emission line

Lines which are given only as r or R are reversals on a general background.

Table 2. Observed Lines of Sn II

Intensity	Air Wavelength (A) and Uncertainty Grating λ	Δλ	Interferometer λ	Δλ	Vacuum Wave Number (cm^{-1}) and Uncertainty ν	Δν	Combination	$\nu_o-\nu_c$ (cm^{-1})
5	10739.22	.07	10739.257	.006	9309.081	.005	9°-14	-0.002
5	10607.41	.07	10607.434	.006	9424.769	.005	10°-13	-0.004
6	9063.57	.06	9063.658	.005	11030.045	.006	5°-34	-0.008
							34 - 6°	-0.006
7	9058.84	.06	9058.880	.004	11035.863	.004	6°-34	+0.005
							34 - 5°	+0.007
2	8055.72	.09			12410.13	.14	18 - 8°	-0.08
16	7903.531	.014	7903.532	.004	12649.092	.005	3°- 5	-0.001
3	7825.97	.09			12774.45	.15	18 - 7°	+0.09
16	7741.409	.014	7741.425	.003	12913.965	.004	4°- 6	-0.003
12	7387.132	.017	7387.1651	.0024	13533.266	.005	4°- 5	-0.002
14	7190.773	.018	7190.776	.003	13902.873	.006	12 - 4°	+0.004
28	6844.188	.017	6844.1859	.0020	14606.911	.004	3°- 4	+0.001
12	6760.87	.03	6760.812	.003	14787.040	.006	12 - 3°	-0.004
24	6453.552	.017	6453.5422	.0012	15491.085	.003	4°- 4	0.000
10	6079.77	.04	6079.7696	.0024	16443.439	.007	21 - 6°	+0.010
10	6077.63	.04	6077.6331	.0019	16449.220	.005	21 - 5°	-0.013
4H	5965.84	.06			16757.46	.17	25 - 8°	0.00[a]
14	5798.89	.04	5798.860	.003	17239.989	.008	5°- 8	-0.002
6	5796.93	.04	5796.9078	.0015	17245.794	.005	6°- 8	-0.001
8h	5596.29	.06	5596.2644	.0015	17864.103	.005	13 - 4°	-0.002
14	5588.84	.06	5588.8152	.0018	17887.913	.006	6°- 7	0.000
14	5561.96	.06	5561.9101	.0016	17974.443	.005	14 - 4°	-0.001
16	5332.38	.04	5332.3391	.0016	18748.281	.006	13 - 3°	+0.001
8	4944.28	.04	4944.2562	.0020	20219.845	.008	8°- 8	0.000
7	4877.20	.04	4877.209	.003	20497.805	.013	7°- 7	+0.001
5h	4792.03	.04	4792.0732	.0019	20861.963	.009	8°- 7	0.000
10	4618.26	.04	4618.2359	.0010	21647.226	.005	4°- 3	+0.002

Table 2. Observed Lines of Sn II (Continued)

Intensity	Air Wavelength (A) and Uncertainty Grating λ	Δλ	Interferometer λ	Δλ	Vacuum Wave Number (cm^{-1}) and Uncertainty ν	Δν	Combination	$\nu_o - \nu_c$ (cm^{-1})
6	4323.09	.04	4323.0925	.0013	23125.086	.007	3° - 2	-0.001
3	3841.38	.03	3841.3756	.0014	26024.959	.010	15 - 4°	-0.004
5	3715.11	.04	3715.1524	.0011	26909.141	.008	15 - 3°	+0.003
3	3620.48	.03	3620.4854	.0015	27612.732	.011	9° - 8	+0.012
2	3582.36	.03	3582.3511	.0014	27906.663	.011	16 - 4°	0.000
5	3575.41	.03	3575.3255	.0012	27961.498	.010	17 - 4°	0.000[a]
4			3472.333	.003	28970.839	.025	16 - 3°	+0.001
20			3351.9523	.0012	29824.787	.011	5° - 6	+0.022
15			3283.1399	.0009	30449.874	.008	6° - 5	+0.004
3			2592.7198	.0017	38558.006	.025	5° - 3	-0.016
13			2486.9666	.0008	40197.497	.013	9° - 6	+0.001
5			2448.9079	.0007	40822.164	.012	10° - 5	+0.019
16			2368.2265	.0006	42212.796	.011	1 - 2°	-0.001
13			2266.0156	.0010	44116.677	.019	2 - 2°	-0.017
5			2151.5135	.0020	46464.29	.04	1 - 1°	0.00[a]
13			2150.8442	.0009	46478.749	.019	3 - 2°	+0.018

[a] This line alone determines the value of one of the levels involved.

The symbols which describe the character of the lines are defined as follows:

h - slightly hazy

H - more hazy

Observed Energy Levels

The energy levels of the arc spectrum of tin are listed in Tables 3 and 4. The values of these levels appear in the second columns and are given with respect to the $5s^2 5p^2\ ^3P_0$ level which is assigned the value zero. Whenever possible, the level values were determined from the measurements of the author. The values for the levels which could not be determined from the lines listed in Table 1 are from the work of Barrow and Rowlinson and were taken from AEL[1] with the exception of level 139° which is from Garton[24]. Of the other two levels with J = 1 given by Garton, the one at 60401 (±5) cm^{-1} is probably the same as level 83° in Table 4. The other level at 61766 (±5) cm^{-1} was not verified by the measurements of Shenstone or Barrow and Rowlinson and was not included in the table for this reason.

The third and fourth columns of the tables give the estimated uncertainties of the levels determined by the author, column three of each table giving the uncertainties with respect to the other levels and column four those with respect to the $5s^2 5p^2\ ^3P_0$ level. The relative uncertainty of this level is rather large because it is determined by only four interferometrically measured lines, one of which could only be measured with the Bausch and Lomb eyepiece. In addition, these four lines are so broad that fringes were obtained only with the 2- and 5-mm interferometer spacers and even these fringes could not be accurately measured because of their breadth.

The fifth columns of the tables give the number of combinations observed by the author between each level and the levels of the opposite parity, and the sixth columns give the number of combinations observed when all of the lines listed in Table 1 are considered. The symbol +

in column six of each table indicates that one or more combinations presently have two possible classifications; these transitions are in addition to the number specified.

The classifications of the levels appearing in the remaining columns of the tables will be discussed in the next chapter. The numbers enclosed in parentheses in the designations given in AEL and by Meggers indicate the probable J-value of the level. The designations given by the author are in jK-coupling notation and, in parentheses, in LS-coupling notation. These types of coupling also will be discussed in the next chapter. Although the LS notation has little meaning for most of the levels, it is included for purposes of comparison with the designations given in AEL and by Meggers. The designations of the levels of the $5s^2 5p^2$ and $5s5p^3$ configurations are given only in LS notation because jK notation has no meaning when the electrons are equivalent since jK coupling requires a distinction between the electrons.

Of the 62 levels of even parity listed in Table 3, 28 are new. Four of the 38 even levels listed in AEL could not be verified and two have been re-classified. Of the 138 levels of odd parity listed in Table 4, 10 are new and four are unclassified. One of the 125 odd levels listed in AEL was not verified and two have been re-classified.

The energy levels of the first spark spectrum of tin which could be determined from the lines measured in this investigation are listed in Tables 5 and 6. The classifications are those given in AEL and the levels are numbered in the order in which they appear in that publication. Even level 34 is new, but since it is determined by only two lines and since its classification is not known, there are two possible values it can have as is indicated in Table 6. The large absolute uncertainties

of the levels are due to the fact that they are connected to the $5s^2 5p\ {}^2P^o_{\frac{1}{2}}$ zero level through a single pair of lines. The interference pattern of one of these lines, 2151.51 A, is not completely resolved from that of a stronger arc line only 0.09 A away. Because of this, accurate measurements for this spark line were impossible.

Table 3. Even Energy Levels of Sn I

Level Number	Level Value (cm^{-1})	Estimated Uncertainty (cm^{-1}) Relative	Absolute	Number of Combinations Author	All	Level Designation Author	AEL[1]	Meggers[2]
1	0.000	.010	.000	4	37+	$5p\ ^3P_0$	$5p\ ^3P_0$	$5p\ ^3P_0$
2	1691.806	.005	.011	15	48+	$5p\ ^3P_1$	$5p\ ^3P_1$	$5p\ ^3P_1$
3	3427.673	.004	.011	19	54	$5p\ ^3P_2$	$5p\ ^3P_2$	$5p\ ^3P_2$
4	8612.955	.003	.010	31	44	$5p\ ^1D_2$	$5p\ ^1D_2$	$5p\ ^1D_2$
5	17162.499	.004	.011	16	16	$5p\ ^1S_0$	$5p\ ^1S_0$	$5p\ ^1S_0$
6	42342.216	.002	.010	27	32	$6p\ (\frac{1}{2},1\frac{1}{2})_1$ $(^3D_1)$	$6p\ ^3P_1$	$6p\ ^3D_1$
7	43368.634	.002	.010	21	29	$6p\ (\frac{1}{2},\frac{1}{2})_1$ $(^1P_1)$	$6p\ ^3D_1$	$6p\ ^3P_1$
8	43430.135	.002	.010	24	29+	$6p\ (\frac{1}{2},1\frac{1}{2})_2$ $(^3D_2)$	$6p\ ^3P_0$	$6p\ ^3P_0$
9	43799.085	.004	.011	8	13	$6p\ (\frac{1}{2},\frac{1}{2})_0$ $(^3P_0)$		
10	46603.517	.003	.010	12	18	$6p\ (1\frac{1}{2},1\frac{1}{2})_1$ $(^3P_1)$	$6p\ ^1P_1$	$6p\ ^1P_1$
11	47006.830	.005	.011	6	8	$6p\ (1\frac{1}{2},2\frac{1}{2})_3$ $(^3D_3)$	$6p\ ^3D_3$	$6p\ ^3D_3$
12	47235.221	.003	.010	9	14	$6p\ (1\frac{1}{2},1\frac{1}{2})_2$ $(^3P_2)$	$6p\ ^3P_2$	$6p\ ^3P_2$

Table 3. Even Energy Levels of Sn I (Continued)

Level Number	Level Value (cm^{-1})	Estimated Uncertainty (cm^{-1}) Relative	Absolute	Number of Combinations Author	All	Level Designation Author		AEL[1]	Meggers[2]
13	47805.840	.003	.010	5	10+	$6p\ (1\frac{1}{2},\frac{1}{2})_1$	$(^3S_1)$	$6p\ ^3S_1$	$6p\ ^3S_1$
14	48189.791	.003	.010	4	10+	$6p\ (1\frac{1}{2},2\frac{1}{2})_2$	$(^1D_2)$	$6p\ ^1D_2$	$6p\ ^1D_2$
15	49406.162	.003	.010	2	2	$6p\ (1\frac{1}{2},\frac{1}{2})_0$	$(^1S_0)$		
16	50756.212	.004	.011	4	5	$7p\ (\frac{1}{2},1\frac{1}{2})_1$	$(^3D_1)$	$7p\ ^3P_1$	$7p\ ^3D_1$
17	51113.059	.004	.011	4	6	$7p\ (\frac{1}{2},\frac{1}{2})_1$	$(^1P_1)$	$7p\ ^3D_1$	$7p\ ^3P_1$
18	51170.993	.003	.010	3	3+	$7p\ (\frac{1}{2},1\frac{1}{2})_2$	$(^3D_2)$	$7p\ ^3D_2$	$7p\ ^3D_2$
19	51375.332	.005	.011	2	3	$7p\ (\frac{1}{2},\frac{1}{2})_0$	$(^3P_0)$	$7p\ ^3P_0$	$7p\ ^3P_0$
20	52248.822	.004	.011	2	4	$4f\ (\frac{1}{2},3\frac{1}{2})_3$	$(^1F_3)$	4f (2?)	4f (1,2,3)
21	52254.28	.13	.13	1	1	$4f\ (\frac{1}{2},3\frac{1}{2})_4$	$(^3F_4)$		
22	52263.589	.004	.010	4	5	$4f\ (\frac{1}{2},2\frac{1}{2})_3$	$(^3F_3)$	4f (2)	4f (2)
23	52265.373	.004	.010	5	5	$4f\ (\frac{1}{2},2\frac{1}{2})_2$	$(^3F_2)$	$7p\ ^1S_0$	$7p\ ^1S_0$
24	54070.814	.006	.011	5	5	$8p\ (\frac{1}{2},1\frac{1}{2})_1$	$(^3D_1)$		
25	54225.628	.005	.011	4	4	$8p\ (\frac{1}{2},\frac{1}{2})_1$	$(^1P_1)$		
26	54234.318	.007	.012	5	5	$8p\ (\frac{1}{2},1\frac{1}{2})_2$	$(^3D_2)$		
27	54288.152	.009	.013	2	2	$8p\ (\frac{1}{2},\frac{1}{2})_0$	$(^3P_0)$		

Table 3. Even Energy Levels of Sn I (Continued)

Level Number	Level Value (cm^{-1})	Estimated Uncertainty (cm^{-1}) Relative	Absolute	Number of Combinations Author	All	Level Designation Author		AEL[1]	Meggers[2]
28	54762.862	.003	.010	5	5+	5f $(\frac{1}{2},2\frac{1}{2})_3$	($^3F_3$)	5f (3?)	5f (2,3)
29	54767.731	.003	.010	3	3	5f $(\frac{1}{2},3\frac{1}{2})_3$	($^1F_3$)	5f (2?)	5f (1,2,3)
30	54770.188	.004	.011	5	5	5f $(\frac{1}{2},2\frac{1}{2})_2$	($^3F_2$)		
31	54771.898	.006	.011	1	1	5f $(\frac{1}{2},3\frac{1}{2})_4$	($^3F_4$)	5f (2?)	5f (2)
32	54990.431	.004	.010	5	5	7p $(1\frac{1}{2},1\frac{1}{2})_1$	($^3P_1$)	7p $^1P_1$	7p $^1P_1$
33	55140.472	.004	.010	3	4	7p $(1\frac{1}{2},2\frac{1}{2})_3$	($^3D_3$)	7p $^3D_3$	7p $^3D_3$
34	55187.151	.004	.010	3	3	7p $(1\frac{1}{2},1\frac{1}{2})_2$	($^3P_2$)	7p $^3P_2$	7p $^3P_2$
35	55373.835	.004	.011	3	3	7p $(1\frac{1}{2},\frac{1}{2})_1$	($^3S_1$)	7p $^3S_1$	7p $^3S_1$
36	55500.973	.004	.010	4	4	7p $(1\frac{1}{2},2\frac{1}{2})_2$	($^1D_2$)	7p $^1D_2$	7p $^1D_2$
37	55751.947	.006	.011	2	2	9p $(\frac{1}{2},1\frac{1}{2})_1$	($^3D_1$)		
38	55856.737	.007	.012	4	4	9p $(\frac{1}{2},\frac{1}{2})_1$	($^1P_1$)		
39	55888.347	.005	.011	3	3	9p $(\frac{1}{2},1\frac{1}{2})_2$	($^3D_2$)		
41	56104.407	.006	.011	2	2+	7p $(1\frac{1}{2},\frac{1}{2})_0$	($^1S_0$)		
42	56132.848	.007	.012	2	2	6f $(\frac{1}{2},3\frac{1}{2})_3$	($^1F_3$)		
43	56134.851	.007	.012	1	1	6f $(\frac{1}{2},2\frac{1}{2})_3$	($^3F_3$)		

Table 3. Even Energy Levels of Sn I (Continued)

Level Number	Level Value (cm^{-1})	Estimated Uncertainty (cm^{-1}) Relative	Absolute	Number of Combinations Author	All	Level Designation Author		AEL[1]	Meggers[2]
44	56135.589	.010	.014	5	5	6f $(\frac{1}{2},2\frac{1}{2})_2$	$(^3F_2)$		
45	56136.159	.008	.013	1	1	6f $(\frac{1}{2},3\frac{1}{2})_4$	$(^3F_4)$		
46	56395.886	.003	.010	5	6	4f $(1\frac{1}{2},3\frac{1}{2})_3$	$(^3G_3)$	4f (2?)	4f (2,3)
47	56400.530	.005	.011	3	4+	4f $(1\frac{1}{2},3\frac{1}{2})_4$	$(^3G_4)$	4f (3?)	4f (4)
48	56486.365	.003	.010	6	6	4f $(1\frac{1}{2},2\frac{1}{2})_3$	$(^3D_3)$	4f (2)	4f (2)
49	56488.327	.003	.010	7	8+	4f $(1\frac{1}{2},2\frac{1}{2})_2$	$(^3D_2)$	4f (1?)	4f (1)
50	56541.05	.11	.11	1	1	4f $(1\frac{1}{2},4\frac{1}{2})_5$	$(^3G_5)$		
51	56549.647	.003	.010	2	3+	4f $(1\frac{1}{2},4\frac{1}{2})_4$	$(^1G_4)$	4f (3?)	4f (4)
52	56630.744	.006	.011	3	4	4f $(1\frac{1}{2},1\frac{1}{2})_1$	$(^3D_1)$		
53	56632.797	.004	.011	7	9+	4f $(1\frac{1}{2},1\frac{1}{2})_2$	$(^1D_2)$	4f $^3D_1$	4f (2)
54	56963.668	.011	.015	3	3	7f $(\frac{1}{2},3\frac{1}{2})_3$	$(^1F_3)$		
55	56965.911	.006	.012	1	1	7f $(\frac{1}{2},3\frac{1}{2})_4$	$(^3F_4)$		
56	56969.725	.010	.014	2	2	7f $(\frac{1}{2},2\frac{1}{2})_3$	$(^3F_3)$		
57	56970.512	.020	.022	2	2	7f $(\frac{1}{2},2\frac{1}{2})_2$	$(^3F_2)$		
59	57498.77	.03	.03	1	1	8f $(\frac{1}{2},3\frac{1}{2})_4$	$(^3F_4)$		

Table 3. Even Energy Levels of Sn I (Continued)

Level Number	Level Value (cm^{-1})	Estimated Uncertainty (cm^{-1}) Relative	Absolute	Number of Combinations Author	All	Level Designation Author	AEL[1]	Meggers[2]
60	57499.57	.04	.04	1	1	8f $(\frac{1}{2},2\frac{1}{2})_3$	$(^3F_3)$	
61	57500.35	.06	.06	1	1	8f $(\frac{1}{2},2\frac{1}{2})_2$	$(^3F_2)$	
62	59039.80	.13	.13	1	1	5f $(1\frac{1}{2},4\frac{1}{2})_5$	$(^3G_5)$	
63	59091.20	.11	.11	1	1	5f $(1\frac{1}{2},1\frac{1}{2})_2$	$(^1D_2)$	
64	60399.93	.18	.18	1	1	6f $(1\frac{1}{2},4\frac{1}{2})_5$	$(^3G_5)$	

The symbol + in column six indicates that one or more combinations presently have two possible classifications; these transitions are in addition to the number specified.

Table 4. Odd Energy Levels of Sn I

Level Number	Level Value (cm^{-1})	Estimated Uncertainty (cm^{-1}) Relative	Absolute	Number of Combinations Author	All	Level Designation Author		AEL[1]	Meggers[2]
1°	34640.758	.003	.010	11	11	6s $(\frac{1}{2},\frac{1}{2})^{\circ}_{0}$	($^3P^{\circ}_0$)	6s $^3P^{\circ}_0$	6s $^3P^{\circ}_0$
2°	34914.282	.002	.010	34	34	6s $(\frac{1}{2},\frac{3}{2})^{\circ}_{1}$	($^3P^{\circ}_1$)	6s $^3P^{\circ}_1$	6s $^3P^{\circ}_1$
3°	38628.876	.002	.010	18	21	6s $(1\frac{1}{2},1\frac{1}{2})^{\circ}_{2}$	($^3P^{\circ}_2$)	6s $^3P^{\circ}_2$	6s $^3P^{\circ}_2$
4°	39257.053	.002	.010	30	32	6s $(1\frac{1}{2},1\frac{1}{2})^{\circ}_{1}$	($^1P^{\circ}_1$)	6s $^1P^{\circ}_1$	6s $^1P^{\circ}_1$
5°	39625.506	.004	.010	7	7	5s5p^3 $^5S^{\circ}_2$		5s5p^3 $^5S^{\circ}_2$	5s5p^3 (2) ?
6°	43682.737	.002	.010	22	24	5d $(\frac{1}{2},2\frac{1}{2})^{\circ}_{2}$	($^1D^{\circ}_2$)	5d $^3F^{\circ}_2$	5d $^3D^{\circ}_2$
7°	44144.368	.002	.010	22	24	5d $(\frac{3}{2},1\frac{1}{2})^{\circ}_{2}$	($^3D^{\circ}_2$)	5d $^3D^{\circ}_2$	5d $^3F^{\circ}_2$
8°	44508.677	.003	.010	15	16	5d $(\frac{1}{2},1\frac{1}{2})^{\circ}_{1}$	($^3D^{\circ}_1$)	5d $^3D^{\circ}_1$	5d $^3D^{\circ}_1$
9°	44576.006	.003	.010	17	19+	5d $(\frac{1}{2},2\frac{1}{2})^{\circ}_{3}$	($^3D^{\circ}_3$)	5d $^3D^{\circ}_3$	5d $^3F^{\circ}_3$
10°	47145.684	.004	.011	9	11	5d $(1\frac{1}{2},2\frac{3}{2})^{\circ}_{2}$	($^3F^{\circ}_2$)	5d $^1D^{\circ}_2$	5d $^1D^{\circ}_2$
11°	47487.696	.003	.010	8	9	5d $(1\frac{1}{2},2_2)^{\circ}_{3}$	($^3F^{\circ}_3$)	5d $^3F^{\circ}_3$	5d $^3D^{\circ}_3$
12°	48107.27	.11	.11	4	5+	5d $(1\frac{1}{2},3\frac{1}{2})^{\circ}_{4}$	($^3F^{\circ}_4$)		

Table 4. Odd Energy Levels of Sn I (Continued)

Level Number	Level Value (cm^{-1})	Estimated Uncertainty (cm^{-1}) Relative	Absolute	Number of Combinations Author	All	Level Designation Author		AEL[1]	Meggers[2]
13°	48216.356	.015	.018	1	3	$7s\ (\frac{1}{2},\frac{1}{2})^{\circ}_{0}$	$(^3P^{\circ}_0)$	$7s\ ^3P^{\circ}_0$	$7s\ ^3P^{\circ}_0$
14°	48222.159	.005	.011	5	9+	$7s\ (\frac{1}{2},\frac{1}{2})^{\circ}_{1}$	$(^3P^{\circ}_1)$	$7s\ ^3P^{\circ}_1$	$7s\ ^3P^{\circ}_1$
15°	48669.409	.007	.012	4	8	$5d\ (1\frac{1}{2},1\frac{1}{2})^{\circ}_{2}$	$(^3P^{\circ}_2)$	$5d\ ^3P^{\circ}_2$	$5d\ ^3P^{\circ}_2$
16°	48981.934	.006	.011	4	9	$5d\ (1\frac{1}{2},1\frac{1}{2})^{\circ}_{1}$	$(^3P^{\circ}_1)$	$5d\ ^3P^{\circ}_1$	$5d\ ^3P^{\circ}_1$
17°	49487.127	.021	.023	1	2	$5d\ (1\frac{1}{2},\frac{1}{2})^{\circ}_{0}$	$(^3P^{\circ}_0)$	$5d\ ^3P^{\circ}_0$	$5d\ ^3P^{\circ}_0$
18°	49893.823	.009	.013	2	3+	$5d\ (1\frac{1}{2},3\frac{1}{2})^{\circ}_{3}$	$(^1F^{\circ}_3)$	$5d\ ^1F^{\circ}_3$	$5d\ ^1F^{\circ}_3$
19°	50125.971	.005	.011	6	9+	$5d\ (1\frac{1}{2},\frac{1}{2})^{\circ}_{1}$	$(^1P^{\circ}_1)$	$5d\ ^1P^{\circ}_1$	$5d\ ^1P^{\circ}_1$
20°	51010.937	.007	.012	4	7	$6d\ (\frac{1}{2},2\frac{1}{2})^{\circ}_{2}$	$(^1D^{\circ}_2)$	$6d\ ^3D^{\circ}_2$	$6d\ ^3D^{\circ}_2$
21°	51160.520	.004	.011	3	5	$6d\ (\frac{1}{2},1\frac{1}{2})^{\circ}_{2}$	$(^3D^{\circ}_2)$	$6d\ ^3F^{\circ}_2$	$6d\ ^3F^{\circ}_2$
22°	51474.718	.007	.012	5	9	$6d\ (\frac{1}{2},1\frac{1}{2})^{\circ}_{1}$	$(^3D^{\circ}_1)$	$6d\ ^3D^{\circ}_1$	$6d\ ^3D^{\circ}_1$
23°	51754.671	.005	.011	3	5	$6d\ (\frac{1}{2},2\frac{1}{2})^{\circ}_{3}$	$(^3D^{\circ}_3)$	$6d\ ^3D^{\circ}_3$	$6d\ ^3F^{\circ}_3$
24°	52415.877	.011	.015	3	10	$7s\ (1\frac{1}{2},1\frac{1}{2})^{\circ}_{2}$	$(^3P^{\circ}_2)$	$7s\ ^3P^{\circ}_2$	$7s\ ^3P^{\circ}_2$
25°	52706.832	.006	.011	5	11	$7s\ (1\frac{1}{2},1\frac{1}{2})^{\circ}_{1}$	$(^1P^{\circ}_1)$	$7s\ ^1P^{\circ}_1$	$7s\ ^1P^{\circ}_1$
26°	52919.767	.004	.011	2	2	$8s\ (\frac{1}{2},\frac{1}{2})^{\circ}_{0}$	$(^3P^{\circ}_0)$		
27°	53020.952	.003	.010	6	9+	$8s\ (\frac{1}{2},\frac{1}{2})^{\circ}_{1}$	$(^3P^{\circ}_1)$	$8s\ ^3P^{\circ}_1$	$8s\ ^3P^{\circ}_1$

Table 4. Odd Energy Levels of Sn I (Continued)

Level Number	Level Value (cm^{-1})	Estimated Uncertainty (cm^{-1}) Relative	Absolute	Number of Combinations Author	All	Level Designation Author		AEL[1]	Meggers[2]
28°	53592.774	.004	.010	6	10	7d $(\frac{1}{2},1\frac{1}{2})^\circ_1$	($^3D^\circ_1$)	7d $^3D^\circ_1$	7d $^3D^\circ_1$
29°	53631.806	.003	.010	4	9	7d $(\frac{1}{2},2\frac{1}{2})^\circ_2$	($^1D^\circ_2$)	7d $^3D^\circ_2$	7d $^3F^\circ_2$
30°	53826.604	.005	.011	2	6	7d $(\frac{1}{2},2\frac{1}{2})^\circ_3$	($^3D^\circ_3$)	7d $^3D^\circ_3$	7d $^3F^\circ_3$
31°	54211.744	.005	.011	3	5	7d $(\frac{1}{2},1\frac{1}{2})^\circ_2$	($^3D^\circ_2$)	7d $^3F^\circ_2$	7d or 8d (2)
32°	54653.830	.004	.011	2	4+	6d $(1\frac{1}{2},2\frac{1}{2})^\circ_3$	($^3F^\circ_3$)	6d $^3P^\circ_2$	6d $^3P^\circ_2$
33°	54713.310	.004	.011	5	7+	6d $(1\frac{1}{2},2\frac{1}{2})^\circ_2$	($^3F^\circ_2$)	8d $^3D^\circ_1$?	7d or 8d (3)
34°	54830.196	.012	.015	2	3	8d $(\frac{1}{2},2\frac{1}{2})^\circ_3$	($^3D^\circ_3$)	8d $^3D^\circ_3$	7d or 8d (3)
35°	55073.194	.004	.011	4	8	6d $(1\frac{1}{2},1\frac{1}{2})^\circ_1$	($^3P^\circ_1$)	6d $^3P^\circ_1$	6d $^3P^\circ_1$
36°	55131.530	.005	.011	2	3	9s $(\frac{1}{2},\frac{1}{2})^\circ_0$	($^3P^\circ_0$)	8d $^3D^\circ_2$	
37°	55156.731	.004	.011	6	9	9s $(\frac{1}{2},\frac{1}{2})^\circ_1$	($^3P^\circ_1$)	9s $^3P^\circ_1$	9s $^3P^\circ_1$
38°	55296.252	.004	.010	4	8	6d $(1\frac{1}{2},1\frac{1}{2})^\circ_2$	($^3P^\circ_2$)	6d $^1D^\circ_2$	6d $^1D^\circ_2$
39°	55444.611	.009	.013	1	1	6d $(1\frac{1}{2},3\frac{1}{2})^\circ_4$	($^3F^\circ_4$)		
40°	55621.90	.07	.07	1	2	6d $(1\frac{1}{2},\frac{1}{2})^\circ_0$	($^3P^\circ_0$)		
41°	55688.377	.005	.011	2	6+	$5s5p^3\ ^3S^\circ_1$		$5s5p^3\ ^3S^\circ_1$	7d or 8d (2)
42°	55741.165	.006	.011	4	5	J = 3		6d $^3F^\circ_3$	6d $^3D^\circ_3$

Table 4. Odd Energy Levels of Sn I (Continued)

Level Number	Level Value (cm^{-1})	Estimated Uncertainty (cm^{-1}) Relative	Absolute	Number of Combinations Author	All	Level Designation Author		AEL[1]	Meggers[2]
43°	55805.362	.005	.011	4	7	J = 2		8d $^2F^\circ_2$	7d or 8d (2)
44°	55854.623	.005	.011	2	3	8d $(\frac{1}{2},1\frac{1}{2})^\circ_2$	($^3D^\circ_2$)		
45°	56242.378	.005	.011	5	7+	6d $(1\frac{1}{2},\frac{1}{2})^\circ_1$	($^1P^\circ_1$)	6d $^1P^\circ_1$	7d or 8d (1)
46°	56298.005	.006	.011	4	5	6d $(1\frac{1}{2},3\frac{1}{2})^\circ_3$	($^1F^\circ_3$)	6d $^1F^\circ_3$	6d $^1F^\circ_3$
47°[a]	56358.901	.009	.013	2	3	10s $(\frac{1}{2},\frac{1}{2})^\circ_0$	($^3P^\circ_0$)		
48°	56390.113	.008	.012	5	9	10s $(\frac{1}{2},\frac{1}{2})^\circ_1$	($^3P^\circ_1$)	10s $^3P^\circ_1$	10s $^3P^\circ_1$
49°	56546.137	.007	.012	3	6	5s5p^3 $^3D^\circ_2$		5s5p^3 $^3D^\circ_2$	7d or 8d (3)
50°[a]	56631.1			0	2	J = 1			
51°	56659.180	.005	.011	5	8	5s5p^3 $^3D^\circ_1$		5s5p^3 $^3D^\circ_1$	6d $^1P^\circ_1$
52°	56780.004	.011	.015	2	2	9d $(\frac{1}{2},1\frac{1}{2})^\circ_2$	($^3D^\circ_2$)		
53°	56839.3			0	2	J = 3		7d $^1F^\circ_3$?	7d or 8d (3)
54°	57094.4			0	2	11s $(\frac{1}{2},\frac{1}{2})^\circ_1$	($^3P^\circ_1$)	11s $^3P^\circ_1$	11s $^3P^\circ_1$
55°	57105.3			0	3	9d $(\frac{1}{2},2\frac{1}{2})^\circ_2$	($^1D^\circ_2$)	9d $^3D^\circ_2$	
56°	57150.177	.004	.010	4	7	8s $(1\frac{1}{2},1\frac{1}{2})^\circ_2$	($^3P^\circ_2$)	8s $^3P^\circ_2$	8s $^3P^\circ_2$
57°	57181.5			0	2	5s5p^3 $^3D^\circ_3$		5s5p^3 $^3D^\circ_3$	

Table 4. Odd Energy Levels of Sn I (Continued)

Level Number	Level Value (cm^{-1})	Estimated Uncertainty (cm^{-1}) Relative	Absolute	Number of Combinations Author	All	Level Designation Author		AEL[1]	Meggers[2]
58°	57283.653	.005	.011	6	9	8s $(1\frac{1}{2},1\frac{1}{2})^{\circ}_{1}$	($^{1}P^{\circ}_{1}$)	8s $^{1}P^{\circ}_{1}$	8s $^{1}P^{\circ}_{1}$
59°	57374.553	.021	.023	1	1	10d $(\frac{1}{2},1\frac{1}{2})^{\circ}_{2}$	($^{3}D^{\circ}_{2}$)		
60°	57517.82	.04	.04	1	2	10d $(\frac{1}{2},2\frac{1}{2})^{\circ}_{3}$	($^{3}D^{\circ}_{3}$)		
61°	57533.5			0	1	10d $(\frac{1}{2},2\frac{1}{2})^{\circ}_{2}$	($^{1}D^{\circ}_{2}$)	10d $^{3}D^{\circ}_{2}$	
62°	57563.0			0	2	12s $(\frac{1}{2},\frac{1}{2})^{\circ}_{1}$	($^{3}P^{\circ}_{1}$)	12s $^{3}P^{\circ}_{1}$	12s $^{3}P^{\circ}_{1}$
63°	57847.0			0	1	11d $(\frac{1}{2},2\frac{1}{2})^{\circ}_{3}$	($^{3}D^{\circ}_{3}$)	11d $^{3}D^{\circ}_{3}$	
64°	57856.1			0	1	11d $(\frac{1}{2},2\frac{1}{2})^{\circ}_{2}$	($^{1}D^{\circ}_{2}$)	11d $^{3}D^{\circ}_{2}$	
65°	57899.0			0	2	13s $(\frac{1}{2},\frac{1}{2})^{\circ}_{1}$	($^{3}P^{\circ}_{1}$)	13s $^{3}P^{\circ}_{1}$	13s $^{3}P^{\circ}_{1}$
66°	57934.7			0	1+	7d $(1\frac{1}{2},1\frac{1}{2})^{\circ}_{1}$	($^{3}P^{\circ}_{1}$)	7d $^{3}P^{\circ}_{1}$	
67°	58100.7			0	1	12d $(\frac{1}{2},2\frac{1}{2})^{\circ}_{2}$	($^{1}D^{\circ}_{2}$)	12d $^{3}D^{\circ}_{2}$	
68°	58143.6			0	1	14s $(\frac{1}{2},\frac{1}{2})^{\circ}_{1}$	($^{3}P^{\circ}_{1}$)	14s $^{3}P^{\circ}_{1}$	14s $^{3}P^{\circ}_{1}$
69°	58324.7			0	1	15s $(\frac{1}{2},\frac{1}{2})^{\circ}_{1}$	($^{3}P^{\circ}_{1}$)	15s $^{3}P^{\circ}_{1}$	15s $^{3}P^{\circ}_{1}$
70°	58521.907	.006	.012	1	1	7d $(1\frac{1}{2},3\frac{1}{2})^{\circ}_{4}$	($^{3}F^{\circ}_{4}$)		
71°	58523.3			0	1	16s $(\frac{1}{2},\frac{1}{2})^{\circ}_{1}$	($^{3}P^{\circ}_{1}$)	16s $^{3}P^{\circ}_{1}$	
72°	58595.0			0	1	15d $(1\frac{1}{2},1\frac{1}{2})^{\circ}_{1}$	($^{3}D^{\circ}_{1}$)	15d $^{3}D^{\circ}_{1}$	

Table 4. Odd Energy Levels of Sn I (Continued)

Level Number	Level Value (cm^{-1})	Estimated Uncertainty (cm^{-1}) Relative	Absolute	Number of Combinations Author	All	Level Designation Author		AEL[1]	Meggers[2]
73°	58607.7			0	1	17s $(\frac{1}{2},\frac{1}{2})^\circ_1$	$(^3P^\circ_1)$	17s $^3P^\circ_1$	
74°	58679.6			0	1	16d $(\frac{1}{2},1\frac{1}{2})^\circ_1$	$(^3D^\circ_1)$	16d $^3D^\circ_1$	
75°	58690.3			0	1	18s $(\frac{1}{2},\frac{1}{2})^\circ_1$	$(^3P^\circ_1)$	18s $^3P^\circ_1$	
76°	58747.8			0	1	17d $(\frac{1}{2},1\frac{1}{2})^\circ_1$	$(^3D^\circ_1)$	17d $^3D^\circ_1$	
77°	58758.9			0	1	19s $(\frac{1}{2},\frac{1}{2})^\circ_1$	$(^3P^\circ_1)$	19s $^3P^\circ_1$	
78°	58970.3			0	1	7d $(1\frac{1}{2},\frac{1}{2})^\circ_1$	$(^1P^\circ_1)$	7d $^1P^\circ_1$	
79°	59190.2			0	1	7d $(1\frac{1}{2},3\frac{1}{2})^\circ_3$	$(^1F^\circ_3)$	7d $^3F^\circ_3$	
80°	59374.2			0	3	9s $(1\frac{1}{2},1\frac{1}{2})^\circ_2$	$(^3P^\circ_2)$	9s $^3P^\circ_2$	9s $^3P^\circ_2$
81°	59453.0			0	1	9s $(1\frac{1}{2},1\frac{1}{2})^\circ_1$	$(^1P^\circ_1)$	9s $^1P^\circ_1$	
82°	60051.4			0	0	8d $(1\frac{1}{2},1\frac{1}{2})^\circ_1$	$(^3P^\circ_1)$	8d $^3P^\circ_1$	
83°	60397.1			0	1	8d $(1\frac{1}{2},\frac{1}{2})^\circ_1$	$(^1P^\circ_1)$	8d $^1P^\circ_1$	
84°	60452.1			0	2	8d $(1\frac{1}{2},3\frac{1}{2})^\circ_3$	$(^1F^\circ_3)$	8d $^3F^\circ_3$	
85°	60598.8			0	1	10s $(1\frac{1}{2},1\frac{1}{2})^\circ_2$	$(^3P^\circ_2)$	10s $^3P^\circ_2$	10s $^3P^\circ_2$
86°[a]	60646.1			0	1	10s $(1\frac{1}{2},1\frac{1}{2})^\circ_1$	$(^1P^\circ_1)$		
87°	60948.4			0	0	9d $(1\frac{1}{2},1\frac{1}{2})^\circ_1$	$(^3P^\circ_1)$	9d $^3P^\circ_1$	

Table 4. Odd Energy Levels of Sn I (Continued)

Level Number	Level Value (cm^{-1})	Estimated Uncertainty (cm^{-1}) Relative	Absolute	Number of Combinations Author	All	Level Designation Author		AEL[1]	Meggers[2]
88°	61215.2			0	1	9d $(1\frac{1}{2},\frac{1}{2})^\circ_1$	($^1P^\circ_1$)	9d $^1P^\circ_1$	
89°	61247.5			0	1	9d $(1\frac{1}{2},3\frac{1}{2})^\circ_3$	($^1F^\circ_3$)	9d $^3F^\circ_3$	
90°	61346.3			0	1	11s $(1\frac{1}{2},1\frac{1}{2})^\circ_2$	($^3P^\circ_2$)		
91°	61534.2			0	0	10d $(1\frac{1}{2},2\frac{1}{2})^\circ_2$	($^3F^\circ_2$)	10d $^1D^\circ_2$	
92°	61556.3			0	0	10d $(1\frac{1}{2},1\frac{1}{2})^\circ_1$	($^3P^\circ_1$)	10d $^3P^\circ_1$	
93°	61746.7			0	1	10d $(1\frac{1}{2},\frac{1}{2})^\circ_1$	($^1P^\circ_1$)	10d $^1P^\circ_1$	
94°	61769.3			0	2	10d $(1\frac{1}{2},3\frac{1}{2})^\circ_3$	($^1F^\circ_3$)	10d $^3F^\circ_3$	
96°	61859.5			0	0	12s $(1\frac{1}{2},1\frac{1}{2})^\circ_1$	($^1P^\circ_1$)	12s $^1P^\circ_1$	
97°	61963.0			0	0	11d $(1\frac{1}{2},2\frac{1}{2})^\circ_2$	($^3F^\circ_2$)	11d $^1D^\circ_2$	
98°	61973.2			0	0	11d $(1\frac{1}{2},1\frac{1}{2})^\circ_1$	($^3P^\circ_1$)	11d $^3P^\circ_1$	
99°	62111.0			0	1	11d $(1\frac{1}{2},\frac{1}{2})^\circ_1$	($^1P^\circ_1$)	11d $^1P^\circ_1$	
100°	62126.9			0	1	11d $(1\frac{1}{2},3\frac{1}{2})^\circ_3$	($^1F^\circ_3$)	11d $^3F^\circ_3$	
101°	62191.5			0	0	13s $(1\frac{1}{2},1\frac{1}{2})^\circ_1$	($^1P^\circ_1$)	13s $^1P^\circ_1$	
102°	62263.9			0	0	12d $(1\frac{1}{2},2\frac{1}{2})^\circ_2$	($^3F^\circ_2$)	12d $^1D^\circ_2$	
103°	62267.3			0	0	12d $(1\frac{1}{2},1\frac{1}{2})^\circ_1$	($^3P^\circ_1$)	12d $^3P^\circ_1$	

Table 4. Odd Energy Levels of Sn 1 (Continued)

Level Number	Level Value (cm^{-1})	Estimated Uncertainty (cm^{-1}) Relative	Absolute	Number of Combinations Author	All	Level Designation Author	AEL[1]	Meggers[2]
104°	62375.6			0	1	12d $(1\frac{1}{2},2\frac{1}{2})^{\circ}_{1}$	($^{1}P^{\circ}_{1}$)	12d $^{1}P^{\circ}_{1}$
105°	62384.7			0	1	12d $(1\frac{1}{2},3\frac{1}{2})^{\circ}_{3}$	($^{1}F^{\circ}_{3}$)	12d $^{3}F^{\circ}_{3}$
106°	62431.0			0	0	14s $(1\frac{1}{2},1\frac{1}{2})^{\circ}_{1}$	($^{1}P^{\circ}_{1}$)	14s $^{1}P^{\circ}_{1}$
107°	62483.1			0	0	13d $(1\frac{1}{2},2\frac{1}{2})^{\circ}_{2}$	($^{3}F^{\circ}_{2}$)	13d $^{1}D^{\circ}_{2}$
108°	62484.0			0	0	13d $(1\frac{1}{2},1\frac{1}{2})^{\circ}_{1}$	($^{3}P^{\circ}_{1}$)	13d $^{3}P^{\circ}_{1}$
109°	62564.5			0	0	13d $(1\frac{1}{2},\frac{1}{2})^{\circ}_{1}$	($^{1}P^{\circ}_{1}$)	13d $^{1}P^{\circ}_{1}$
110°	62609.4			0	0	15s $(1\frac{1}{2},1\frac{1}{2})^{\circ}_{1}$	($^{1}P^{\circ}_{1}$)	15s $^{1}P^{\circ}_{1}$
111°	62647.8			0	0	14d $(1\frac{1}{2},2\frac{1}{2})^{\circ}_{2}$	($^{3}F^{\circ}_{2}$)	14d $^{1}D^{\circ}_{2}$
112°	62651.8			0	0	14d $(1\frac{1}{2},1\frac{1}{2})^{\circ}_{1}$	($^{3}P^{\circ}_{1}$)	14d $^{3}P^{\circ}_{1}$
113°	62716.4			0	0	14d $(1\frac{1}{2},\frac{1}{2})^{\circ}_{1}$	($^{1}P^{\circ}_{1}$)	14d $^{1}P^{\circ}_{1}$
114°	62745.9			0	0	16s $(1\frac{1}{2},1\frac{1}{2})^{\circ}_{1}$	($^{1}P^{\circ}_{1}$)	16s $^{1}P^{\circ}_{1}$
115°	62774.6			0	0	15d $(1\frac{1}{2},2\frac{1}{2})^{\circ}_{2}$	($^{3}F^{\circ}_{2}$)	15d $^{1}D^{\circ}_{2}$
116°	62776.2			0	0	15d $(1\frac{1}{2},1\frac{1}{2})^{\circ}_{1}$	($^{3}P^{\circ}_{1}$)	15d $^{3}P^{\circ}_{1}$
117°	62827.5			0	0	15d $(1\frac{1}{2},\frac{1}{2})^{\circ}_{1}$	($^{1}P^{\circ}_{1}$)	15d $^{1}P^{\circ}_{1}$
118°	62852.6			0	0	17s $(1\frac{1}{2},1\frac{1}{2})^{\circ}_{1}$	($^{1}P^{\circ}_{1}$)	17s $^{1}P^{\circ}_{1}$

Table 4. Odd Energy Levels of Sn I (Continued)

Level Number	Level Value (cm^{-1})	Estimated Uncertainty (cm^{-1}) Relative	Absolute	Number of Combinations Author	All	Level Designation Author		AEL[1]	Meggers[2]
119°	62871.2			0	0	16d $(1\frac{1}{2},2\frac{1}{2})^{\circ}_{2}$	$(^3F^{\circ}_2)$	16d $^1D^{\circ}_2$	
120°	62878.1			0	0	16d $(1\frac{1}{2},1\frac{1}{2})^{\circ}_{1}$	$(^3P^{\circ}_1)$	16d $^3P^{\circ}_1$	
121°	62919.6			0	0	16d $(1\frac{1}{2},\frac{1}{2})^{\circ}_{1}$	$(^1P^{\circ}_1)$	16d $^1P^{\circ}_1$	
122°	62954.2			0	0	17d $(1\frac{1}{2},2\frac{1}{2})^{\circ}_{2}$	$(^3F^{\circ}_2)$	17d $^1D^{\circ}_2$	
123°	62956.4			0	0	17d $(1\frac{1}{2},1\frac{1}{2})^{\circ}_{1}$	$(^3P^{\circ}_1)$	17d $^3P^{\circ}_1$	
124°	62992.5			0	0	17d $(1\frac{1}{2},\frac{1}{2})^{\circ}_{1}$	$(^1P^{\circ}_1)$	17d $^1P^{\circ}_1$	
125°	63018.1			0	0	18d $(1\frac{1}{2},2\frac{1}{2})^{\circ}_{2}$	$(^3F^{\circ}_2)$	18d $^1D^{\circ}_2$	
126°	63025.9			0	0	18d $(1\frac{1}{2},1\frac{1}{2})^{\circ}_{1}$	$(^3P^{\circ}_1)$	18d $^3P^{\circ}_1$	
127°	63051.3			0	0	18d $(1\frac{1}{2},\frac{1}{2})^{\circ}_{1}$	$(^1P^{\circ}_1)$	18d $^1P^{\circ}_1$	
128°	63072.6			0	0	19d $(1\frac{1}{2},2\frac{1}{2})^{\circ}_{2}$	$(^3F^{\circ}_2)$	19d $^1D^{\circ}_2$	
129°	63080.3			0	0	19d $(1\frac{1}{2},1\frac{1}{2})^{\circ}_{1}$	$(^3P^{\circ}_1)$	19d $^3P^{\circ}_1$	
130°	63104.2			0	0	19d $(1\frac{1}{2},\frac{1}{2})^{\circ}_{1}$	$(^1P^{\circ}_1)$	19d $^1P^{\circ}_1$	
131°	63122.5			0	0	20d $(1\frac{1}{2},1\frac{1}{2})^{\circ}_{1}$	$(^3P^{\circ}_1)$	20d $^3P^{\circ}_1$	
132°	63160.4			0	0	21d $(1\frac{1}{2},1\frac{1}{2})^{\circ}_{1}$	$(^3P^{\circ}_1)$	21d $^3P^{\circ}_1$	
133°	63191.6			0	0	22d $(1\frac{1}{2},1\frac{1}{2})^{\circ}_{1}$	$(^3P^{\circ}_1)$	22d $^3P^{\circ}_1$	

Table 4. Odd Energy Levels of Sn I (Continued)

Level Number	Level Value (cm^{-1})	Estimated Uncertainty (cm^{-1}) Relative	Absolute	Number of Combinations Author	All	Level Designation Author	AEL[1]	Meggers[2]
134°	63220.7			0	0	23d $(1\frac{1}{2},1\frac{1}{2})^{\circ}_{1}$ $(^{3}P^{\circ}_{1})$	23d $^{3}P^{\circ}_{1}$	
135°	63244.3			0	0	24d $(1\frac{1}{2},1\frac{1}{2})^{\circ}_{1}$ $(^{3}P^{\circ}_{1})$	24d $^{3}P^{\circ}_{1}$	
136°	63267.9			0	0	25d $(1\frac{1}{2},1\frac{1}{2})^{\circ}_{1}$ $(^{3}P^{\circ}_{1})$	25d $^{3}P^{\circ}_{1}$	
137°	63283.5			0	0	26d $(1\frac{1}{2},1\frac{1}{2})^{\circ}_{1}$ $(^{3}P^{\circ}_{1})$	26d $^{3}P^{\circ}_{1}$	
138°	63297.5			0	0	27d $(1\frac{1}{2},1\frac{1}{2})^{\circ}_{1}$ $(^{3}P^{\circ}_{1})$	27d $^{3}P^{\circ}_{1}$	
139°[b]	75952.	10.	10.	0	0	$5s5p\,^{3}\,^{1}P^{\circ}_{1}$		

[a] This level was found by Shenstone.

[b] This level was found by Garton[24].

The symbol + in column six indicates that one or more combinations presently have two possible classifications; these transitions are in addition to the number specified.

Table 5. Observed Odd Energy Levels of Sn II

Level Number	Level Value (cm^{-1})	Estimated Uncertainty (cm^{-1}) Relative	Absolute	Number of Combinations	Level Designation AEL[1]
1°	0.000	.05	.000	1	$5p\ ^2P^\circ_{\frac{1}{2}}$
2°	4251.494	.015	.05	3	$5p\ ^2P^\circ_{1\frac{1}{2}}$
3°	71493.275	.004	.05	7	$6p\ ^2P^\circ_{\frac{1}{2}}$
4°	72377.450	.003	.05	10	$6p\ ^2P^\circ_{1\frac{1}{2}}$
5°	89288.248	.007	.05	5	$4f\ ^2F^\circ_{3\frac{1}{2}}$
6°	89294.052	.005	.05	5	$4f\ ^2F^\circ_{2\frac{1}{2}}$
7°	91903.942	.015	.05	2	$7p\ ^2P^\circ_{\frac{1}{2}}$
8°	92268.102	.008	.05	4	$7p\ ^2P^\circ_{1\frac{1}{2}}$
9°	99660.977	.007	.05	3	$5f\ ^2F^\circ_{3\frac{1}{2}}$
10°	99666.327	.008	.05	2	$5f\ ^2F^\circ_{2\frac{1}{2}}$

Table 6. Observed Even Energy Levels of Sn II

Level Number	Level Value (cm^{-1})	Estimated Uncertainty (cm^{-1}) Relative	Absolute	Number of Combinations	Level Designation AEL[1]
1	46464.291	.018	.05	2	$5s5p^2\ {}^4P_{\frac{1}{2}}$
2	48368.188	.008	.05	2	$5s5p^2\ {}^4P_{1\frac{1}{2}}$
3	50730.225	.006	.05	3	$5s5p^2\ {}^4P_{2\frac{1}{2}}$
4	56886.365	.004	.05	2	$6s\ {}^2S_{\frac{1}{2}}$
5	58844.182	.004	.05	4	$5s5p^2\ {}^2D_{1\frac{1}{2}}$?
6	59463.482	.006	.05	3	$5s5p^2\ {}^2D_{2\frac{1}{2}}$?
7	71406.139	.006	.05	3	$5d\ {}^2D_{1\frac{1}{2}}$?
8	72048.257	.005	.05	4	$5d\ {}^2D_{2\frac{1}{2}}$?
12	86280.319	.006	.05	2	$7s\ {}^2S_{\frac{1}{2}}$
13	90241.555	.005	.05	3	$6d\ {}^2D_{1\frac{1}{2}}$
14	90351.894	.005	.05	2	$6d\ {}^2D_{2\frac{1}{2}}$
15	98402.413	.008	.05	2	$8s\ {}^2S_{\frac{1}{2}}$
16	100284.113	.011	.05	2	$7d\ {}^2D_{1\frac{1}{2}}$
17	100338.947	.011	.05	1	$7d\ {}^2D_{2\frac{1}{2}}$
18	104678.31	.12	.13	2	$9s\ {}^2S_{\frac{1}{2}}$
21	105737.480	.011	.05	2	$6g\ {}^2G_{3\frac{1}{2},4\frac{1}{2}}$
25	109025.56	.17	.18	1	$9d\ {}^2D_{2\frac{1}{2}}$
34[a]	$\left(\begin{matrix}78258.194\\100324.103\end{matrix}\right)$	.006	.05	2	$J = 2\frac{1}{2}$ or $3\frac{1}{2}$

[a] This is a new level.

ANALYSIS OF RESULTS

Theoretical Considerations

Predicted Terms

The normal, unexcited tin atom contains 50 electrons in the configuration $1s^2 2s^2 2p^6 3s^2 3p^6 3d^{10} 4s^2 4p^6 4d^{10} 5s^2 5p^2$. The observed arc spectrum can be almost completely accounted for as resulting from the excitation of one of the 5p electrons to higher energy states; that is, by the addition of an electron to the $5s^2 5p$ configuration of singly ionized tin, Sn II. The $^2P^o$ term associated with this latter configuration consists of two levels, $^2P^o_{\frac{3}{2}}$ and $^2P^o_{1\frac{1}{2}}$, which become the parent levels of the terms of the $5s^2 5pnx$ configurations of the arc spectrum. The predicted terms of these configurations are given in Tables 7 and 8 in LS- and jK-notation, respectively. The coupling schemes associated with these notations will be discussed later. Table 7 is a reproduction of Table 9 of reference 1.

Other terms of the arc spectrum result from the excitation of one of the 5s electrons to higher states and some of these terms also are given in Table 7. However, the parent levels of these terms are the levels of the $5s5p^2$ configuration of Sn II and, since the lowest of these levels, $^4P_{\frac{1}{2}}$, lies 46464 cm^{-1} above the $5s^2 5p\ ^2P^o_{\frac{1}{2}}$ level of Sn II, the terms of Sn I built upon these levels would in general be expected to lie above the first ionization limit and thus not be readily observed. However, in the case of the $5s5p^3$ configuration, which has the lowest energy of all of the $5s5p^2 nx$ configurations, many of the levels are

Table 7. Predicted Terms of Sn I (LS Coupling)

Configuration $1s^2 2s^2 2p^6 3s^2 3p^6 3d^{10} 4s^2 4p^6 4d^{10}$ +	Predicted Terms									
$5s^2 5p^2$	^1S	^3P	^1D							
$5s5p^3$	$^3S^\circ$	$^5S^\circ$	$^3P^\circ$	$^1P^\circ$	$^3D^\circ$	$^1D^\circ$				
	ns ($n \geq 6$)		np ($n \geq 6$)			nd ($n \geq 5$)			nf ($n \geq 4$)			. . . . .
$5s^2 5p(^2P^\circ)nx$	$^3P^\circ$		^3S	^3P	^3D	$^3P^\circ$	$^3D^\circ$	$^3F^\circ$	^3D	^3F	^3G	. . . . .
	$^1P^\circ$		^1S	^1P	^1D	$^1P^\circ$	$^1D^\circ$	$^1F^\circ$	^1D	^1F	^1G	. . . . .
$5s5p^2(^4P)nx'$	^5P		$^5S^\circ$	$^5P^\circ$	$^5D^\circ$	^5P	^5D	^5F	$^5D^\circ$	$^5F^\circ$	$^5G^\circ$	. . . . .
	^3P		$^3S^\circ$	$^3P^\circ$	$^3D^\circ$	^3P	^3D	^3F	$^3D^\circ$	$^3F^\circ$	$^3G^\circ$	. . . . .

Table 8. Predicted Terms of Sn I (jK Coupling)

Configuration	Predicted Terms				
	ns ($n \geq 6$)	np ($n \geq 6$)	nd ($n \geq 5$)	nf ($n \geq 4$)	. . . . .
	$(\frac{1}{2},\frac{1}{2})^{\circ}_{0,1}$	$(\frac{1}{2},\frac{1}{2})_{0,1}$	$(\frac{1}{2},1\frac{1}{2})^{\circ}_{1,2}$	$(\frac{1}{2},2\frac{1}{2})_{2,3}$	. . . . .
$1s^2 2s^2 2p^6 3s^2 3p^6 3d^{10}$		$(\frac{1}{2},1\frac{1}{2})_{1,2}$	$(\frac{1}{2},2\frac{1}{2})^{\circ}_{2,3}$	$(\frac{1}{2},3\frac{1}{2})_{3,4}$	. . . . .
$4s^2 4p^6 4d^{10}$	$(1\frac{1}{2},1\frac{1}{2})^{\circ}_{1,2}$	$(1\frac{1}{2},\frac{1}{2})_{0,1}$	$(1\frac{1}{2},\frac{1}{2})^{\circ}_{0,1}$	$(1\frac{1}{2},1\frac{1}{2})_{1,2}$	. . . . .
$5s^2 5p(^2P^{\circ})nx$		$(1\frac{1}{2},1\frac{1}{2})_{1,2}$	$(1\frac{1}{2},1\frac{1}{2})^{\circ}_{1,2}$	$(1\frac{1}{2},2\frac{1}{2})_{2,3}$	. . . . .
		$(1\frac{1}{2},2\frac{1}{2})_{2,3}$	$(1\frac{1}{2},2\frac{1}{2})^{\circ}_{2,3}$	$(1\frac{1}{2},3\frac{1}{2})_{3,4}$	. . . . .
			$(1\frac{1}{2},3\frac{1}{2})^{\circ}_{3,4}$	$(1\frac{1}{2},4\frac{1}{2})_{4,5}$	. . . . .

expected to lie below the first ionization limit; in particular, the $^5S^\circ_2$ level of the $5s5p^3$ configuration should lie quite low[39].

There are endless other terms which are theoretically possible, but their energies lie so high that there is no hope of observing any combinations with them.

Types of Coupling

The first type of vector coupling to be recognized was LS coupling[40] and, for this reason, LS notation has been used in many cases where it is clearly incorrect. Later, a second type of coupling, jj[41], was found and, much later, jK (jl)[42] and LK (Ls)[43]. Although the actual coupling in an atom is never completely of one type, certain generalizations about the types of coupling can be made. LS coupling, which is predominant when the magnetic interaction (spin-orbit) between the spin of each electron and the field caused by its orbital motion is small compared to the electrostatic interactions between the electrons, is generally true for the ground state and low excited configurations of elements of low atomic number. For elements of high atomic number, the spin-orbit interaction tends to be dominant and the coupling is close to jj. Special cases of jj- and LS-coupling are the pair couplings, jK and LK. For jK coupling, the electrostatic interactions of the parent ion and the outer electron are weak compared to the spin-orbit coupling of the parent ion but are strong compared to the spin coupling of the outer electron. This occurs for orbits of high angular momentum for elements of medium and high atomic number. In LK coupling, the spin-orbit interaction of the parent ion is weak compared to the electrostatic interactions but strong compared to the spin coupling of the outer electron. This tends to occur

for the high angular momentum orbits of elements of low atomic number.

In order to illustrate LS- and jK-coupling notation, consider the $5s^2 5p4f$ configuration of tin. Since closed shells contribute zero angular momentum, we need deal with only the two outer electrons. For LS coupling, we have $\underline{L} = \underline{l}_1 + \underline{l}_2$ or, since $l_1 = 1$ and $l_2 = 3$, L = 2, 3, or 4; and $\underline{S} = \underline{s}_1 + \underline{s}_2$, where $s_1 = s_2 = \frac{1}{2}$, so that S = 0 or 1. Thus, one would expect to find levels arising from singlet and triplet terms. These would be written in the form $^{2S+1}L_J$, where 2S+1 is the multiplicity and $\underline{J} = \underline{L} + \underline{S}$. Thus, we would have twelve levels, $^1D_2$, $^1F_3$, $^1G_4$, $^3D_{1,2,3}$, $^3F_{2,3,4}$, and $^3G_{3,4,5}$.

In jK coupling, for the same configuration, we have $\underline{j}_1 = \underline{l}_1 + \underline{s}_1$, so that $j_1 = \frac{1}{2}$ or $1\frac{1}{2}$; and $\underline{K} = \underline{j}_1 + \underline{l}_2$ which gives, for $j_1 = \frac{1}{2}$, $K = 2\frac{1}{2}$ or $3\frac{1}{2}$ and, for $j_1 = 1\frac{1}{2}$, $K = 1\frac{1}{2}$, $2\frac{1}{2}$, $3\frac{1}{2}$, or $4\frac{1}{2}$. Thus, one would expect to find six pairs of levels. These would be written in the form $(j_1,K)_J$, where $\underline{J} = \underline{K} + \underline{s}_2$. So again we would have twelve levels with the same set of J values, $(\frac{1}{2},2\frac{1}{2})_{2,3}$, $(\frac{1}{2},3\frac{1}{2})_{3,4}$, $(1\frac{1}{2},1\frac{1}{2})_{1,2}$, $(1\frac{1}{2},2\frac{1}{2})_{2,3}$, $(1\frac{1}{2},3\frac{1}{2})_{3,4}$, and $(1\frac{1}{2},4\frac{1}{2})_{4,5}$.

Therefore, it is seen that, if LS coupling were valid for this configuration, we would expect to find three singlet terms and three triplet terms, and, if jK coupling were valid, we should find six close pairs of levels, four pairs approaching the upper limit, $5s^2 5p\ ^2P^o_{1\frac{1}{2}}$ of Sn II, and two pairs approaching the lower limit, $5s^2 5p\ ^2P^o_{\frac{1}{2}}$, as the principal quantum number of the outer electron increases. The levels listed in Table 3 clearly indicate that, for the levels of the $5s^2 5p4f$ configuration, the coupling is definitely jK since there is a large j_1 separation and they occur in close pairs.

For the ground configuration, $5s^2 5p^2$, jK coupling has no meaning

because the p-electrons are equivalent (they have the same n- and l-quantum numbers) and jK coupling requires an essential distinction between the electrons. The coupling in this case lies between LS and jj, being somewhat closer to the former[44]. However, for the $5s^2 5p6s$ levels, we find two pairs rather than the singlet and triplet predicted by LS coupling. The pair separations are relatively large, indicating that the coupling is closer to jj than to jK. Nevertheless, the jK notation is used in the level tables to avoid the confusion which would result if a third notation were introduced. As the orbital angular momentum of the valence electron increases, the coupling more closely approaches pure jK.

Selection Rules

While some of the selection rules governing the usual electric dipole transitions between energy levels depend upon the type of coupling present, there are two rules that are independent of the coupling. These are $\Delta J = 0$ or ± 1 with $J = 0$ to $J = 0$ forbidden and Laporte's rule[45]: "even levels can combine only with odd levels," where a level is defined as even (odd) if the configuration has Σl even (odd).

One additional selection rule applies in the usual case where only one electron is involved in the transition, namely, $\Delta l = \pm 1$. In the case in which two electrons are involved in the transition, $\Delta l_i = \pm 1$ and $\Delta l_j = 0$ or ± 2. Several examples of the latter transitions were found in the tin spectrum, namely, $5s^2 5p6p - 5s5p^3$, $5s^2 5pnf - 5s5p^3$, and $5s^2 5pnf - 5s^2 5p6s$. At first sight, the last of these appears to be a one-electron transition, but, if this were true, then l would have to change by three, violating the selection rule; thus, it must be that $\Delta l_1 = -1$ (5p to 6s) and $\Delta l_2 = -2$ (nf to 5p).

For LS coupling, we have the additional selection rules that $\Delta S = 0$ and $\Delta L = 0$ or ± 1. The first of these rules prohibits singlet-triplet intercombinations and the second prohibits transitions of the type $5s^2 5p4f\ {}^3F - 5s^2 5p6s\ {}^3P^o$. As the coupling conditions deviate from LS, these selection rules are among the first characteristics of LS coupling to disappear. Both of these rules are frequently violated in the case of tin, giving one indication that the actual coupling differs from pure LS.

For jK coupling, the additional selection rules are $\Delta j_1 = 0$ and $\Delta K = 0$ or ± 1 with $K = 0$ to $K = 0$ forbidden. Both of these rules also are violated for tin, indicating that the coupling is not pure jK, either. However, the relative positions of the $5s^2 5p4f$ levels and the intensities of the $5s^2 5pnf - 5s^2 5p5d$ transitions indicate that the actual coupling must be close to jK for these configurations.

Classification of the Levels

The designations of the levels of the arc spectrum of tin listed in Tables 3 and 4 were assigned on the basis of the selection rules, the relative intensities of the transitions observed, the values of the quantum defects of the levels, the designations given the corresponding levels in the arc spectrum of germanium[46], and, of course, the designations given by previous investigators. One means which could not be employed was the reference to the corresponding spectra of the isoelectronic series, Sb II, Te III, etc., as these spectra are not as well known as that of Sn I.

The selection rules have already been discussed. The one of importance in classifying the levels is the J selection rule since it enables

one to determine the J-value of a level from other levels whose J-values are known.

The intensities of the transitions between the levels proved to be of limited value in the classification of the levels because of the breakdown of the selection rules for the different types of coupling. In terms of LS coupling, the singlet-triplet transitions usually were weaker than the singlet-singlet and triplet-triplet transitions. Or, in terms of jK coupling, transitions which violated the $\Delta j_1 = 0$ rule usually were weak compared to those that did not. Beyond this, however, the intensities could not be relied upon in determining the classifications of the levels.

The quantum defect of a level is defined as n - n*, where n is the principal quantum number and n* is the effective quantum number defined by $n^* = \sqrt{R/T}$, where R is the Rydberg constant (109736.8 cm^{-1} for tin) and T is the term value which is equal to the difference between the value of the limit and the level value. A non-zero quantum defect arises because of penetration of the core by the outer electron and because of polarization of the core in the field of the outer electron, the former being dominant for small values of the angular momentum and the latter for large values. Since there are two possible limits for the levels of the $5s^2 5pnx$ configurations, two values for the quantum defect of each level were calculated, one for each limit. In the absence of perturbations, the quantum defect of a level series varies smoothly with n and a plot of the quantum defect versus the level values of the series will result in a smooth curve. Also, the quantum defects of the levels decrease as l increases, and they are nearly zero for levels of the $5s^2 5pnf$ and higher configurations.

Because of the above-mentioned relations, not only is the quantum defect of value in classifying the levels, it also provides a simple means of locating new levels. Since the approximate value of the quantum defect of the level being sought can be extrapolated from the other levels of that series, the approximate value of the level can be calculated and this, in turn, can be used to calculate the approximate wave numbers of the expected transitions with the level. If the transitions have been observed, they usually are unclassified and are easily identified so that the correct value of the new level can then be determined. This method was used to locate most of the new levels listed in Tables 3 and 4.

$5s^2 5p^2$ Ground-State Configuration

The five levels of the ^3P, ^1D, and ^1S terms belonging to the ground-state configuration of the arc spectrum of tin were first identified by Sur[20], and the Zeeman effect measurements of Back[22] and of Green and Loring[23] definitely established the quantum numbers of these levels. In addition, their relative positions agree very well with those predicted[44] so that there is no question about their classification.

$5s^2 5pns$ Configurations ($n \geq 6$)

The four levels of the $5s^2 5p6s$ configuration also were first identified by Sur and their quantum numbers were verified by Back and by Green and Loring. Since these are the lowest excited levels, one would expect the lines resulting from combinations between these levels and the levels of the ground configuration to be the most intense and this is verified by observation.

Many levels of the other $5s^2 5pns$ configurations have been identified

by other investigators and are listed in AEL[1]. Plots of the quantum defect versus level value for the observed levels of these configurations are given in Figure 7. The arrows beside the designations of the configurations indicate to which limit the levels go, as do the points themselves, an erect triangle indicating a level going to the upper limit and an inverted triangle indicating one going to the lower limit. The J-values of the levels are written beside the points to aid in following the series.

The 8s- and 9s-$(\frac{1}{2},\frac{1}{2})^{\circ}_{0}$ ($^3P^{\circ}_0$) levels and the 11s$(1\frac{1}{2},1\frac{1}{2})^{\circ}_{2}$ ($^3P^{\circ}_2$) level were found in the present investigation by the method previously described. The 9s$(\frac{1}{2},\frac{1}{2})^{\circ}_{0}$ level was classified as 8d $^3D^{\circ}_2$ in AEL, but it combines only with even levels with J = 1 and, on the basis of this and the quantum defect, the new classification is undoubtedly correct.

The irregularities in the quantum defect curve for the ns$(\frac{1}{2},\frac{1}{2})^{\circ}_{1}$ ($^3P^{\circ}_1$) levels can be accounted for as resulting from perturbations due to neighboring levels. (A level can be perturbed only by other levels having the same parity and the same J-value.) In particular, the 7s- and 9s-$(\frac{1}{2},\frac{1}{2})^{\circ}_{1}$ levels are pushed down and the 8s- and 10s-$(\frac{1}{2},\frac{1}{2})^{\circ}_{1}$ levels are pushed up by the 5d- and 6d-$(1\frac{1}{2},\frac{1}{2})^{\circ}_{1}$ ($^1P^{\circ}_1$) levels, respectively. Similar perturbations are found in the germanium spectrum[46]. Also, the 7s-, 8s-, 9s-, and 10s-$(\frac{1}{2},\frac{1}{2})^{\circ}_{0}$ ($^3P^{\circ}_0$) levels are slightly affected by the 5d- and 6d-$(1\frac{1}{2},\frac{1}{2})^{\circ}_{0}$ ($^3P^{\circ}_0$) levels. The discontinuity in the quantum defect curve between 15s- and 16s-$(\frac{1}{2},\frac{1}{2})^{\circ}_{1}$ levels might be accounted for by the presence of an odd level with J = 1 at about 58400 cm^{-1}, as was suggested by Professor Shenstone in a private communication to Miss Charlotte E. Moore prior to the publication of the third volume of Atomic Energy Levels. A careful search for such a level was made but without success.

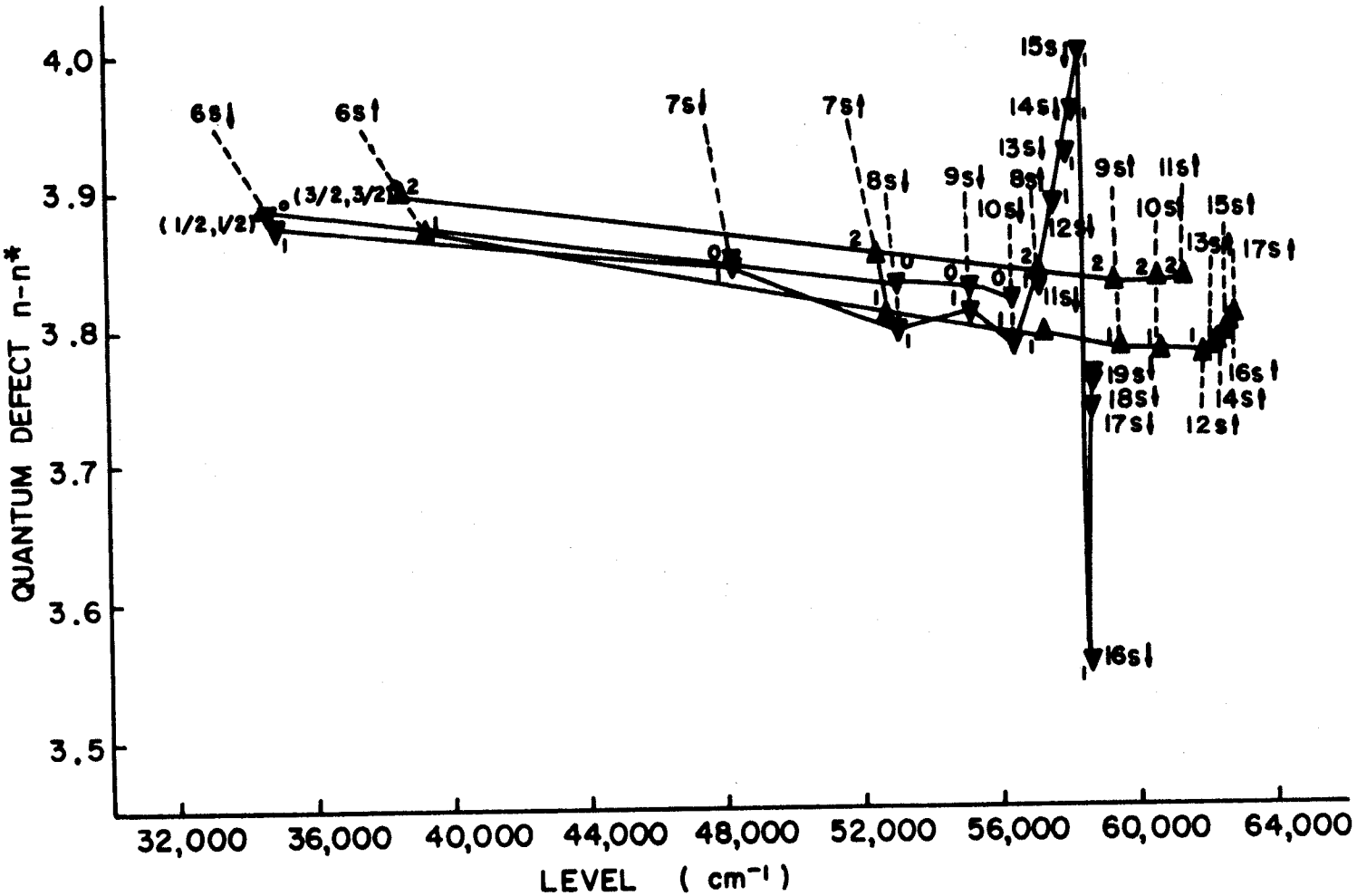

FIGURE 7 QUANTUM DEFECT VERSUS LEVEL VALUE FOR THE $5s^2 5p\ ns$ CONFIGURATIONS

A further verification of the classifications of the $5s^2 5pns$ levels is provided by the relation $ns(1\tfrac{1}{2},1\tfrac{1}{2})^\circ_2 - ns(\tfrac{1}{2},\tfrac{1}{2})^\circ_0 \rightarrow L_2 - L_1$ as $n \rightarrow \infty$, where L_2 and L_1 are the limits of these configurations, the $5s^2 5p\ {}^2P^\circ_{1\frac{1}{2}}$ and ${}^2P^\circ_{\frac{1}{2}}$ levels, respectively, of Sn II. This regularity is illustrated below.

n	$ns(1\tfrac{1}{2},1\tfrac{1}{2})^\circ_2 - ns(\tfrac{1}{2},\tfrac{1}{2})^\circ_0$
6	3988.12 cm^{-1}
7	4199.52 cm^{-1}
8	4230.41 cm^{-1}
9	4242.7 cm^{-1}
10	4239.9 cm^{-1}
$L_2 - L_1$	4251.49 cm^{-1}

$5s^2 5pnp$ Configurations ($n \geq 6$)

Although AEL lists values for all of the twenty predicted levels of the $5s^2 5p6p$ and $5s^2 5p7p$ configurations, three of the former and one of the latter were not verified in this investigation. It was first noted that most of the lines which could be classified as resulting from combinations with the AEL $6p\ {}^3P_0$ level at 43430 cm^{-1} resulted in a violation of the ΔJ selection rule, but, if the level had $J = 2$, then the transitions were no longer forbidden. However, this gave two levels with $J = 2$ and two with $J = 1$ going to the lower limit instead of the predicted one with $J = 0$, two with $J = 1$, and one with $J = 2$. The other $J = 2$ level, $6p\ {}^3D_2$ at 43238 cm^{-1}, belonging to the lower limit appeared to be well established by four lines, three of which had been measured interferometrically; however, it was discovered that each of these lines could be classified in a different way so that this level was rejected. The search for a level with $J = 0$ led to the discovery of level 9 (Table 3)

at 43779 cm^{-1} and permitted the classification of several relatively strong lines which had resisted previous efforts at classification.

The 6p $^1S_0$ level at 46396 cm^{-1} given in AEL was determined by a single line and had a value considerably lower than would be expected after noting the position of the corresponding level in germanium. A search for a level of higher energy immediately led to the discovery of level 15 with J = 0 at 49406 cm^{-1}.

The only change made in the levels of the $5s^2 5p7p$ configuration as given in AEL involved the level there classified as $^1S_0$ at 52265 cm^{-1}. From the observed transitions, it was apparent that this level had J = 2 and, from its quantum defect, it appeared that it belonged to the $5s^2 5p4f$ configuration as it had been classified by Randall and Wright[3]. This led to the discovery of level 41 with J = 0 at 56104 cm^{-1}.

In the manner previously descrived, the levels of the $5s^2 5p8p$ and $5s^2 5p9p$ configurations belonging to the lower limit were found with the exception of the $9p(\frac{1}{2},\frac{1}{2})_0$ ($^3P_0$) level. None of the levels belonging to the higher limit were found for these configurations.

Plots of the quantum defect versus level value for the $5s^2 5pnp$ configurations are shown in Figure 8. The regularity of the curves supports the present classifications. The perturbation of the $(\frac{1}{2},\frac{2}{2})_1$, $(\frac{2}{2},1\frac{1}{2})_2$, and $(\frac{1}{2},\frac{1}{2})_0$ levels of the 7p and 8p configurations must be due to the $(1\frac{1}{2},\frac{1}{2})_1$, $(1\frac{1}{2},1\frac{1}{2})_2$, and $(1\frac{1}{2},\frac{1}{2})_0$ levels, respectively, of the 6p and 7p configurations.

$5s^2 5pnd$ Configurations ($n \geq 5$)

The classification of the levels of the $5s^2 5pnd$ configurations proved to be the most difficult, primarily because of the perturbing

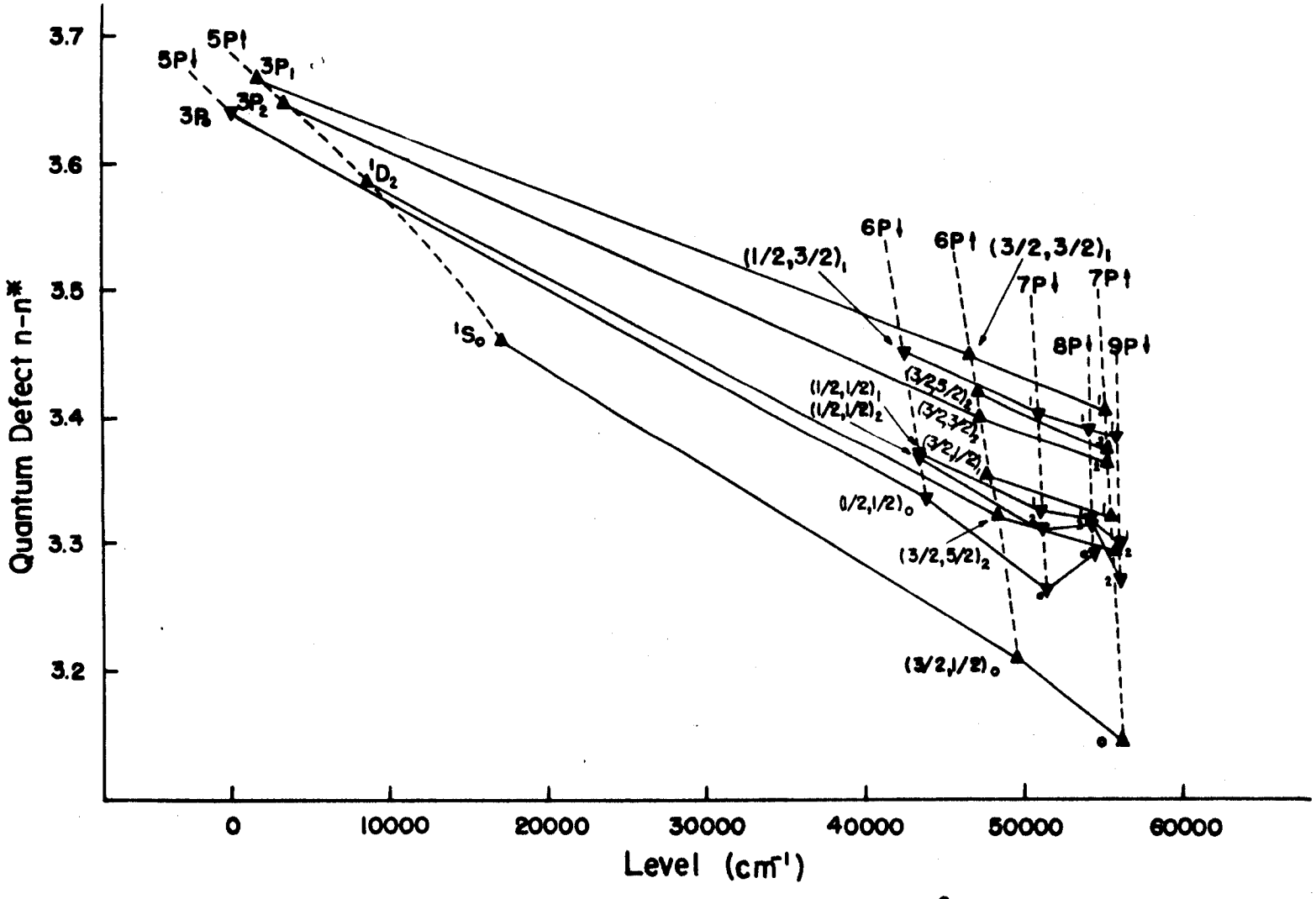

Figure 8. Quantum Defect Versus Level Value for the $5s^2 5pnp$ Configurations

effects of the levels of the $5s5p^3$ configuration. This latter configuration will be discussed in detail later. The author believes that, even though a few of the present classifications are somewhat doubtful, they are the most reasonable in view of the present knowledge of the tin spectrum.

Figure 9 shows the quantum defect curves for the $5s^2 5pnd$ configurations. The levels going to the upper limit for n greater than 15 have been omitted for the sake of clarity as they have no bearing on this investigation.

The classifications of the 5d levels as given in AEL agree very well with those of the 4d configuration of germanium. No changes have been made except that the designations of the 5d $^1D^\circ_2$ and 5d $^3F^\circ_2$ levels have been interchanged. The $5d(1\frac{1}{2},3\frac{1}{2})^\circ_4$ ($^3F^\circ_4$) level was found after its position was estimated from the relative position of the corresponding level in germanium. The 6d- and 7d-$(1\frac{1}{2},3\frac{1}{2})^\circ_4$ levels were then found on the basis of quantum defects and intensities. These levels are not perturbed as they are the only odd levels with J = 4.

Level 32°, classified as 6d $^3P^\circ_2$ in AEL, combines only with levels with J = 2, so that its J-value is probably three. For this reason, and because of its quantum defect, this level was re-classified as $6d(1\frac{1}{2},2\frac{1}{2})^\circ_3$ ($^3F^\circ_3$). Similarly, level 33° was classified as 8d $^3D^\circ_1$? in AEL, but the lack of transitions between it and levels with J = 0 strongly suggests that its J-value is two. Because of this and its quantum defect, this level has been re-classified as $6d(1\frac{1}{2},2\frac{1}{2})^\circ_2$ ($^3F^\circ_2$).

Level 40° is new and is classified as $6d(1\frac{1}{2},1\frac{1}{2})^\circ_0$ ($^3P^\circ_0$). The 6d $^3P^\circ_0$ level listed in AEL was determined by a single line which has been given a different classification in this investigation.

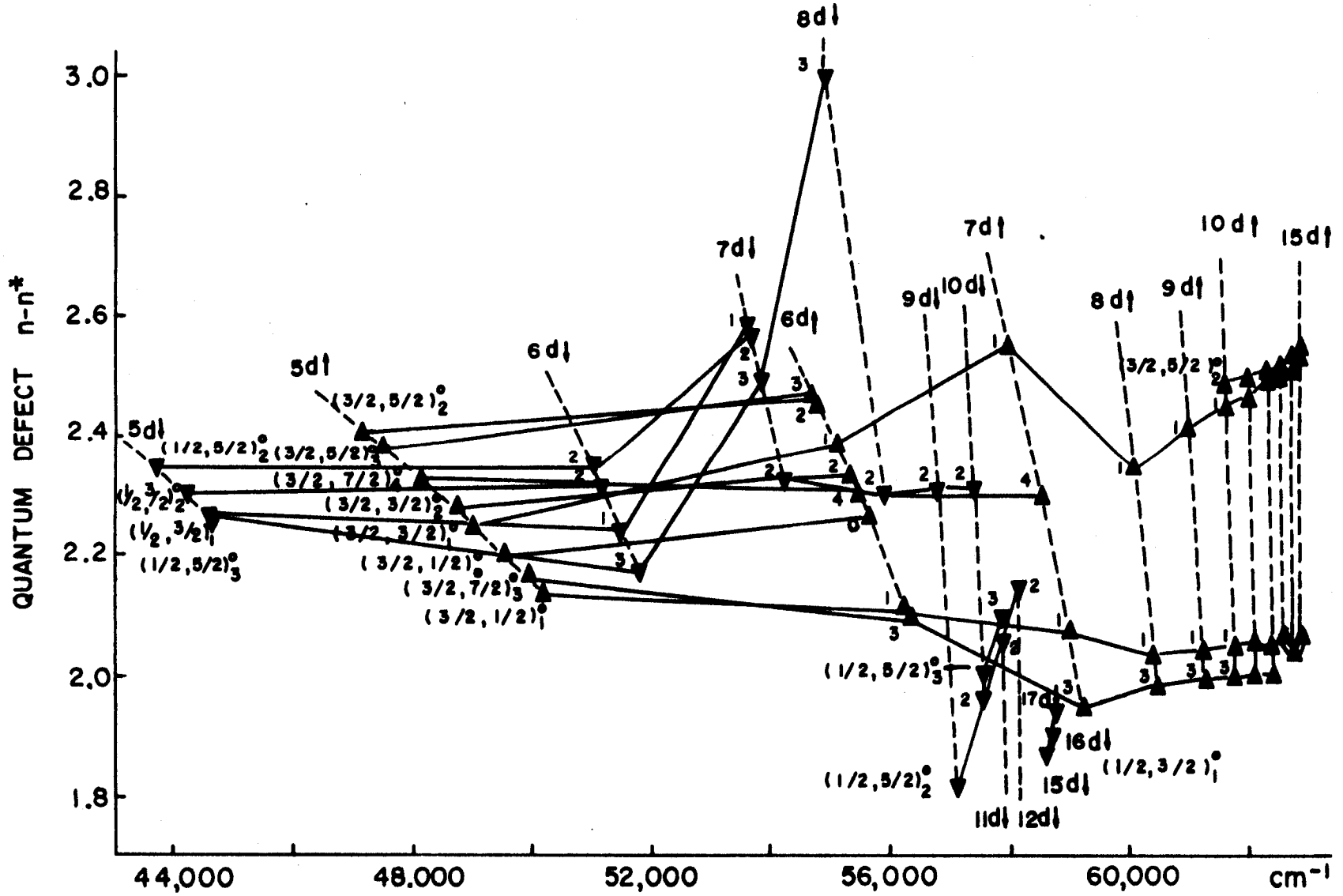

FIGURE 9 QUANTUM DEFECT VERSUS LEVEL VALUE FOR THE $5s^2\,5p\,nd$ CONFIGURATIONS

The perturbations of the $7d(\frac{1}{2},1\frac{1}{2})^\circ_1$ ($^3D^\circ_1$), the $7d(\frac{1}{2},2\frac{1}{2})^\circ_2$ ($^1D^\circ_2$), and the 7d- and 8d-$(\frac{1}{2},2\frac{1}{2})^\circ_3$ ($^3D^\circ_3$) levels are no doubt due to the $^3D^\circ_{1,2,3}$ levels of the $5s5p^3$ configuration.

The 8d-, 9d-, and 10d-$(\frac{1}{2},1\frac{1}{2})^\circ_2$ ($^3D^\circ_2$) levels are new and were located by means of the quantum defects and line intensities. The classification of level 38° has been changed from 6d $^1D^\circ_2$ to $6d(1\frac{1}{2},1\frac{1}{2})^\circ_2$ ($^3P^\circ_2$) because of its quantum defect. The classifications of all nd $^3F^\circ_3$ levels for $n \geq 7$ have been changed to $nd(1\frac{1}{2},3\frac{1}{2})^\circ_3$ ($^1F^\circ_3$) because the quantum defects are much too small for the former classifications to be correct.

Levels 42° and 43°, formerly classified as 6d $^3F^\circ_3$ and 6d $^3F^\circ_2$, respectively, are now unclassified. This is also true of level 53° which was classified as 7d $^1F^\circ_3$?, the quantum defect of this level being much too large for this classification to be correct, even if the level were greatly perturbed by the $5s5p^3$ $^3D^\circ_3$ level. Level 50°, found by Shenstone, also is unclassified. Both it and level 53° are established by only two combinations, so that there is some doubt as to their existence; nevertheless, none of the four lines resulting from transitions with these levels could be classified in any other way.

The classifications of the remaining $5s^25pnd$ levels were not changed except that the designations of the nd $^1D^\circ_2$ levels of AEL for $n \geq 10$ were changed to $nd(1\frac{1}{2},2\frac{1}{2})^\circ_2$ ($^3F^\circ_2$) and those of the nd $^3D^\circ_2$ levels for $n \geq 9$ were changed to $nd(\frac{1}{2},2\frac{1}{2})^\circ_2$ ($^1D^\circ_2$).

The perturbations of the 7d- and 8d-$(1\frac{1}{2},1\frac{1}{2})^\circ_1$ ($^3P^\circ_1$) levels tend to confirm the existence of the previously mentioned level with J = 1 at about 58400 cm^{-1}.

$5s^2 5pnf$ Configurations ($n \geq 4$)

There are eight levels listed in AEL as belonging to the $5s^2 5p4f$ configuration and four as belonging to the $5s^2 5p5f$ configuration, but, with one exception, no level designations are given. All but one of these levels were verified in this investigation, although in many cases the J-values do not agree with those given in AEL. The level not verified was that at 59406 cm^{-1} which was determined by one line, a line which is classified differently in the present investigation.

The quantum defect curves for the nf configurations are given in Figure 10. The effect of the jK pair coupling is very evident for the levels of the 4f configuration. However, the 5f- and 6f-$(\frac{1}{2},2\frac{1}{2})_{2,3}$ ($^3F_{2,3}$) levels are perturbed by the 7p$(1\frac{1}{2},2\frac{1}{2})_{2,3}$ ($^3D_{2,3}$) levels, respectively, and the levels of the 6f and 7f configurations are perturbed by the 4f$(1\frac{1}{2},3\frac{1}{2})_{3,4}$ ($^3G_{3,4}$) levels and by the 4f$(1\frac{1}{2},2\frac{1}{2})_{2,3}$ ($^3D_{2,3}$) levels.

Because the quantum defect for the nf levels is nearly zero, and because the coupling is nearly pure jK, the identification of the levels is not as difficult as for the other configurations. The identification also was aided by the fact that the strongest (and sometimes only) combination with the nf$(j_1,K)_J$ levels was always such that $\Delta j_1 = 0$ and $\Delta K = \Delta J = -1$.

All of the levels going to the lower limit for the 4f, 5f, 6f, 7f, and 8f configurations have been found with the exception of the 8f$(\frac{1}{2},3\frac{1}{2})_3$ level. All of the levels going to the upper limit for the 4f configuration have been found, but the only higher levels found are the 5f- and 6f-$(1\frac{1}{2},4\frac{1}{2})_5$ levels and the 5f$(1\frac{1}{2},1\frac{1}{2})_2$ level. This is no doubt due to the fact that the nf levels going to the upper limit lie above the first

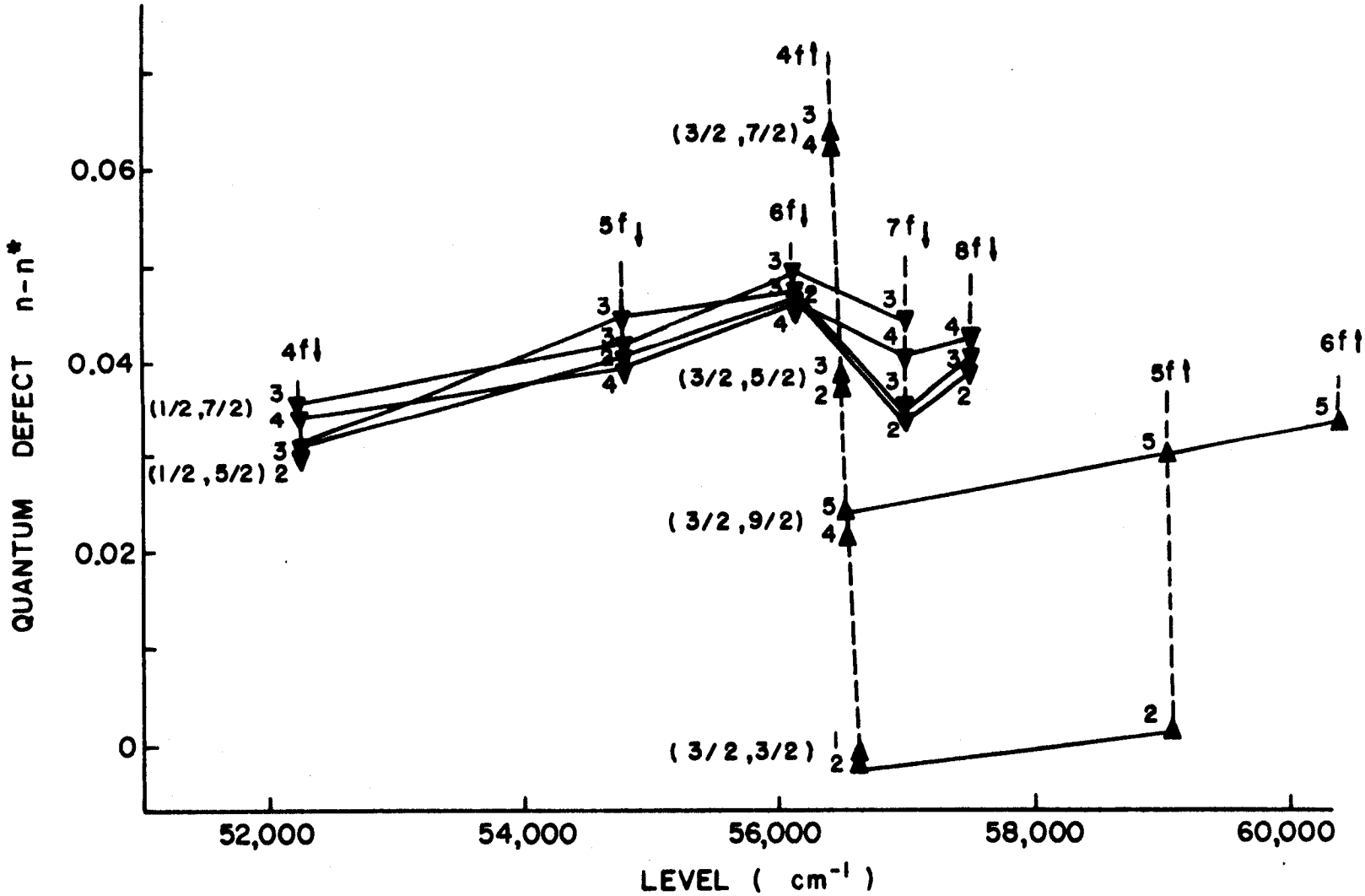

FIGURE 10 QUANTUM DEFECT VERSUS LEVEL VALUE FOR THE $5s^2 5p\ nf$ CONFIGURATIONS

ionization limit for $n \geq 5$ and therefore suffer from the effects of auto-ionization. These effects also probably account for the fact that no levels of the $5s^2 5pnp$ configurations were found above the first ionization limit. Auto-ionization occurs when levels of one series interact with the continuum associated with another series. This latter series corresponds to the unquantized orbits of free electrons and has the same parity and total angular momentum as the series of discrete levels to which it forms an extension. In cases of strong interaction between these series, there is a high probability that the atom in the quantized state will become ionized whereby the atom returns to the level of the first ionization limit and the excess energy is carried off by the ejected electron. This situation cannot occur for the $J = 5$ levels since only the one series exists, but it should occur for the $5f(1\frac{1}{2},1\frac{1}{2})_2$ level and, since this level is established by only one combination, it must be considered somewhat doubtful.

$5s5p^3$ Configuration

The $^5S^\circ_2$, $^3S^\circ_1$, and $^3D^\circ_{1,2,3}$ levels of the $5s5p^3$ configuration are given in AEL. Attempts to find new classifications of these levels yielded results which were incompatible with the observations; therefore, no change was made in the classification of these levels.

The $^5S^\circ_2$ level lies close to the expected position[39], and it and the other four levels agree well with the corresponding levels of germanium. Level 139°, which was found by Garton[24], has been classified as $5s5p^3\ ^1P^\circ_1$ in this investigation as the value of this level is close to that determined by the use of Slater parameters[47]. None of the levels of the $5s5p^3$ ^3P and ^1D terms have been found.

Forbidden Transitions

Two lines of the arc spectrum of tin with wavelengths 7278 A and 6462 A were discovered to be due to the forbidden transitions $5s^2 5p^2$ ($^1S_0 - {}^3P_2$) and $5s^2 5p^2$ ($^1S_0 - {}^3P_1$), respectively. Both of these transitions violate the Laporte rule since they are between levels of the same parity. In addition, the first transition violates the ΔJ selection rule. However, these rules are valid only for electric dipole radiation. For electric quadrupole radiation, transitions can occur only between levels of the same parity and $\Delta J = 2$ is no longer forbidden. One would expect electric quadrupole transitions to be comparatively weak and this is as observed. Of the remaining seven quadrupole transitions between the five levels of the $5s^2 5p^2$ configuration, three lie outside the region of observation and the other four lie above 11600 A, a region in which only lines of relatively high intensity are found.

CONCLUSION

The author feels that the objectives of this investigation have been achieved. Quite satisfactory light sources have been developed and employed to investigate the tin arc spectrum with emphasis on the photographic infrared region. Accurate wavelength measurements have been made throughout the region accessible with the spectrographic equipment available. The analysis of the arc spectrum of tin has yielded several new levels of the $5s^2 5pnp$ and $5s^2 5pnf$ configurations.

Nevertheless, work on the arc spectrum of tin still remains to be done. Measurements in the vacuum ultraviolet should be performed using a light source of the type developed by the author in order to avoid the shifts that are present when different light sources are used. This should result in the discovery of new odd energy levels and, hopefully, remove many of the questions arising from the present analysis of the $5s^2 5pnd$ and $5s5p^3$ configurations. In addition, it should permit the determination of more accurate series limits.

The apparent wavelength shifts between the $SnCl_2$- and the $SnBr_2$- electrodeless discharge light sources should be investigated. They may very well be real, as they were in germanium[48], and may shed additional light on the classification of some of the levels.

And, of course, more measurements are needed in the long wavelength region. Many of the strong lines of the tin spectrum lie considerably above the present 25000 A limit of the measurements.

In connection with the use of lines of the tin arc spectrum as

calculated Ritz standards in the vacuum ultraviolet region, it is the feeling of the author that the lines emitted by the electrodeless discharge tubes of the type employed by him may not be sufficiently sharp for this purpose. The lines which would be used, of course, result from combinations with the ground state, and lines in the region observed in this investigation which resulted from conbinations with these levels were particularly broad. Grating spectrograms in the vacuum ultraviolet obtained with electrodeless discharge light sources are needed to determine the sharpness and intensity of the lines. A hollow-cathode light source should emit sharper lines, but its use would require new measurements in the higher wavelength region with this source.

BIBLIOGRAPHY

BIBLIOGRAPHY

1. C. E. Moore, Atomic Energy Levels (U. S. Government Printing Office, Washington, D. C., 1958), Natl. Bur. Standards Circ. 467, Vol. III.

2. W. F. Meggers, "First Spectrum of Tin," J. Research Natl. Bur. Standards 24, 153 (1940).

3. H. M. Randall and N. Wright, "The Infrared Spectrum of Sn I," Phys. Rev. 38, 457 (1931).

4. P. G. Wilkinson and K. L. Andrew, "Proposed Standard Wavelengths in the Vacuum Ultraviolet. Spectra of Ge, Ne, C, Hg, and N," J. Opt. Soc. Am. 53, 710 (1963).

5. H. Kayser, Handbuch der Spectroscopie (S. Hirzel, Leipzig, 1912), Vol. VI, p. 509.

6. C. Wheatstone, "On the Prismatic Decomposition of Electrical Light," Phil. Mag. (3) 7, 299 (1835).

7. C. Wheatstone, "On the Prismatic Decomposition of the Electric, Voltaic, and Electro-Magnetic Sparks," Chem. News 3, 198 (1861).

8. J. Plücker, "Ueber die Constitution der elektrischen Spectra der verschiedenen Gase und Dämpfe," Annalen der Physik und Chemie (Poggendorff) 107, 497 (1859).

9. G. D. Liveing and J. Dewar, "On the Ultra-Violet Spectra of the Elements," Phil. Trans. 174, 187 (1883).

10. H. Kayser and C. Runge, "Über die Spectren der Elemente VII," Physikalische Abhandlungen der Koniglichen Akademie der Wissenschaften zu Berlin, Paper No. 3 (1893) and "Ueber die Spectra von Zinn, Blei, Arsen, Antimon, Wismuth," Annalen der Physik und Chemie (Wiedemann) 52, 93 (1894).

11. P. Zeeman, "Measurements concerning Radiation-Phenomena in the Magnetic Field I," Phil. Mag. (5) 45, 197 (1898).

12. H. M. Randall, "Some Infra-red Spectra," Astrophys. J. 34, 1 (1911).

13. R. Arnolds, "Das Bogen- und Funkenspektrum von Zinn in I. A.," Z. wiss. Phot. 13, 313 (1914).

14. F. A. Saunders, "Notes on Certain Ultra-Violet Spectra," Astrophys. J. 43, 234 (1916).

15. R. V. Zumstein, "Regularities in the Spectra of Lead and Tin," Trans. Roy. Soc. Can. (Sect. III) 12, 59 (1918).

16. F. M. Walters, Jr., "Wave-Length Measurements in Arc Spectra Photographed in the Yellow, Red, and Infrared," Sci. Papers Bur. Standards 17, (No. 411), 161 (1921).

17. J. C. McLennan, J. F. T. Young, and A. B. McLay, "On the Absorption and Series Spectra of Tin," Trans. Roy. Soc. Can. (Sect. III) 18, 57 (1924).

18. H. Sponer, "Bemerkungen zum Serienspektrum von Blei und Zinn," Z. Physik 32, 19 (1925).

19. R. V. Zumstein, "The Absorption Spectrum of Tin Vapor in the Ultraviolet," Phys. Rev. 27, 150 (1926).

20. N. K. Sur, "Über das Bogenspektrum des Zinns," Z. Physik 41, 791 (1927).

21. F. Hund, "Zur Deutung verwickelter Spektren," Z. Physik 33, 345 (1925) and 34, 296 (1925).

22. E. Back, "Das Zinnbogenspektrum nach seiner magnetischen Zerlegung," Z. Physik 43, 309 (1927).

23. J. B. Green and R. A. Loring, "The Spectra of Tin and their Zeeman Effects," Phys. Rev. 30, 574 (1927).

24. W. R. S. Garton, "Absorption Spectrum of Tin Vapour in the Schumann Region," Letter in Nature 166, 690 (1950).

25. W. R. S. Garton, "Ultra-Violet Absorption Spectra of Tin Vapour in Atmospheres of Helium and Hydrogen," Letter in Proc. Phys. Soc. (London) A64, 591 (1951).

26. C. H. Corliss, W. R. Bozman, and F. O. Westfall, "Electrodeless Metal-Halide Lamps," J. Opt. Soc. Am. 43, 398 (1953).

27. A. L. Wannlund, Jr., "The Purdue Concave Grating Spectrograph," Master's Thesis (unpublished), Purdue University (1949).

28. J. L. Sirks, "On the Astigmatism of Rowland's Concave Gratings," Astronomy and Astro-Physics 13, 763 (1894).

29. F. S. Tomkins and M. Fred, "A Photoelectric Setting Device for a Spectrum Plate Comparator," J. Opt. Soc. Am. 41, 641 (1951).

30. R. L. Kelly, Vacuum Ultraviolet Emission Lines (University of California Lawrence Radiation Laboratory, Livermore), UCRL 5612.

31. E. K. Pyler and N. Gailar, "Near Infrared Absorption Spectra of Deuterated Acetylene," J. Research Natl. Bur. Standards 47, 248 (1951).

32. American Institute of Physics Handbook (McGraw-Hill Book Company, Inc., New York, 1957), p. 789.

33. R. W. Stanley and W. F. Meggers, "Wavelengths From Iron-Halide Lamps," J. Research Natl. Bur. Standards 58, 41 (1957).

34. C. J. Humphreys and E. Paul, Jr., "Infrared Atomic Spectra," Quarterly Report, Foundational Research Projects, Naval Ordnance Laboratory, Corona, California, (Oct. - Dec. 1958), p. 47.

35. C. C. Kiess and C. H. Corliss, "Description and Analysis of the First Spectrum of Iodine," J. Research Natl. Bur. Standards A63, 1 (1959).

36. K. W. Meissner, "Interference Spectroscopy I," J. Opt. Soc. Am. 31, 405 (1941).

37. A. Davison, "Interferometric Wavelength Measurements of Thorium in the Ultraviolet," Master's Thesis (unpublished), Purdue University, p. 41 (1960).

38. B. Edlén, "Vacuum Corrections for Wavelengths from 2000 to 13500 A," Lunds Universitet, Lund, Sweden (1952).

39. K. L. Andrew and K. W. Meissner, "$^5S^\circ_2$ Term of Neutral Germanium," J. Opt. Soc. Am. 47, 850 (1957).

40. H. N. Russell and F. A. Saunders, "New Regularities in the Spectra of the Alkaline Earths," Astrophys. J. 61, 38 (1925).

41. S. Goudsmit and G. E. Uhlenbeck, "Die Kopplungsmöglichkeiten der Quantenvektoren im Atom," Z. Physik 35, 618 (1925).

42. G. Racah, "On a New Type of Vector Coupling in Complex Spectra," Letter in Phys. Rev. 61, 537 (1942).

43. K. B. S. Eriksson, "Pair coupling in p^2f with application to O II," Arkiv Fysik 19, 229 (1961).

44. E. U. Condon and G. H. Shortley, The Theory of Atomic Spectra (The Cambridge University Press, New York, 1935), p. 275.

45. O. Laporte, "Die Struktur des Eisenspektrums," Z. Physik 23, 135 (1924).

46. K. L. Andrew and K. W. Meissner, "Arc Spectrum of Germanium," J. Opt. Soc. Am. 49, 146 (1959).

47. See reference 44, p. 199.

48. V. Kaufman and K. L. Andrew, "Germanium Vacuum Ultraviolet Ritz Standards," J. Opt. Soc. Am. 52, 1223 (1962).

General References

J. H. Pollok, "On the Vacuum Tube Spectra of the Vapours of Some Metals and Metallic Chlorides I," Sci. Proc. Roy. Dublin Soc. 13, 202 (1912).

T. van Lohuizen, "Series in the spectra of Tin and Antimony," Koninklijke Akademie van Wetenschappen te Amsterdam 15, 31 (1912) and "Reihen in den Spektren von Zinn und Antimon," Z. wiss. Phot. 11, 397 (1913).

J. M. Eder, "Messungen im ultravioletten Funkenspektrum von Metallen nach dem internationalen System (Ag, Al, As, Au, Ba, Bi, C, Ca, Cd, Cu, Pb, Sb, Sn, Sr, Tl, Zn)," Kaiserliche Akademie der Wissenschaften, Wien 122, IIa, 607 (1913).

D. S. Ainslie and D. S. Fuller, "New Lines in the Extreme Ultra-Violet of Certain Metals," Trans. Roy. Soc. Can. (Sect. III) 12, 65 (1918).

J. C. McLennan, D. S. Ainslie, and D. S. Fuller, "Vacuum Arc Spectra of various Elements in the Extreme Ultra-violet," Proc. Roy. Soc. (London) A95, 316 (1919).

P. A. van der Harst, "Researches on the Spectra of Tin, Lead, Antimony, and Bismuth in the Magnetic Field," Koninklijke Akademie van Wetenschappen te Amsterdam 22, 300 (1920).

J. C. McLennan, J. F. T. Young, and H. J. C. Ireton, "Arc Spectra in vacuo and Spark Spectra in Helium of Various Elements," Proc. Roy. Soc. (London) A98, 95 (1920).

L. Bloch and E. Bloch, "Spectres d'étincelle de quelques éléments dans l'ultraviolet extrême," Compt. rend. 171, 709 (1920) and "Spectres d'étincelle dans l'ultraviolet extrême," J. phys. radium (6) 2, 229 (1921).

G. A. Hemsalech and A. de Gramont, "Observations and Experiments on the Occurrence of Spark Lines (Enhanced Lines) in the Arc. Part I. Lead and Tin," Phil. Mag. (6) 43, 287 (1922).

L. Bloch and E. Bloch, "Sur les spectres d'étincelle dans l'eau," Compt. rend. 174, 1456 (1922) and "Spectres d'étincelles dans l'eau," J. phys. radium (6) 3, 309 (1922).

W. Grotrian, "Die Absorptionsspektren einiger Metalldämpfe," Z. Physik 18, 169 (1923).

L. Bloch and E. Bloch, "Nouvelle extension des spectres d'étincelle d'étain et du zinc dans la région de Schumann," Compt. rend. 177, 1025 (1923).

M. Kimura and G. Nakamura, "Cathode Spectra of Metals and Their Salts," Japan. J. Phys. 3, 29 (1924).

R. J. Lang, "On the Ultra-Violet Spark Spectra of some of the Elements," Phil. Trans. A224, 371 (1924).

M. Kimura and G. Nakamura, "A Classification of Enhanced Lines of Various Elements," Japan. J. Phys. 3, 197 (1924).

M. Kimura, "Classification of Enhanced Lines of Various Elements," Japan. J. Phys. 3, 217 (1924).

J. A. Carroll, "The Vacuum Spark Spectra of Some of the Heavier Elements, and Series Classification of the Spectra of Ionised Atoms Homologous with Copper, Silver, and Gold," Phil. Trans. A225, 357 (1925).

K. R. Rao, "On the Spectrum of Ionised Tin (Sn III)," Proc. Phys. Soc. (London) 39, 161 (1927).

R. J. Lang, "Series Spectra of Silver-Like Atoms," Proc. Natl. Acad. Sci. U. S. 13, 341 (1927).

K. R. Rao, "Series in the Spectrum of Trebly-Ionised Tin (Sn IV)," Proc. Phys. Soc. (London) 39, 408 (1927).

M. Fukuda, "Reversed Spectra of Metals produced by Explosion under Increased Pressure," Sci. Papers Inst. Phys. Chem. Research (Tokyo) 6, No. 85, 1 (1927).

A. L. Narayan and K. R. Rao, "Serien im ersten Funkenspektrum des Zinns (Sn II)," Z. Physik 45, 350 (1927).

R. C. Gibbs and H. E. White, "Analysis of Spectra Arising from Quadruply Ionized Tin, Sn V," Proc. Natl. Acad. Sci. U. S. 14, 345 (1928).

K. R. Rao, A. L. Narayan, and A. S. Rao, "A Note on the Series Spectra of Sn IV and In III," Indian J. Phys. 2, 477 (1928),

A. T. Williams and F. Charola, "Les séries du spectre d'arc de l'étain," J. phys. radium (6) 9, 377 (1928).

R. J. Loyarte and A. T. Williams, "Die Absorptionsspektren der Dämpfe des Zinns, Silbers, und Mangans zwischen 5500 und 2140 Angströmeinheiten," Physik. Z. 30, 68 (1929).

R. J. Lang, "On the Spectra of Zn II, Cd II, In III, and Sn IV," Proc. Natl. Acad. Sci. U. S. 15, 414 (1929).

R. J. Lang, "The Second Spark Spectrum of Antimony and a Note on the First Spark Spectrum of Tin," Phys. Rev. 35, 445 (1930).

H. Schüler and H. Westmeyer, "Das Kernmoment des Zinns," Letter in Naturwissenschaften 21, 660 (1933).

S. Tolansky, "The Nuclear Spin of Tin," Proc. Roy. Soc. (London) A144, 574 (1934).

H. Westmeyer, "Bemerkung über die Hyperfeinstruktur der roten Cd-linie λ6438 and über Hyperfeinstrukturen bei Sr, Sn, und Mg," Z. Physik 94, 590 (1935).

T. Yuasa, "Wave-Length Shifts of the Spectral Lines of Sn due to the Change of Pressure," Science Reports of the Tokyo Bunrika Daigaku, Sect. A, 2, No. 45, 267 (1935).

T. Futagami, "On the Electric Explosion Spectrum of Metals," Sci. Papers Inst. Phys. Chem. Research (Tokyo) 31, No. 671, 1 (1937)

J. G. Winans and R. M. Williams, "Sensitized Fluorescence of Tin," Phys. Rev. 52, 930 (1937).

W. W. McCormick and R. A. Sawyer, "The Classification of the Spectrum of Singly Ionized Tin. Sn II," Phys. Rev. 54, 71 (1938).

M. Green, "The Spectra of Cd IV, In V and Sn VI in the Isoelectric Sequence Rh I to Sn VI," Phys. Rev. 60, 117 (1941).

S. Tolansky and G. O. Forester, "Hyperfine Structure in the Arc Spectrum of Tin," Phil. Mag. (7) 32, 315 (1941).

M. Gurevitch, "On the Stability of the Isobaric Pair In^{115}-Sn^{115}," Phys. Rev. 75, 767 (1949).

W. G. Proctor, "The Magnetic Moments of Sn^{117}, Sn^{119}, and Pb^{207}," Letter in Phys. Rev. 76, 684 (1949).

W. G. Proctor and F. C. Yu, "On the Magnetic Moments of Sn^{115}, Cd^{111}, Cd^{113}, Pt^{195}, and Hg^{199}," Letter in Phys. Rev. 76, 1728 (1949).

W. G. Proctor, "On the Magnetic Moments of Tl^{203}, Tl^{205}, Sn^{115}, Sn^{117}, Sn^{119}, Cd^{111}, Cd^{113}, and Pb^{207}," Phys. Rev. 79, 35 (1950).

W. R. Hindmarsh, H. Kuhn, and S. A. Ramsden, "Isotope Shifts in the Atomic Spectra of Tin and Cadmium," Letter in Proc. Phys. Soc. (London) A67, 478 (1954).

K. Murakawa, "Isotope Shift in the Spectra of Tin and Lead," Note in J. Phys. Soc. Japan 9, 876 (1954).

W. R. Hindmarsh and H. Kuhn, "Isotope Shifts and Hyperfine Structure in the Atomic Spectrum of Tin," Proc. Phys. Soc. (London) A68, 433 (1955).

C. W. Allen and A. S. Assad, "Oscillator Strengths from Arc Spectra of Diluted Copper Alloys," Monthly Notices Roy. Astrom. Soc. 117, 36 (1957).

C. W. Allen, "Absolute Oscillator Strength Measurements in Mg, Ca and Other Atoms," Monthly Notices Roy. Astrom. Soc. 117, 622 (1957).

R. A. Fisher, W. C. Knopf, Jr., and F. E. Kinney, "Laboratory Wave Lengths and Intensities in the Near Infrared Spectra of Nine Elements," Astrophys. J. 130, 683 (1959).

V. K. Proko'ev, I. M. Nagibina, and G. P. Petrova, "Determination of Absolute Oscillator Strengths from Spectral Line Widths," Optics and Spectroscopy 8, 195 (1960).

N. P. Penkin and I. Yu. Yu. Slavenas, "Oscillator Strengths of the Spectral Lines Sn I and Pb I," Optics and Spectroscopy 15, 83 (1963).

VITA

Wilfred Grenfell Brill, son of Hazel E. and Ira C. Brill, was born on [redacted], in [redacted]. He received his elementary education in the public school at Albion, graduating in 1948. He attended Manchester College, located in North Manchester, Indiana, for four years and received the B. A. degree with a major in physics in May 1952. He enrolled in the graduate school of Purdue University in September of that year and was awarded the M. S. degree in January 1955, after which he continued in the graduate school of Purdue, working on his doctorate.